

INFORMATION TO USERS

This manuscript has been reproduced from the microfilm master. UMI films the text directly from the original or copy submitted. Thus, some thesis and dissertation copies are in typewriter face, while others may be from any type of computer printer.

The quality of this reproduction is dependent upon the quality of the copy submitted. Broken or indistinct print, colored or poor quality illustrations and photographs, print bleedthrough, substandard margins, and improper alignment can adversely affect reproduction.

In the unlikely event that the author did not send UMI a complete manuscript and there are missing pages, these will be noted. Also, if unauthorized copyright material had to be removed, a note will indicate the deletion.

Oversize materials (e.g., maps, drawings, charts) are reproduced by sectioning the original, beginning at the upper left-hand corner and continuing from left to right in equal sections with small overlaps.

Photographs included in the original manuscript have been reproduced xerographically in this copy. Higher quality 6" x 9" black and white photographic prints are available for any photographs or illustrations appearing in this copy for an additional charge. Contact UMI directly to order.

ProQuest Information and Learning
300 North Zeeb Road, Ann Arbor, MI 48106-1346 USA
800-521-0600

UMI[®]

**PHOTO-SWITCHING OF PROTEIN ACTIVITIES BY
CONJUGATION OF PHOTO-RESPONSIVE POLYMERS
TO PROTEINS**

Tsuyoshi Shimoboji

**A dissertation submitted in partial fulfillment of the
requirements for the degree of**

Doctor of Philosophy

University of Washington

2001

Program Authorized to Offer Degree: Department of Bioengineering

UMI Number: 3014117

Copyright 2001 by
Shimoboji, Tsuyoshi

All rights reserved.

UMI[®]

UMI Microform 3014117

Copyright 2001 by Bell & Howell Information and Learning Company.
All rights reserved. This microform edition is protected against
unauthorized copying under Title 17, United States Code.

Bell & Howell Information and Learning Company
300 North Zeeb Road
P.O. Box 1346
Ann Arbor, MI 48106-1346

© Copyright 2001
Tsuyoshi Shimoboji

Doctoral Dissertation

In presenting this thesis in partial fulfillment of the requirements for the Doctoral degree at the University of Washington, I agree that the Library shall make its copies freely available for inspection. I further agree that extensive copying of the dissertation is allowable only for scholarly purposes, consistent with "fair use" as prescribed in the U.S. Copyright Law. Requests for copying or reproduction of this dissertation may be referred to UMI Dissertation Services, 300 North Zeeb Road, P.O. Box 1346, Ann Arbor, MI 48106-1346, to whom the author has granted "the right to reproduce and sell (a) copies of the manuscript in microform and/or (b) printed copies of the manuscript made from microform."

Signature *Junyachi Shimada*

Date March 2, 2001

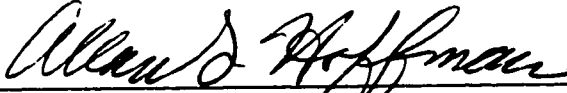
University of Washington
Graduate School

This is to certify that I have examined this copy of a doctoral dissertation by

Tsuyoshi Shimoboji


and have found that it is complete and satisfactory in all respects,
and that any and all revisions required by the final
examining committee have been made.

Chair of Supervisory Committee:

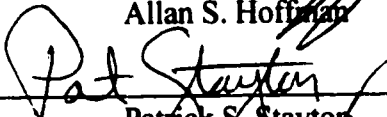


Allan S. Hoffman

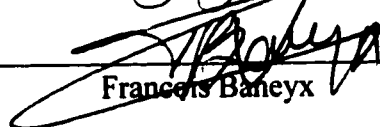
Reading Committee:



Allan S. Hoffman



Patrick S. Stavton



Francis Baeyx

Date:

3/2/01

University of Washington

Abstract

**PHOTO-SWITCHING OF PROTEIN ACTIVITIES BY
CONJUGATION OF PHOTO-RESPONSIVE POLYMERS
TO PROTEINS**

by Tsuyoshi Shimoboji

Chairperson of the Supervisory Committee:
Professor Allan S. Hoffman
Department of Bioengineering

Photo-switching of protein functions has recently become more actively investigated by many researchers. Our objective is to create novel photo-switchable proteins by conjugating photo-responsive polymers to proteins site-specifically.

We synthesized N,N-dimethylacrylamide (DMA)-co-phenylazophenylacrylate copolymer (DMAA) and DMA-co-phenylazophenylacrylamide copolymer (DMAAm) with vinylsulfone termini for conjugation to a protein containing a cysteine. These polymers exhibited temperature-induced phase transitions, and opposite and reversible photo-responses; DMAA became soluble, while DMAAm became insoluble upon the same UV light irradiation.

The mutant streptavidins (SAs), E116C and S139C, were conjugated to these polymers site-specifically. The conjugates bound the ligand, biotin, below the phase transition temperature of the polymer, and released it above the phase transition temperature. The E116C-DMAA conjugate released biotin upon VIS light, while the E116C-DMAAm conjugate released it upon UV light. These opposite photo-responses corresponded to the opposite photo-induced phase transitions of the conjugated polymers. The E116C conjugate, which contains the conjugation site at a critical position for biotin-binding, exhibited larger responses than the S139C conjugate which contains it on the opposite

side to biotin-binding. The conjugation of larger MW polymer and the addition of free polymer also increased the responses.

The mutant endoglucanaseIII, S25C and N55C, were also conjugated to the polymers. The conjugates exhibited similar temperature- and photo-responsive activity changes to the SA conjugates. Polymers with higher MW and the addition of the free polymer enhanced the switching activity. The N55C conjugates, which locate the conjugated polymer closer to the catalytic site than S25C, exhibited higher switching activity than the S25C conjugates. Both conjugates exhibited less activity toward a large substrate, hydroxyethylcellulose, than toward a small substrate, o-nitrophenylcellobioside. Kinetic studies revealed that the activity shut-off stemmed from the sterical inhibition by the shrunken polymers.

Therefore, the photo-switching of molecular recognition processes and catalytic activity were achieved by photo-responsive polymer-protein site-specific conjugation. The MW of the polymer, the position of conjugation, the size of the substrate and the addition of free polymer were key factors in the design of such molecular switches. This methodology can be utilized to develop novel photo-switchable proteins in the fields of biomedicine, bioprocesses, and bioelectronics.

TABLE OF CONTENTS

LIST OF FIGURES	v
LIST OF TABLES	x
LIST OF ABBREVIATIONS.....	xi
CHAPTER 1 INTRODUCTION.....	1
1.1 Objectives	1
1.2 Photo-responsive Processes in Biology	1
1.3 Photochromes	2
1.4 Photo-Control of Conformations and Functions of Biomolecules.....	3
1.4.1 Classification of Photo-switchable Biomolecules	3
1.4.2 Photo-Control of Conformations of Polypeptides	7
1.4.3 Photo-Control of Specific Binding Processes of Proteins	8
1.4.4 Photo-Control of Catalytic Activities of Enzymes	8
1.4.5 Photo-Control of the Absolute Zero Catalytic Activity	10
1.5 Photo-responsive Polymer	12
1.5.1 Stimuli-Responsive Polymer.....	12
1.5.2 Photo-Responsive Polymer	13
1.5.3 Opposite Photo-Responsive Polymer	16
1.6 Site-Specific Conjugation of polymer to Protein.....	17
1.7 Target Model Proteins	18
1.7.1 Streptavidin (SA).....	18
1.7.2 Endoglucanase III (EG III)	20
1.7.2.1 Cellulase	20
1.7.2.2 EG III	21
1.7.2.3 Methods for Measuring Activities of Cellulases	23
1.8 Perspective Applications of Photo-switchable Biomolecules	24
1.8.1 Therapeutics	24
1.8.2 Biosensor & Diagnostics.....	24
1.8.3 Affinity Separations.....	25
1.8.4 Bioprocesses.....	25
1.8.5 Bioelectronics.....	25
1.9 Summary of Our Strategy : Site-Specific Conjugation of Photo-Responsive Polymers to Proteins.....	26
1.10 Significance.....	28

CHAPTER 2 SYNTHESIS OF TEMPERATURE- AND PHOTO- DUAL STIMULI- RESPONSIVE POLYMERS FOR CONJUGATION TO PROTEINS	29
2.1 Introduction.....	29
2.2 Materials and Methods	29
2.2.1 Materials.....	29
2.2.2 Methods.....	30
2.2.2.1 Synthesis of Photo-Responsive Monomers.....	30
2.2.2.2 Synthesis of Photo-Responsive Polymers.....	30
2.2.2.3 Determination of Contents of AZAAm and AZAA	33
2.2.2.4 Determination of Molecular Weights (MWs) of the Polymers	33
2.2.2.5 Derivatization of End Groups of Copolymers with Vinylsulfone Groups.....	33
2.2.2.6 UV or VIS Irradiation	33
2.2.2.7 LCST Measurement	34
2.2.2.8 Photo-Responsive Temperature Measurement.....	34
2.2.2.9 Determination of VS in Polymers.....	34
2.3 Results and Discussions.....	36
2.3.1 Synthesis and Characterization of DMAAm and DMAA Copolymers.....	36
2.3.2 Effects of Photoirradiations on Phase Transitions.....	36
2.3.3 Effects of Azobenzene Monomer Contents on LCST Phase Transition	41
2.3.4 Effects of Polymer and Salt Concentrations on LCSTs.....	44
2.3.5 Isothermal Photo-Responses	47
2.3.6 Design and Synthesis of End-Reactive Photo-Responsive Polymers for Conjugation to EG III.....	47
2.3.7 Synthesis and Determination of Reactive VS content of DMAAm-VS and DMAA-VS.....	53
2.4 Conclusions.....	54
CHAPTER 3 STREPTAVIDIN-PHOTORESPONSIVE POLYMER CONJUGATES.....	56
3.1 Introduction.....	56
3.2 Materials and Methods	57
3.2.1 Materials.....	57
3.2.2 Genetic Engineering of SA.	57
3.2.3 Conjugation of Polymer to SA.	58
3.2.4 Conjugation of Azobenzene to SA.	60
3.2.5 Photo-Irradiation.....	62
3.2.6 Temperature-Responsive Biotin-Binding Assay	62
3.2.7 Photo-Responsive Biotin-Binding Assay	63

3.3 Results and Discussion	66
3.3.1 Preparation of SA Mutants.....	66
3.3.2 SA-DMAA or DMAAm Conjugation	66
3.3.3 SA-AZ Conjugation.....	67
3.3.4 Temperature-Responsive Biotin-Binding	68
3.3.5 Photo-Responsive Biotin-Binding.....	77
3.4 Conclusions.....	84
CHAPTER 4 SITE-DIRECTED MUTAGENESIS OF EG III.....	85
4.1 Introduction.....	85
4.2 Materials and Methods	85
4.2.1 Materials.....	85
4.2.2 Confirmation of EG III Gene in the Plasmid	86
4.2.3 Site-Directed Mutation of EG III	87
4.2.4 Determination of DNA Concentration.....	88
4.2.5 DNA Sequencing.....	88
4.2.6 Gel Electrophoresis for DNA.....	88
4.2.7 Expression of the Mutant EG IIIs.....	88
4.2.8 Purification of the Mutant EG IIIs.....	89
4.2.9 Determination of the Mutant EG IIIs.....	89
4.2.10 Determination of Purity of the Mutant EG IIIs	89
4.2.11 Conjugation of Fluorescein-5-Maleimide (F-MI) to EG III Mutants.....	90
4.2.12 Catalytic Activity Assay	90
4.2.12.1 ONPC Assay.....	90
4.2.12.2 HEC Assay	92
4.3 Results and Discussion	95
4.3.1 Structure and Property of WT EG III	95
4.3.2 Site-Directed Mutation of EG III	96
4.3.3 Expression, Purification and Evaluation of the Site-Directed Mutants of EG IIIs	97
4.3.4 Determination of the Kinetic Parameters of Catalytic Activity of WT and Mutant EG IIIs by ONPC Assay	102
4.3.5 Determination of the Kinetic Parameters of Catalytic Activity of WT and Mutant EG IIIs by HEC Assay	104
4.4 Conclusions.....	105
CHAPTER 5 EG III – PHOTO-RESPONSIVE POLYMER CONJUGATES.....	106
5.1 Introduction.....	106
5.2 Materials and Methods	107

5.2.1 Materials.....	107
5.2.2 Derivatization of End Groups of Copolymers with Acrylate Groups	107
5.2.3 Conjugation of Photo-Responsive Polymers to EG III Mutants	109
5.2.4 Immobilization of the Conjugates on Magnetic Beads.....	109
5.2.5 Conjugation of 4-Phenylazomaleinanil (AZ-MI) to EG III Mutants	113
5.2.6 Conjugation of Photo-Responsive Polymers to Wild Type EG III	114
5.2.7 Catalytic Activity Assay of the Conjugates	114
5.2.7.1 Substrates	114
5.2.7.2 Thermo-Responsive Activity Assay of the Conjugates	115
5.2.7.3 Photo-Responsive Activity Assay of the Conjugates	115
5.2.7.4 Activity Assay for the Immobilized Conjugates	115
5.2.7.5 Cyclic Activity Assay	115
5.2.7.6 Kinetic Studies of the Conjugates.....	116
5.3 Results and Discussions.....	116
5.3.1 Conjugations of Mutant EG IIIs to the Photo-Responsive Polymers.....	116
5.3.2 Thermo-Responsive Activity Changes of the Conjugates	119
5.3.3 Photo-Responsive Activity Changes of the Conjugates	125
5.3.4 Photo-Responsive Activity Changes of EG III – Azobenzene (AZ) Conjugate.....	131
5.3.5 Photo-Switching Hydrolysis of Cotton Cloth by the Conjugates	132
5.3.6 Temperature-Responsive Activity Changes of the Immobilized Conjugates....	137
5.3.7 The Effect of Addition of Free Polymer on Switching Activity	139
5.3.8 Photo-Responsive Activity Changes of the Immobilized Conjugates.....	142
5.3.9 Cyclic Switching of the Activity	144
5.3.10 Mechanism Analysis of the Thermo- and Photo-Response	150
5.4 Conclusions.....	154
CHAPTER 6 CONCLUSIONS AND RECOMMENDATIONS.....	157
6.1 Conclusions.....	157
6.1.1 Conclusions of Photo-Responsive Polymer Research.....	157
6.1.2 Conclusions of SA-Photo-Responsive Polymer Conjugate Research.....	158
6.1.3 Conclusions of EG III - Photo-Responsive Polymer Conjugate Research.....	159
6.2 Recommendations for the Future Research.....	162
6.2.1 Improvement of the Conjugate.....	162
6.2.1.1 Switching Response	162
6.2.1.2 Conjugation Reaction Efficacy on the Yield.....	163
6.2.2 Practical Process Using Our Photo-Switchable EG III.....	164
6.2.3 Application of Our Methodology	165
6.2.4 Oppositely Photo-Responsive Polymers and Hydrogels	166
BIBLOGRAPHY	167

LIST OF FIGURES

<i>Number</i>	<i>Page</i>
Figure 1.1. Typical photochromes used for photo-switchable biomolecules.	4
Figure 1.2. Methods for tailoring reversible photo-switchable biomolecules.	6
Figure 1.3. Schematic illustration of photo-responsive phase transition of polymer.	15
Figure 1.4. Schematic molecular model of endoglucanase III (EG III).....	22
Figure 1.5. Rationale of photo-switchable protein.....	27
Figure 2.1. Scheme of synthesis of photo-responsive monomer (AZAA and AZAAm)	31
Figure 2.2. Scheme of synthesis of photo-responsive polymer (DMAA and DMAAm)	32
Figure 2.3. Scheme of vinylsulfonation of DMAA and DMAAm	35
Figure 2.4. UV/VIS spectra of DMAA	38
Figure 2.5. UV/VIS spectra of DMAAm	39
Figure 2.6. Effect of photo-irradiation on the phase transition temperature of DMAA and DMAAm.....	40
Figure 2.7. Effect of photo-irradiation and azobenzene content on the LCSTs of DMAA and DMAAm.	42
Figure 2.8. Speculated explanation of the opposite photo-responses of DMAA and DMAAm.....	43
Figure 2.9. Effect of polymer concentration on the LCSTs of DMAA and DMAAm. ...	45
Figure 2.10. Effect of salt concentration on the LCST of DMAA and DMAAm.	46
Figure 2.11. Photo-induced phase transition of DMAA and DMAAm.	48
Figure 2.12. Effect of photo-irradiation and azobenzene content on the LCSTs of DMAA and DMAAm in the EG III buffer.	49
Figure 2.13. Effect of Mw (molecular weight) on PT (photo-responsive temperature) and AZ (azobenzene content) of DMAA and DMAAm.....	50

Figure 2.14. Effect of AZ (azobenzene content) on PT (photo-responsive temperature) and Mw (molecular weight) of DMAA and DMAAm.....	52
Figure 3.1. Specific conjugation of a photo-responsive polymer to a streptavidin (SA).....	59
Figure 3.2. Scheme of purification of the conjugate.....	61
Figure 3.3. Specific conjugation of an azobenzene to a streptavidin (SA).	62
Figure 3.4. Temperature responsive biotin-binding assay.....	64
Figure 3.5. Photo-responsive biotin-binding assay	65
Figure 3.6. 3-D molecular structure model of streptavidin (SA).....	67
Figure 3.7. Effect of temperature on biotin-binding activity of E116C-DMAA and E116C-DMAAm conjugates containing free polymers.....	69
Figure 3.8. Effect of incubation time and temperature on biotin-binding capacity of E116C-DMAA conjugate containing free polymer.....	70
Figure 3.9. Effect of incubation time and temperature on biotin-binding capacity of E116C-DMAAm conjugate containing free polymer.....	71
Figure 3.10. Effect of incubation time and temperature on biotin-binding capacity of E116C.....	72
Figure 3.11. Effect of thermal cycling on biotin-binding capacity of E116C conjugates containing free polymer.....	74
Figure 3.12. Effect of thermal cycling on biotin-binding capacity of S139C conjugates containing free polymer.....	75
Figure 3.13. Effect of thermal cycling on biotin-binding capacity of the purified E116C conjugates.....	76
Figure 3.14. Effect of addition of free polymer on biotin-binding capacity of the purified conjugates.....	78
Figure 3.15. Effect of temperature and photo-irradiation on biotin-binding activity of E116C-DMAA conjugate containing free polymer.....	79

Figure 3.16. Effect of temperature and photo-irradiation on biotin-binding activity of E116C-DMAAm conjugate containing free polymer.....	80
Figure 3.17. Photo-cycling effect on biotin-binding activity of E116C-DMAA conjugate containing free polymer.	82
Figure 3.18. Photo-cycling effect on biotin-binding activity of E116C-DMAAm conjugate containing free polymer.	83
Figure 4.1. Catalytic activity assay of EG III using o-nitrophenyl- β -D-cellobioside (ONPC) as a substrate.	91
Figure 4.2. Catalytic activity assay of EG III using hydroxyethyl cellulose (HEC) as a substrate.	93
Figure 4.3. Molecular model of endoglucanase III (EG III).	95
Figure 4.4. SDS-PAGE of wild type (WT) endoglucanase III (EG III) and the mutants.	97
Figure 4.5. Comparison of catalytic activities of EG III mutants.....	98
Figure 4.6. SDS-PAGE of EF III-F (fluorescein) conjugates.....	99
Figure 4.7. UV/VIS spectra of EG III-F conjugates.	100
Figure 4.8. Lineweaver-Burk plot.....	101
Figure 5.1. Scheme of synthesis of DMAA-AA and DMAAm-AA.....	106
Figure 5.2. Specific conjugation of a VS-terminated polymer to an EG III mutant.....	108
Figure 5.3. Specific conjugation of an AA-terminated polymer to an EG III mutant. ..	109
Figure 5.4. Biotinylation of Polymer-EG III conjugate.	110
Figure 5.5. SDS-PAGE of EG III-DMAA and EG III-DMAAm conjugates.....	115
Figure 5.6. The LCSTs of DMAA and DMAAm.	117
Figure 5.7. Thermo-responsive activity changes of the conjugates.....	120
Figure 5.8. Thermo-responsive activity changes of the conjugates.....	121
Figure 5.9. Thermo-responsive activity changes of the conjugates.....	122
Figure 5.10. Photo-responsive LCST changes of DMAA and DMAAm.	124

Figure 5.11. Effects of temperature and photo-irradiation on catalytic activity of N55C-DMAA conjugate toward ONPC.	125
Figure 5.12. Effects of temperature and photo-irradiation on catalytic activity of N55C-DMAAm conjugate toward ONPC.	126
Figure 5.13. Effects of temperature and photo-irradiation on catalytic activity of N55C-DMAA conjugate toward HEC.	127
Figure 5.14. Effects of temperature and photo-irradiation on catalytic activity of N55C-DMAA conjugate toward HEC.	128
Figure 5.15. Photo-responsive relative activity changes of N55C-DMAA and N55C-DMAAm conjugates.	131
Figure 5.16. UV/VIS spectra of EG III-AZ conjugates.	132
Figure 5.17. Photo-responsive relative activity changes of N55C-AZ and S25C-AZ conjugates.	133
Figure 5.18. Photo-responsive relative activity changes of the N55C conjugates toward cotton cloth.	134
Figure 5.19. Thermo-responsive activity changes of the conjugates immobilized on magnetic beads.	138
Figure 5.20. Thermo-responsive activity changes of the conjugates immobilized on magnetic beads.	139
Figure 5.21. Effect of addition of free polymer on the shut-off activity of the conjugates immobilized on magnetic beads.	140
Figure 5.22. Photo-responsive activity changes of the conjugates immobilized on magnetic beads.	141
Figure 5.23. Sequential thermo-switching of activity of N55C-DMAA and N55C-DMAAm conjugates.	143
Figure 5.24. Sequential photo-switching of activity of N55C-DMAA and N55C-DMAAm conjugates.	144

Figure 5.25. Effect of thermal cycling on the activity of N55C, N55C-DMAA and N55C-DMAAm conjugates.....	145
Figure 5.26. Effect of photo-cycling on the activity of N55C, N55C-DMAA and N55C-DMAAm conjugates.....	146
Figure 5.27. Retained activities of N55C, N55C-DMAA and N55C-DMAAm conjugates as a function of the number of thermal cycling.....	147
Figure 5.28. Retained activities of N55C, N55C-DMAA and N55C-DMAAm conjugates as a function of the number of photo-cycling.	148
Figure 5.29. Kinetic parameters of the conjugates toward ONPC in response to temperature and photo-irradiation.	150
Figure 5.30. Kinetic parameters of the conjugates toward HEC in response to temperature and photo-irradiation.	151
Figure 6.1. EG III reactor.	163

LIST OF TABLES

<i>Number</i>	<i>Page</i>
Table 2.1. Characteristics of DMAAm and DMAA	37
Table 2.2. Characteristics of DMAA and DMAAm for Conjugation to EG III.....	53
Table 2.3. Percentages of the active VS in DMAA and DMAAm	54
Table 3.1. Polymer/streptavidin (SA) ratios of the purified conjugates.....	68
Table 4.1. Expression yields of the endoglucanase III (EG III) mutants.	96
Table 4.2. Comparison of kinetic parameters of EG III mutants toward o-nitrophenyl- β-D-cellobioside (ONPC).	102
Table 4.3. Comparison of kinetic parameters of EG III mutants toward hydroxyethyl cellulose (HEC).	103
Table 5.1. Conversion of EG III-DMAA or DMAAm Conjugate.....	116
Table 5.2. Degrees of biotinylation of the conjugates.....	135
Table 5.3. Immobilized amount of the conjugates and WT EG III.	136

LIST OF ABBREVIATIONS

AIBN	2,2'-azoisobutyronitrile
DMF	dimethylformamide
THF	tetrahydrofuran
DVS	divinyl sulfone
DMA	N,N-dimethylacrylamide
MEO	mercaptoethanol
DTNB	5,5'-thiobis (2-nitrobenzoic acid)
EDTA	ethylenediaminetetraacetic acid
NIPAAm	N-isopropylacrylamide
PNIPAAm	poly(N-isopropylacrylamide)
TCEP	Tris-(2-carboxyethyl) phosphine (HCl)
HABA	4'-hydroxyazobenzene-2-carboxylic acid
AZ-MI	4-phenylazomaleinanyl
AZ-F	fluoresein maleimide
Da	Dalton, unit of molecular weight (gram/mol)
MW	molecular weight
M _w	weight average molecular weight
M _n	number average molecular weight
LCST	lower critical solution temperature
GPC	gel permeation chromatography
VS	a vinyl sulfone group
AZ	azobenzene
AZAA	phenylazophenylacrylate
AZAAm	phenylazophenylacrylamide
DMAA	DMA-co-AZAA copolymer
DMAAm	DMA-co-AZAAm copolymer
PT	photo-responsive temperature
ONPC	o-nitrophenyl-β-cellobioside
HEC	hydroxyethyl cellulose
PHBAH	p-hydroxybenzoic acid
PB	sodium phosphate buffer
AB	sodium acetate buffer
DTT	dithiothreitol
WT	wild type
CBB	coomasie brilliant blue
HABA	4'-hydroxyazobenzene-2-carboxylic acid

ACKNOWLEDGMENTS

I would like to gratefully thank my advisors: Professor Allan S. Hoffman and Professor Patrick S. Stayton, who guided me throughout this Ph.D. research work. Their continuous support and encouragement during the past three and half years helped me accomplish my educational goal. I was attracted and inspired by them not only because of their vast knowledge of science and the fascinating fields of Biomaterials and Molecular Bioengineering, but also because of their attitude and consideration to people as scientists and educators.

I also appreciate my Supervisory Committee: Professor Hoffman, Professor Stayton, Professor Francois Baneyx, Professor Viola Vogel and Professor Paul B. Hopkins, for their helpful advise and suggestions on my research progress. Special thanks to Professor Hoffman, Stayton and Baneyx for reading this dissertation and providing valuable comments.

I am also grateful to Dr. Edmund Larenas and Dr. Tim Fowler at Genencor International Inc., for providing EG III cloned gene, expressing the mutants and providing lots of suggestions and information about EG III. I also owe Dr. Deb McMillen at University of Oregon for N-terminus sequencing of EG III. Thanks go to Dr. Zhongli Ding and Dr. Richard To, great collaborators who not only assisted me with their experiences in protein conjugation and protein engineering but also provided significant suggestions. I also sincerely appreciate to my colleagues. Thanks to Chantal Lackey, Robin Fong, Todd McDevitt, Hyre David, Kjell Nelson, Niren Murthy, Charles Cheung, Chad Brown, Monica Woodward, Calvin Hu, Dr. Natalie Winblade, Dr. De Tapas, Dr. Fiona Black and all the other friendly members of Hoffman and Stayton groups, for their full-hearted assistance, stimulating discussions. I would like to express my gratitude to the National Institutes of Health for sponsoring this research (Grant No. GM53771-02 to 04).

Finally, I would like to thank my family, especially my wife, Kaori, and my daughter, Yuki, for their persistent support, unconditional love, and continuous understanding. In addition, I am grateful to my parents in Japan who always support us and pray for my success.

DEDICATION

I wish to dedicate this thesis to my wife, my daughter, and my parents

CHAPTER 1 INTRODUCTION

1.1 OBJECTIVES

There are diverse and numerous needs for controlling protein functions, such as specific molecular recognition or catalytic activities, by external stimuli in the fields of bioprocesses (food, detergent, paper, and fabrics), diagnostics, therapeutics, and bioelectronics. Among various stimuli, light is an ideal stimulus, because, in general, light doesn't influence protein functions like temperature and pH, and it is easy and quick to apply and control.

The principal goal of this research is to provide a fundamental design strategy to create photo-switchable proteins using site-specific conjugation of photo-responsive polymers to proteins. Of central importance will be to achieve complete on / off switching of protein functions by UV and visible (VIS) light irradiation.

In this chapter, I will provide background and literature review related to photo-control of biomolecular functions, and explain our strategy to develop novel photo-switchable proteins.

1.2 PHOTO-RESPONSIVE PROCESSES IN BIOLOGY

Biological systems have evolved various kinds of sophisticated photo-responsive systems, such as photo-movement, photo-morphogenesis, photosynthesis, and vision [1-4]. In these systems, optical signals are recorded and transduced as physicochemical events.

The common feature to all these systems is that they contain photochromic molecules (chromophores) embedded in biomolecular matrices. The absorbed light activates a series

of chemical transformations in the chromophore (photo-isomerization), which controls the conformation and assembly of the surrounding biomembranes or proteins. These photo-induced changes lead to subsequent biochemical reactions. It is worthwhile to mimic these processes and to apply them to the design of photo-switchable biomolecules in which the physicochemical properties can be controlled reversibly by photo-irradiation. Referring to biological photo-responsive systems, the artificial photo-switchable molecules should be composed of at least two key elements. One is a photo-sensitive element, which captures optical signals and converts them to physicochemical signals, and another is a functional element, which senses the physicochemical signals and exhibits new output functions.

1.3 PHOTOCROMES

The photochemistry of photochromic materials has been extensively researched in the past four decades [5-8]. These materials can be transformed to other isomers under photo-irradiation, which return to the initial state either thermally or photochemically [5]. The discrete photo-isomeric states exhibit distinct spectral and chemical features. Various classes of reversibly photo-isomerizable compounds are commercially available, including isomerization across double bonds (stilbenes, azobenzenes, indigo, and thioindigo derivatives), $(4n+2)\pi$ -electron ring closures and openings (fulgides, spiropyran, and spirooxazines), $(4n)\pi$ -electron ring closures and openings (oxiranes and aziridines), light-induced tautomerism (N-salicylideneanilines, aniles, aci-nitro compounds), and cycloaddition reactions.

Figure 1.1 shows typical photochromes, which have been used extensively in the research of photo-switchable polymers and biomolecules. Azobenzene undergoes trans to cis photo-isomerization under UV light, which increases the dipole moment from 0 to 3.0 Debye, and also induces geometrical structure changes. Spiropyran generates zwitter ions upon UV light, while it is nonionic under VIS light. Triphenylmethaneleuco hydroxide

(TML) dissociates into a cation under UV light, which results in the electrostatic repulsion among the TMLs. Fulgide isomerizes between ring-closed and -opened structure by photo-irradiation. Since these isomerizations are always accompanied by certain changes in physical and chemical properties of the chromophores, they have been utilized to induce conformational and functional changes in polymers and biomolecules coupled with these photochromes.

1.4 PHOTO-CONTROL OF CONFORMATIONS AND FUNCTIONS OF BIOMOLECULES

1.4.1 CLASSIFICATION OF PHOTO-SWITCHABLE BIOMOLECULES

Photo-switching of biomolecular functions, such as enzymatic reaction or specific molecular recognition and binding, have attracted broad interests of many researchers [9-31]. Photo-switching can be utilized for various applications, such as photo-controlled bioreactors, photo-triggered targeted drug delivery systems, macromolecular light signal amplification devices and photo-controlled separation / recovery systems

In general, there are two fundamental classes of photo-switchable biomolecules that have been developed [24]. They are single-cycle and multi-cycle photo-switches.

Single-cycle photo-switches are activated by the removal of the protective groups upon photo-irradiation to restore the biologically active structure [32, 33]. This is a non-reversible reaction. Light-triggered activation of enzymes [34-36] and important biological components such as AMP [37], c-GMP [38], ATP [39], and InP_3 [40], and also ion-chelators formations [41-43] have been investigated by this approach.

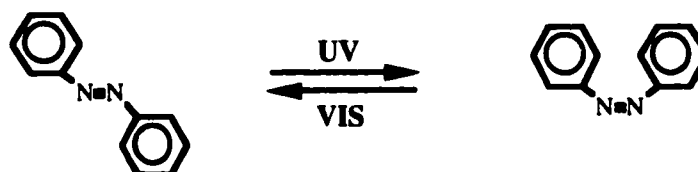
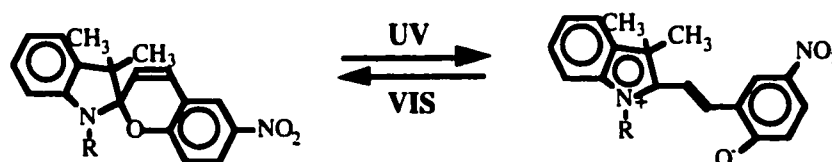
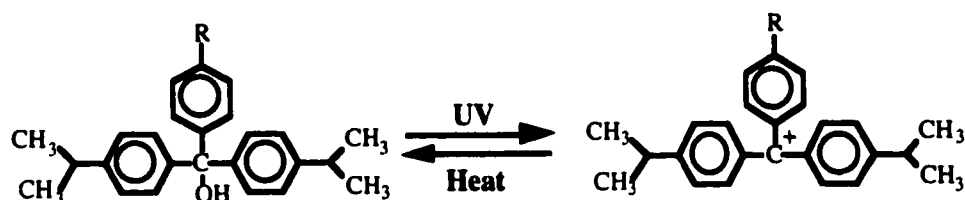
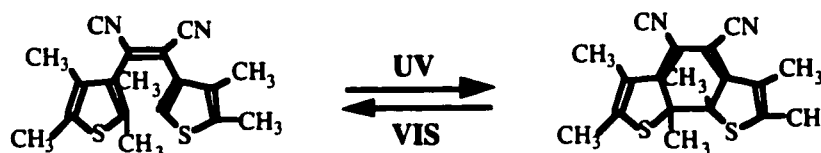
1. Trans - cis isomerization**azobenzene****2. Zwitter ion formation****spiropyran****3. Ionic dissociation****triphenylmethane/leuco hydroxide****4. Ring-formation and ring-cleavage****fulgide**

Figure 1.1. Typical photochromes used for photo-switchable biomolecules.

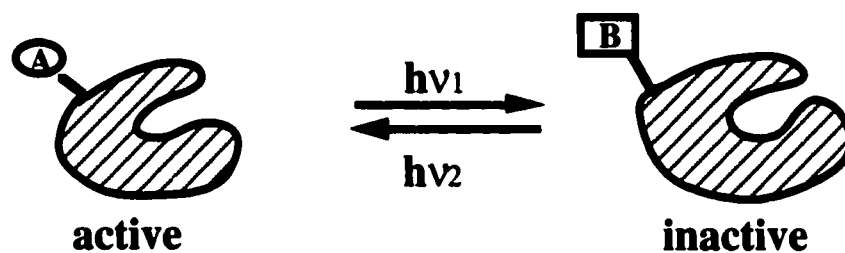
Multi-cycle photo-switches can work reversibly between active (on) and inactive (off) states by specific photo-irradiation. Three kinds of methodologies for tailoring multi-cycle photo-switches have been investigated so far, and are summarized in Figure 1.2 [24]. The first method is the chemical modification of biomolecules by photochromes. In state A, the photochrome doesn't disturb the biomolecule or its active site. Upon photo-isomerization of the photochrome to state B, the structure is perturbed and the biomolecule is deactivated. Cyclic activation/deactivation of the biomolecular functions can be switched by reversible photo-isomerization.

The second method is provided by the entrapment of biomolecules in the photo-responsive environments. In state A, the matrix is permeable to the substrate or the ligand, and the biomolecule can perform its function. In photo-isomerized state B, the matrix becomes nonpermeable to the substrate or the ligand and the entrapped biomolecule is switched off. The diffusion of the substrate is controlled by light.

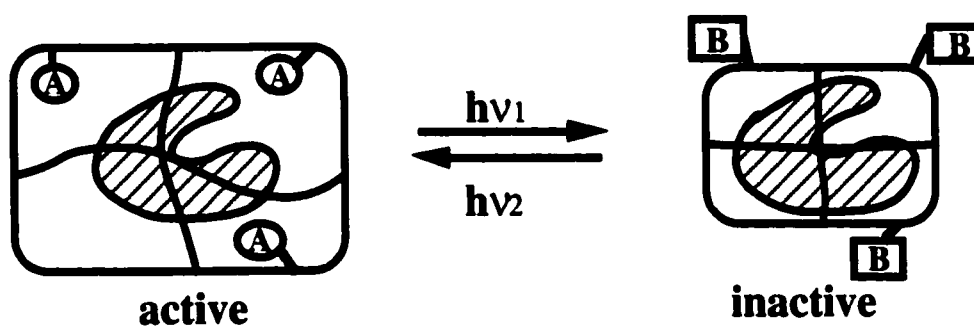
The third method involves photo-isomerizable low molecular weight compounds such as inhibitor or cofactor, which are recognized by proteins. In state A, the inhibitor blocks the active site of the protein and the biological function is switched off. In the complementary state B, the structure of the inhibitor has changed, and it can't bind to the protein, resulting in the active state of the protein.

In our project, the reversible multi-cycle photo-switches combines the concepts of the first and second methodologies in Figure 1.2, i.e., chemical modification and immobilization in polymer matrix, to create more effective photo-switches. The literature on photo-controlled structures and functions of biomolecules are reviewed briefly in the following sections.

1. Chemical Modification



2. Physical Immobilization in Photoresponsive Environment



3. Photoresponsive Inhibitor or Cofactor

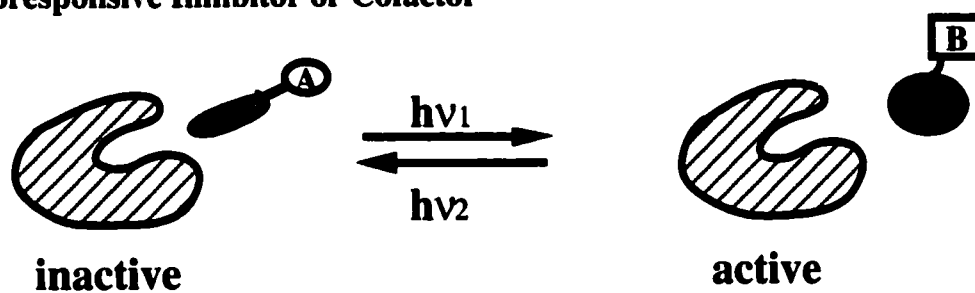


Figure 1.2. Methods for tailoring reversible photo-switchable biomolecules.

(modified from [24])

1.4.2 PHOTO-CONTROL OF CONFORMATIONS OF POLYPEPTIDES

Polypeptides are synthetic analogs of proteins. There have been many reports on the reversible photo-control of the secondary structure of polypeptides, such as α -helix, β -sheet, and random coil.

Azobenzene-modified poly(L-glutamate) [44, 45] and poly(L-lysine) [46, 47] demonstrated transitions between β -sheet and random coil, or α -helix and random coil associated with the photo-isomerization of azobenzene. These conformational transitions were ascribed to the different geometries and polarities of azobenzene units in the different photo-isomerized states, *cis* and *trans*. The planar structure and hydrophobic nature due to the lower dipole moment in the *trans* form contributed to the stabilization of organized structures.

Such photo-regulation of polypeptides was also accomplished with spiropyran-modified poly(L-glutamate) [48] and poly(L-lysine) [49]. Spiropyran generates twitter ions (merocyanine) and becomes more hydrophilic under UV irradiation, which disturbs the organized structure. Thus, in the dissociated state, the polypeptides underwent transitions from α -helix to random coil.

Triphenylmethanloicohydroxide (TML) was also used as a photochrome to be coupled with poly (L-glutamate) [50]. It exhibited α -helix to random coil transition under UV light, which was induced by the electrical repulsion among the generated charges by photo-induced dissociation of TML.

In these systems, the photo-isomerizations of the photochromes attached to polypeptides have triggered pronounced structural transitions. These conformational changes might be utilized to elicit changes in specific binding affinity or catalytic activity in real proteins, which are composed of such secondary structures.

1.4.3 PHOTO-CONTROL OF SPECIFIC BINDING PROCESSES OF PROTEINS

Molecular recognition and specific binding are fundamental functions of biomolecules. They play a primary role in enzymatic catalysis, transport of specific substrates across membranes, and storage of compounds. Photo-control of molecular binding events was reported by Willner *et al.* [12, 51]. Lectin concanavalin A (Con. A) was modified by thiophenefulgide or nitrospiropyran. Con. A is a globular lectin that binds to α -D-mannopyranose. The affinity was weakened in the ring-opening state of fulgide, or in the dissociated state of spiropyran (the association constant K_a decreased by 33-36 %). The different association properties were attributed to the enhanced perturbations of the structure of Con. A, and especially its active site by the photo-isomeric states.

A more sophisticated system was reported by Harada *et al.* [52]. Molecular recognition between antigen and antibody was controlled by light using photo-isomerizable antigen. They prepared a monoclonal antibody against a hapten, Glu-(trans-azobenzene Ala)-Gly₂. The trans state hapten exhibited high affinity for the antibody, whereas the cis state hapten resulted in poor affinity for the antibody. Uptake and release of the hapten from the antibody were accomplished reversibly and completely by UV/VIS photo-irradiation. Antibodies recognize antigens very selectively. Thus, these results suggest that the photo-isomerization at the critical position for the specific molecular recognition expands the photo-responsive affinity change significantly.

1.4.4 PHOTO-CONTROL OF CATALYTIC ACTIVITIES OF ENZYMES

Direct conjugations of photochromes to enzymes have been investigated for developing photo-switchable enzymes (Figure 1.2-1). In this system, one photo-isomeric state preserves the conformation of its active site, while another photo-isomeric state distorts the protein structure by either electrostatic interaction between isomer and protein, steric distortion, or disruption of hydrogen bonding.

The first attempt of this method was reported by Montagnoli *et al.* [19, 20]. They prepared diazo-modified aldolase, which exhibited little difference in their catalytic properties. Willner *et al.* reported the conjugation of azobenzene to lysine residues in papain [21]. The trans isomer displayed higher activity than the cis isomer (2.75 times) towards the hydrolysis of N-benzyl-D,L-arginine-nitroanilide. Kinetic analyses showed similar V_{\max} (maximum velocity) values and different K_m (Michaelis constant) values between the two photo-isomeric states. These results suggested that the binding of the substrate to the enzyme active site was inhibited, but the catalytic function of the active center was not influenced by the photo-isomerization.

Similar approaches were reported for a series of spiropyran-modified enzymes [25-28]. Spiropyran units were covalently linked to the lysines of α -amylase, β -amylase, urease, β -glucosidase, and α -chymotrypsin. The catalytic activities of α -amylase and β -amylase were decreased, and those of urease, β -glucosidase, and α -chymotrypsin were increased by UV irradiation. These opposite photo-responses were ascribed to the affinity changes of the substrates with the enzymes by photo-induced K_m changes. The photo-isomerization changed the hydrophobicity of the enzyme, which influenced the affinity. The hydrophilic substrates were easy to bind to enzymes in the dissociated state of spiropyran, while hydrophobic substrates bound more in the undissociated state of spiropyran. The highest photo-switchable activity difference was observed for β -amylase, in which the activity in the dissociated state was 13 % of that in the undissociated state. It could be speculated that the conjugated position in β -amylase was the most critical for influencing the activity.

These photo-switchable enzymes have demonstrated photo-responsive catalytic activity changes. However, most of them demonstrated little ability to affect the catalytic activity when photo-irradiated. Moreover, even in the off state, they still retain activity. One reason might be that the photo-sensitivities of the photochromes were not necessarily perfect. For example, azobenzene is expected to undergo photo-isomerization from trans

to cis form under UV irradiation, which increases the dipole moment and allows the molecule to become more hydrophilic; however, there is still some trans form remaining even upon UV irradiation. Other possible reasons might be that the connected positions were not placed at the critical positions for controlling the biomolecular functions, or the amount of photochromic changes were not enough to turn off the function completely. Therefore, we have to consider these points for designing novel photo-switchable enzymes to improve the photo-responses.

1.4.5 PHOTO-CONTROL OF THE ABSOLUTE ZERO CATALYTIC ACTIVITY

The control of the absolute zero activity in “off” state is crucial for some applications, because, for example, enzyme reaction cascades will amplify even only a small amount of activity to an enormous production in the practical situation. To date, there have been only three reports that have achieved complete off state of enzymatic activity by photo-regulation.

The first complete “off” state of enzymatic activity by photo-regulation was demonstrated by Willner *et al.* [31]. They immobilized α -chymotrypsin physically in three different kinds of photo-responsive polymer hydrogels (azobenzene, spiropyran, and TML-modified polyacrylamide hydrogel), and regulated the enzymatic activity by controlling the substrate diffusion through the gel matrix by light. The gels showed expanding / shrinking phase transitions in response to UV/VIS light irradiation. Hydrolysis activity of α -chymotrypsin was completely switched off in the shrunken state of the gels. And it became active in the expanded state of the gels. In these systems, they did not control the real enzymatic activity directly, but controlled the permeability of the substrate into the caged enzyme physically. These results suggest that the photo-responsive polymers, which exhibit large conformational changes around the enzymes and regulate the physical access of the substrate, might be one of the key factors to achieve the zero activity.

Hohsaka *et al.* reported complete on/off control of catalytic activity using photo-isomerizable antigen/antibody system [16]. A monoclonal antibody against trans-azobenzene-modified-NAD⁺ cofactor was prepared. Coupling of NAD⁺/NADH-dependent enzymes, alcohol dehydrogenase and diaphorase, with the antibody provided a mechanism for controlling the availability of the cofactor. The cofactor in the trans state was associated with the antibody, and the activities of the two enzymes were completely blocked. Photo-isomerization of azobenzene to the cis form induced the release of cofactor from the antibody; thereby the enzymes were switched on. In this indirect approach, they achieved absolute zero catalytic activity of the enzymes. These results may be due to the sophisticated molecular recognition ability of the antibody, which can distinguish even a small change of the antigen. This suggests that the modification at the critical position for the molecular recognition might be another key strategy to achieve the zero activity.

Photo-switchable enzymes introduced above were developed by random chemical substitution of the proteins by photochromes. Site-specific incorporations of photochromes into an enzyme were investigated by Ueda *et al.* [53]. They employed a semisynthetic method for the preparation of a photo-isomerizable mutant of phospholipase A. The mutants were synthesized by Edman degradations and subsequent reconstitutions by stepwise synthesis of the tripeptide including azobenzene-phenylalanine and coupling to the original enzyme. The mutant in the trans form of azobenzene didn't exhibit any hydrolytic activity towards the lipid hydrolysis. On the contrary, the mutant in the cis form retained about 10 % of the native activity. The CD spectra have revealed that α -helical content in the cis isomer was substantially higher than that in the trans isomer. The enzyme recognition site adopted the α -helical conformation and was the active counterpart for the lipid hydrolysis. This suggested that, in the trans form, the recognition site was perturbed and enzyme activity was blocked. Upon photo-isomerization to the cis isomer, the recognition site was reconstituted and the enzyme was switched on. They did not compare the effect of the conjugated positions of the photochromes on the activity.

However, this result indicated that, if the conjugated position is critical for controlling enzyme activity, complete zero activity could be achieved. Therefore, this suggests again that the site-directed conjugation of photochromes to the appropriate position for the enzyme activity might improve the response of the photo-switches significantly, retaining zero activity in its off state.

1.5 PHOTO-RESPONSIVE POLYMER

One of the key components of our research is a photo-responsive polymer. I will review the literature related to photo-responsive polymers in the following sections:

1.5.1 STIMULI-RESPONSIVE POLYMER

Some water-soluble polymers undergo phase transition in aqueous solution at a critical point upon small changes in the environment, such as temperature, pH, solvent, chemical, electric field, or light. These polymers are called stimuli-responsive or “smart” polymers [54, 55].

The phase transition is the result of changes in the interactions between water and the polymer. For example, temperature-responsive polymers show phase separation at a critical temperature, which is called the lower critical solution temperature (LCST). At a temperature below the LCST, hydrogen bonding between the polymer and water is dominant for hydration. The hydrophobic components of the polymer are shielded from the bulk water by a layer of ordered water molecules, called “ice-berg water” [56]. When the temperature is raised, the hydrogen bonds between the water and polymer chains become weaker, and the iceberg water becomes less stable. The breaking of hydrogen bonds contributes to a positive enthalpy change ($+\Delta H$) and the melting of the iceberg water results in a positive entropy change ($+\Delta S$). The increase of the hydrophobic interactions between the hydrophobic components of the polymer contributes an additional positive entropy change on phase separation [57]. Thus, at the LCST, phase

separation is thermodynamically favored ($\Delta G < 0$) and the polymer collapses and aggregates. For the other stimuli-responsive polymers, the stimuli, which induce the changes in the hydrophobicity of the polymers, are different; however, the mechanism of the resultant phase transitions are common.

1.5.2 PHOTO-RESPONSIVE POLYMER

Polymers having photochromes in the side chain or the backbone main chain have been investigated to demonstrate the photo-responsive conformational changes of polymers.

Poly(methacrylic acid) with pendant azobenzene groups showed an increase in viscosity under UV irradiation in aqueous solution [58]. The trans to cis photo-isomerization of azobenzene was considered to decrease the hydrophobic interaction between azobenzene moieties, allowing the polymer coil to expand. Polyamides with rigid main chains and azobenzene groups in the polymer backbone also have been investigated [59, 60]. These polymers showed reversible viscosity changes as much as 60 % by alternately irradiated UV/VIS light in N,N-dimethylacetamide. Azobenzene undergoes a large structural change during isomerization. The distance between the 4 and 4' carbons decreases from 9.0 to 5.5 Å accompanied by a trans to cis transition [61]. This configurational change was expected to induce the conformational changes in the polymer chains. Before the photo-irradiation, the polymer had a rod-like conformation. The isomerization from trans to cis form kinked the polymer main chain, resulting in a compact conformation and a decrease in the viscosity.

Electric repulsion between photo-generated charges was also used as the driving force for the conformational changes. Poly(N,N-dimethylacrylamide) having pendant TML groups demonstrated a viscosity increase from 0.6 to 1.6 dl/g in methanol upon UV irradiation [62]. After the light was shut off, the viscosity returned to the initial value. Thus, the photo-induced electrostatic repulsion resulted in the expansion of the polymer conformation, and increased the viscosity.

The effect of photo-induced twitter ion formation was investigated using poly(methyl methacrylate) (PMMA) with spiropyran pendant groups [63]. The polymer showed photo-induced viscosity decrease in benzene (17 %). This was explained by the argument that the photo-generated merocyanine was solvated by the ester group of PMMA, and that this intramolecular solvation competed with the solvation by benzene, resulting in the shrinkage of the polymer. Similar phenomenon was observed with poly(methacrylic acid) with pendant spiropyran in methanol [64].

These polymers exhibited photo-induced viscosity changes mostly in organic solvents. Further, these conformational changes might not be large enough for switching applications. To develop molecular switches by means of protein conjugation, we need larger and sharper conformational changes of polymers in aqueous systems.

Since photo-responsive polymers change their properties in proportion to the number of photons they absorb, one method to increase the photo-sensitivity is to incorporate more photochromes in the polymer. Another method is to introduce an amplification mechanism into the system. A convenient way to employ the second method is to utilize the photo-responsive phase transition of polymers. At a temperature close to the phase transition temperature, the polymer is in an unstable state, and thereby a small perturbation may bring about a large effect on it. When such a system is perturbed by a photo-isomerization, the absorption of a few photons will trigger a large property change. Figure 1.3 shows a schematic illustration of this concept. When the polymer has a LCST at T_a and T_b for isomer A and isomer B, respectively, the solubility of the polymer can be changed by light irradiation isothermally at the temperature between T_a and T_b . In this system, a few photons can induce a marked change to cause the phase separation [66].

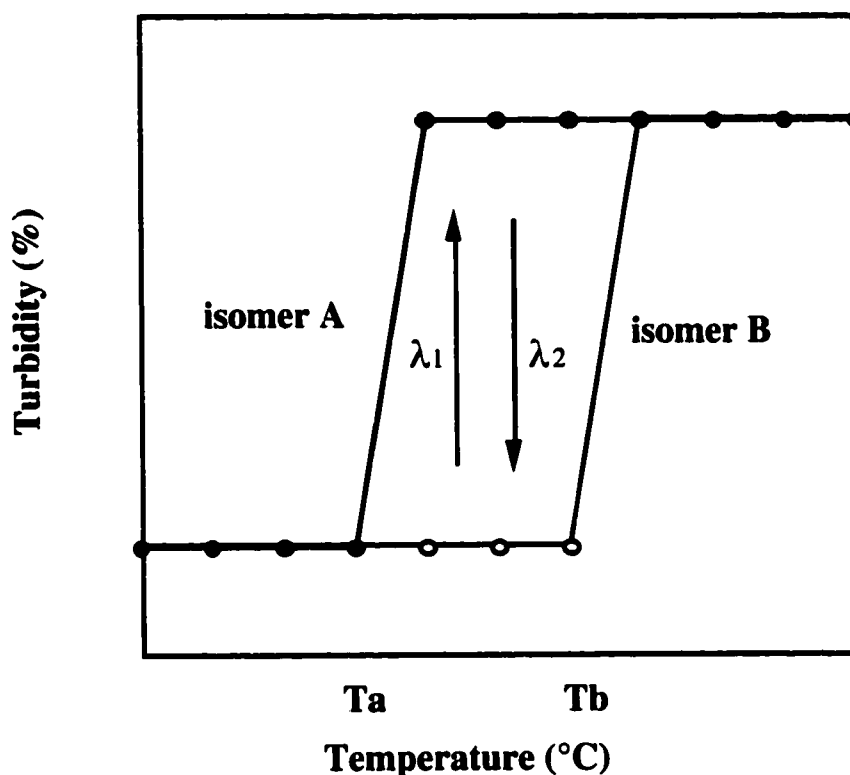


Figure 1.3. Schematic illustration of photo-responsive phase transition of polymer.

(modified from [66])

There have been several reports of photo-responsive polymers, which can be used in aqueous systems [65-68]. These polymers exhibited temperature differences between their lower critical solution temperatures (LCSTs) when under UV vs. visible (VIS) light irradiations. The first aqueous photo-responsive polymer, N-isopropyl acrylamide (NIPAAm)-co-N-4-phenylazophenyl acrylamide (AZAAm) copolymer, was described by Irie *et al.* [65]. However, the photo-response was restricted to a narrow range of composition and temperature. Kröger *et al.* [66] reported the largest differences in LCST

detected in aqueous solution using N,N-dimethyl acrylamide (DMA)-co-4-phenylazophenyl acrylate (AZAA) copolymer. This copolymer was the combination of a more hydrophilic monomer (DMA vs. NIPAAm) with a very hydrophobic monomer (AZAA). This reduced the LCST of the copolymer significantly and permitted wider photo-responsive temperature ranges. In addition, for the photo-response, it was possible to incorporate a higher content of azobenzene in this copolymer than NIPAAm copolymers, and still retain aqueous solubility; this enhanced the magnitude of the photo-response. Since the isomerization wave length of azobenzene (350 nm) does not damage proteins [69, 70], we have incorporated this group into our polymers for site-specific conjugation to proteins for application as photo-switchable proteins.

However, these polymers became more hydrophilic under UV irradiations due to the increase of the dipole moment of azobenzene in its *cis* form. In using these polymers for photo-switchable proteins, we have to irradiate with UV light continuously so as to keep the soluble state of the conjugated proteins. This is not practical for many of the applications. Thus, the opposite photo-responsive polymer, which can become hydrophobic under UV light irradiation, is also desired for tailoring photo-switchable biomolecular devices.

1.5.3 OPPOSITE PHOTO-RESPONSIVE POLYMER

Menzel *et al.* reported the opposite photo-response for poly(N-ethyl-N-2-hydroxy ethyl)acrylamide modified by azobenzene derivatives at higher content of azobenzene [71]. When they incorporated more hydrophobic azobenzene derivatives into the polymer, the opposite photo-response started at lower azobenzene content. Irie *et al.* showed the normal photo-response of NIPAAm-co-AZAAm copolymer [65]. However, the photo-response disappeared above 3.6 mol % of AZAAm content. These results might be due to the packing effects of azobenzene at high azobenzene content. Azobenzene has self-assembling properties, making clusters in aqueous solution because of its hydrophobicity and π -electron interaction between benzene rings. This aggregate

might be destroyed by UV irradiation, because the *cis* form can not stack [72-74]. This breakage may induce release of individual azobenzene into the solution, and make the polymer more hydrophobic, because an azobenzene in the *cis* form is still hydrophobic in water. Therefore, if we incorporate higher contents of AZAAm, the reverse photo-response might be expected. When DMA is used as the counter part of the copolymerization with AZAAm, higher incorporations of azobenzene monomers may be possible keeping the LCST at proper temperatures for protein conjugates (30 – 40 °C), because DMA is more hydrophilic than NIPAAm.

Thus, in this research, we have synthesized two kinds of copolymers, DMA-co-AZAA copolymer (DMAA) and DMA-co-AZAAm copolymer (DMAAm), as photo-responsive polymers.

1.6 SITE-SPECIFIC CONJUGATION OF POLYMER TO PROTEIN

In order to control protein functions by means of phase transition of the conjugated polymers, the position of conjugation is an important factor. Thus, the conjugation should be performed in a site-specific manner. The chemistry for the conjugation of various chemicals to proteins has been developed intensively [75]. The target functional groups in protein for conjugation are limited. They involve amine groups on lysine and the N-terminus, carboxyl groups on glutamate, aspartate, and the C-terminus, phenol group on tyrosine, and thiol group on cysteine. Thiol groups on cysteines are good targets for specific conjugation, because the number of cysteines in wild-type protein is usually less than that of any other reactive group. Further, it is more nucleophilic than amines, thereby generally being the most reactive functional group on a protein. There are several groups reactive with thiols, such as maleimide, iodoacetamide, vinylsulfone, and acrylate groups. The specificity of the reaction is controlled by the pH of the conjugation solution. Since thiol-reactive reagents react rapidly at neutral pH, they can be reacted with thiols selectively in the presence of amine groups.

In our project, we have employed thiol/vinylsulfone (VS) specific reactions for the conjugation of photo-responsive polymers to proteins. Photo-responsive polymers have been synthesized to have a VS group at the end of the polymer by free radical polymerization using mercaptoethanol as a chain transfer reagent to make a hydroxyl terminus, which is subsequently converted to a VS group. On the other hand, a site-directed mutagenesis technique was utilized to construct genetically engineered proteins, which have a cysteine residue at the selected position. Since the conjugation site has to be located close to the active site or critical residues so that the conjugated polymer may exert its influence effectively on the active site, the position of the cysteine in the protein was selected based on the understanding of the structure-function relationship by considering the 3D-structure of the protein.

1.7 TARGET MODEL PROTEINS

Another key component of our research is a site-directed mutant protein. We have selected streptavidin (SA) as a model protein to develop a photo-switchable protein to control ligand-receptor specific recognition and binding. In addition, we have also selected endoglucanase III (EG III) as a model protein to create a photo-switchable enzyme where the catalytic activity is controlled by light.

1.7.1 STREPTAVIDIN (SA)

SA, a protein produced by *Streptomyces avidinii*, is a tetramer and shows a remarkably high affinity with the ligand, biotin ($K_d = 10^{-13}$ M), which is the highest known in nature [76–78]. This unusual interaction is utilized in various kinds of biological, clinical, and diagnostic processes. SA is one of the most widely utilized proteins in biotechnologies.

SA is an exceptionally stable protein. The binding efficiency to biotin is insensitive to pH changes in the range of 2 to 13 [79]. A native SA has a pI of 6.5, a relatively high molecular weight (Mw) (66 - 75 kDa) and can be converted to a lower-mass form (i.e. 60

kDa) by proteolytic digestion at both the N and C termini [80]. The truncated protein, called core SA, has a Mw of 53 kDa, a molecule size of 54 x 58 x 48 Å [81], and retains full binding activity.

SA is a good model protein because there is a convenient genetic engineering system and a high resolution crystal structure [81–84] available guiding the design of switching locations. The mechanism to induce this high affinity was also investigated and the structure-function relationship was elucidated. SA displays many common molecular recognition motifs. One of the strongest interactions related to biotin binding is hydrophobic and van der Waals interaction stemming from the aromatic side chains of Trp. The role of Trp for biotin-binding was investigated by site-directed mutagenesis method which convert Trp to Phe or Ala [85, 86]. It was indicated that these single amino acid conversions reduced the biotin binding affinity substantially.

SA does not have a cysteine in the primary sequence, and thus it is straightforward to employ genetically engineered side chains with thiol groups. We have described the site-specific conjugation of a temperature-sensitive polymer, poly (N-isopropylacrylamide) (PNIPAAm), to a streptavidin (SA) mutant, N49C [87]. This conjugate exhibited blocking of biotin-binding in the shrunken state of the polymer, above the lower critical solution temperature (LCST). However, the first conjugate at position 49 did not demonstrate ejection of bound biotin. Ding *et al.* reported that another SA mutant E116C-PNIPAAm conjugate showed reversible, thermally-induced blocking and release of biotin [88], and E116C-NIPAAm-co-acrylic acid copolymer conjugate exhibited pH control of biotin-binding to and triggered release from E116C SA [89]. The 116 position lies at a solvent accessible site and is relatively close to Trp120, which was previously shown to be a key site for biotin binding [85].

These results suggest that site-specific conjugation of other stimuli-responsive polymers to proteins at critical positions for controlling the protein recognition process could produce efficient molecular switches.

Therefore, E116C was selected as the first target mutant for conjugation with the photo-responsive polymers, DMAA and DMAAm, to create photo-switchable SA for controlled biotin-binding.

1.7.2 ENDOGLUCANASE III (EG III)

1.7.2.1 Cellulase

Cellulose is a major world bioresource, which is a linear polymer made of glucose subunits linked by $\beta(1-4)$ bonds. Cellulose chains form numerous intra- and intermolecular hydrogen bonds, which account for the rigid insoluble microfibril formation. The chains are oriented in parallel and form highly ordered crystalline domains interspersed by disordered amorphous regions. The degree of crystallinity of most commercial celluloses varies between 30 and 70 %.

Cellulase is a class of inducible extracellular enzymes produced by a variety of bacteria and fungi. They are traditionally used in food processing to grow edible mushrooms, facilitate the filtration of beer, and clear fruit juices from remaining pulp particles. In paper and pulp processing, they are used to reduce the amount of chlorine required to bleach the pulp, which results in the decrease of pollution from paper mill effluent [90]. Moreover, they have become increasingly important in recent years in textile processing because of their ability to provide the soft feel of stone washed jeans, and fabric care benefits such as color crispness when used in a laundry detergent [91]. For this application, the most commercially used cellulases are endoglucanases, which preferentially hydrolyze the internal $\beta(1-4)$ linkages of amorphous cellulose. Furthermore, in a long-term challenge for very large scale applications, cellulase will be utilized to degrade cellulose to glucose. Fermentation of glucose into solvents and fuels, particularly ethanol and butanol, could provide a partial substitution for fossil fuels. For this goal, starch alone accounts for too small a fraction of plants to sustain a positive

energy balance, and cellulose will have to be utilized as well, if biomass is to be used as an energy source [90].

Due to the heterogeneous supra-molecular structure, degradation of cellulose requires widely differing cellulases [90]. Cellulolytic microorganisms have evolved a battery of enzymes having different specificities with respect to endo/exo mode of action, activity towards amorphous or crystalline regions, or preference for substrates of different chain length. They act together in synergism.

Despite the considerable diversity, they have the common mechanisms for the glucoside hydrolysis, which have been elucidated by the combination approaches of genetics, biochemistry, and structural biology [90, 92]. Catalytic active sites of cellulases are composed of two key carboxyl groups. Two classes of mechanisms have been proposed. One is an “inverting mechanism”, in which one acid acts as a general acid and another as a general base. Thus, this is operated via a direct displacement of the leaving group by water. Another is a “retaining mechanism”, which utilize a double displacement mechanism involving a glycosyl-enzyme intermediate. In this mechanism, one acid functions as acid and base, and another acid acts as a nucleophile and a leaving group. The primary distinction between these two classes is the degree of separation of the two carboxyl groups. In inverting enzymes, they have greater separation (9.0 - 9.5 Å), which allows the insertion of a water molecule for direct attack. In retaining enzymes, they are close together (4.5 – 5.5 Å), resulting in the formation of a covalent glycosyl-enzyme intermediate. Both mechanisms operate via common transition states, an oxocarbenium ion, which is stabilized by these two carboxyl groups.

1.7.2.2 EG III

T. reesei is an acidophilic filamentous cellulolytic fungus, which secretes various cellulases that have evolved to function optimally in low pH environments. Two major endo-1,4-β-glucanases from *T. reesei* are EGI and EGII, which possess cellulose binding

domains (CBD), catalytic domains (CD), and linker regions. They have molecular weights of 55 and 48 kDa, and isoelectric points (pI) of 4.5 and 5.5, respectively [93].

EGIII is one of the minor endoglucanases of *T. reesei*. It is a single-domain cellulase, which doesn't have a separate CBD or a linker region, but solely a catalytic domain [94]. This simplification makes EGIII an attractive model for studying cellulase. EGIII has a Mw of 23.5 kDa and a near-neutral pI of 7.4. It consists of 218 amino acid residues with two cysteines at positions 4 and 32, which form an internal disulfide linkage to stabilize the protein (7 kcal / mol) [94]. Figure 1.4 shows a 3-D schematic structure of EG III (PDB was provided by Genencor International, Inc.). It has a crescent shape, which provides a groove to clamp a cellulose main chain to facilitate hydrolysis. EG III has an optimum pH at pH 5.5 and an optimum temperature at 40 - 50 °C for the hydrolysis of cellulose.

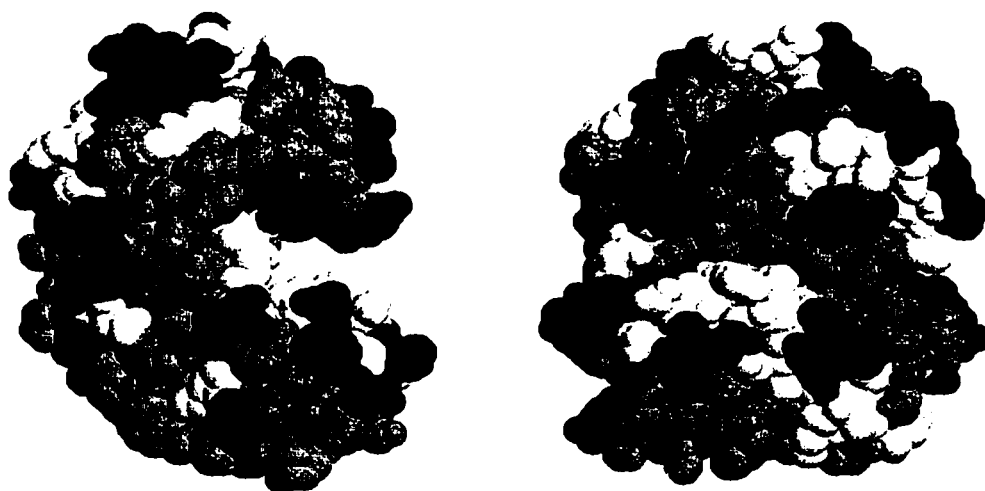


Figure 1.4. Schematic molecular model of endoglucanase III (EG III)

EGIII has been industrially used in textile processing. One of the problems encountered using cellulases in textile application is fiber strength loss. Thus, fine control of cellulase activity is desired. Photo-switchable EGIII would be preferable for this application.

1.7.2.3 Methods for Measuring Activities of Cellulases

In order to degrade crystalline cellulose, such as cotton fiber, filter paper, or Avicel (microcrystalline cellulose), the complete set of cellulase complex (cellobiohydrazase, endo-1,4- β -glucanase, and β -glucosidase) is indispensable. Since EG III is an endo-1,4- β -glucanase, it can't degrade crystalline region of cellulose.

In general, carboxymethyl cellulose, hydroxyethyl cellulose (HEC), cellooligosaccharide, alkali- or phosphoric acid- swollen amorphous cellulose have been used as substrates for endo-1,4- β -glucanase [95]. As more convenient substrates, chromogenic or fluorogenic substrates, in which colored or fluorescent compounds are linked to the anomeric carbon of cellobiose by a β -glucosidic bond have been utilized. O- or p-nitrophenyl- β -D-cellobioside (ONPC or PNPC) [96] and methylumbelliferyl- β -D-cellobioside [97] are the most frequently used compounds.

Catalytic activity of cellulase is usually assayed by measuring the release of soluble reducing sugars, which are expressed as glucose equivalents. HPLC or specific determination methods for reducing sugars are used for quantification. There are a number of published assay methods for the specific assay, but only a few are commonly used in cellulase studies. Of note, in this respect, are the dinitrosalicylic acid method [98], Somogyi-Nelson method [99], ferricyanide method [100], copper-neocuprine method [101], o-toluidine method [102], and p-hydroxybenzoic acid hydrazide (PHBAH) method [103]. Alternatively, residual insoluble cellulose can be determined gravimetrically, colorimetrically, or by turbidimetry.

Among these methods, we have selected two methods to investigate the effect of the size of the substrates on the activity of EG III. We have used ONPC as a small dye model

substrate and HEC as a soluble large substrate. The PHBAH method was used for detecting released glucose from HEC, because the PHBAH method is very specific to glucose, and the reaction condition is mild.

1.8 PERSPECTIVE APPLICATIONS OF PHOTO-SWITCHABLE BIOMOLECULES

Photo-regulation of biomolecular activities provides a general approach to utilize the functions of biomolecules, such as biocatalysts and affinity bindings, as light-controlled on/off switching systems. To date, there have been numerous potential applications of photo-switchable biomolecules proposed. They include the fields of therapeutics, biosensors, diagnostics, affinity separations, bioprocesses, and bioelectronics.

1.8.1 THERAPEUTICS

Since many proteins and their reaction products act as therapeutic agents [104, 105], reversible light-triggered activation/deactivation of proteins allows targeting and controlled release of the therapeutic agents by local specific light irradiation. The light can be irradiated directly by exposing the position using optical fiber, or indirectly by transdermal photo-irradiation. The penetration of UV light through skin was studied for the photo-polymerization of an implantation material by R. Langer *et al.* [106]. They reported that the transdermal photo-polymerization by UV light was slower than VIS light, however, after 15 min irradiation, the conversions were same. Thus, the transdermal photo-control of drug delivery might be possible when used close to the skin surface.

1.8.2 BIOSENSOR & DIAGNOSTICS

Numerous biosensors transduce the binding process between an analyte and the biological sensing receptor into a physical output such as color, fluorescence, or

electrochemical response [107-109]. However, due to the strong receptor-analyte interactions, many of the biosensors operate as single-cycle devices. Reversible photo-switchable biomolecules enable the biosensor to be recycled. The photo-switchable receptor in the active state permits the binding of the analyte and the sensing process. Photo-isomerization to the inactive state yields the sensor molecule to low affinity for the analyte, which facilitates its release. The analyte is then washed off, and further reisomerization of the receptor to the active state regenerates the active state for the subsequent analysis cycles [110].

1.8.3 AFFINITY SEPARATIONS

Isolation and purification of valuable proteins, such as cytokines, growth hormones, and vaccines, are based on affinity separation technology. Cell separation and sorting are also important in bone marrow transplantation and gene therapies using stem cells. For these applications, photo-regulation of protein affinity will provide an easier and more effective separation method without applying denaturing conditions.

1.8.4 BIOPROCESSES

A lot of enzymes have been already utilized in industry, such as food, detergent, paper, fabrics, and medicine. Fine and sharp control of enzyme activity is desired for optimizing the production and improving the efficiency. It is difficult to change the temperature or pH of the reactor sharply to control the enzyme activity. Thus, photo-switchable enzymes might be ideal for these purposes, because light is easy and quick to apply and the magnitude is controllable.

1.8.5 BIOELECTRONICS

Recording and readout of optical signals are the basis for optical memory devices and biocomputers. Amplification of weak light signals by a photo-switchable enzyme represents a further optoelectronic application. Absorption of a weak light signal by

photochromes activates the enzyme, and the chemical transformation is driven, which amplifies the light signal by the cyclic formation of the reaction product. Therefore, photo-switchable enzymes are prospective candidates for bioelectronics applications in the future.

1.9 SUMMARY OF OUR STRATEGY : SITE-SPECIFIC CONJUGATION OF PHOTO-RESPONSIVE POLYMERS TO PROTEINS

The goal of this research is to provide a novel design strategy to create photo-switchable proteins where the function is controlled reversibly and completely by specific light irradiation. Willner *et al.* showed complete on/off switching of enzymatic activity by caging an enzyme in photo-responsive polymer hydrogels [31]. This suggested the possibility that photo-responsive polymers conjugated to enzymes might control the catalytic activities effectively. Photo-responsive polymers are a sort of amplification system of small physicochemical changes of photochromes, and the collapse of the polymer may induce efficient affinity decrease or diffusion blocking of substrates like hydrogels. On the other hand, Ueda *et al.* demonstrated that the conjugation of photochromes to the critical position of the enzyme resulted in zero activity [53]. Thus, when the conjugated position of photo-responsive polymers to proteins is selected to be critical for controlling the protein functions, more effective photo-switching of the function might be possible. The combination of these two strategies might enable us to control the protein activity completely by light. The direct conjugations of proteins and photo-responsive polymers have not been reported much less the site-specific conjugations between them.

Figure 1.5 illustrates our strategy to develop photo-switchable proteins by site-specific conjugation of a photo-responsive polymer to a protein. When the polymer is expanded, it doesn't disturb the protein function. However, when the polymer is shrunken by photo-induced phase transition, it perturbs the protein, and the protein function is switched off.

This switching will be reversible because of the reversible phase transition of the conjugated polymer. We have selected SA as a model protein to control specific molecular recognition and binding, and EG III to control catalytic activity.

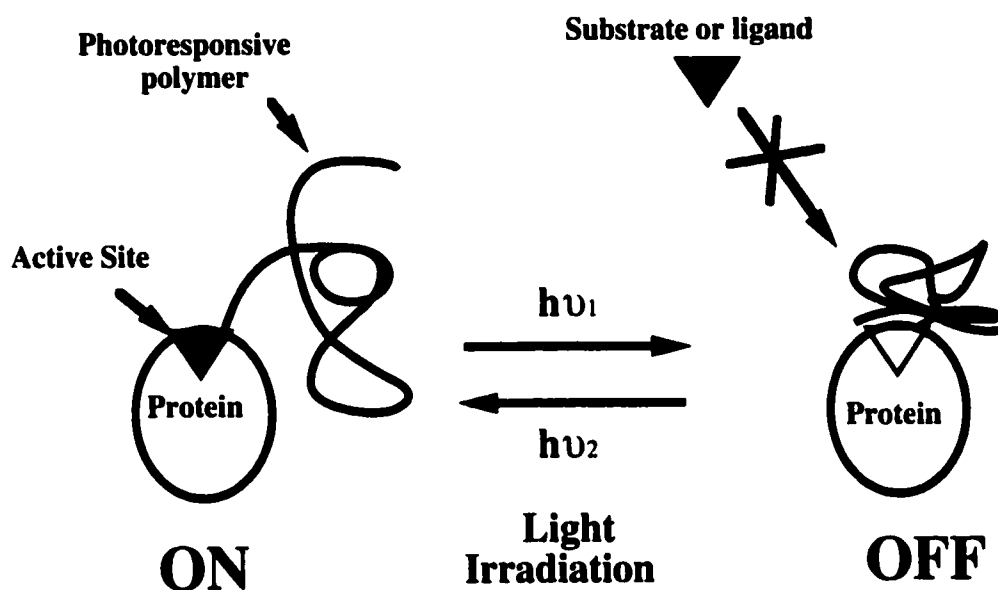


Figure 1.5. Rationale of photo-switchable protein.

We have created site-specific conjugates of mutant SA and EG III with photo-responsive polymers, DMAA and DMAAm. They have been designed to elucidate the effect of conjugated position, MW of the polymer, size of the substrates and addition of free polymer on the switching activities. In addition, since these two polymers have opposite photo-responses, we have switched the protein activities in two opposite directions by the same light irradiation. We have also conjugated an azobenzene directly to the mutated site to clarify the “polymer” effect on the efficacy for controlling the activity. These

investigations will elucidate the key factors and open a novel strategy to design photo-responsive proteins.

1.10 SIGNIFICANCE

Photo-control of specific binding between ligand and receptor or enzymatic activities are desirable for numerous applications in bioelectronics, bioprocesses and biomedical field. At the level of practical applications, it is important to develop molecular switches, which are designed to turn on and off in both directions effectively by the light signals safe to the proteins that are targeted in our project. To our knowledge there have not been any reports of on/off molecular switching of molecular recognition and binding or enzymatic activities in both directions controlled by the same light. This research will break new ground and begin to establish a fundamental strategy to develop photo-switchable biomolecules, and will be applied for designing a number of molecular photo-switches, which will be utilized in various practical applications.

CHAPTER 2 SYNTHESIS OF TEMPERATURE- AND PHOTO- DUAL STIMULI- RESPONSIVE POLYMERS FOR CONJUGATION TO PROTEINS

2.1 INTRODUCTION

The objective of this chapter is to create opposite photo-responsive polymers with reactive end groups for conjugation to proteins. We have investigated the synthesis of two kinds of end-reactive photo-responsive polymers, DMA-co-AZAAm copolymer (DMAAm), and DMA-co-AZAA copolymer (DMAA), terminated with a vinylsulfone (VS) group for further conjugation to proteins. Since SA and EG III were selected as target proteins to develop photo-switchable proteins, the tailored DMAA and DMAAm for conjugation to SA or EG III have been designed and synthesized, respectively. The thermo- and photo-responsive properties of these polymers in each buffer solution were studied.

2.2 MATERIALS AND METHODS

2.2.1 MATERIALS

4-Aminoazobenzene and 4-hydroxyazobenzene (Aldrich, Milwaukee, WI) were recrystallized from ethanol and water, and dried *in vacuo*. N,N-Dimethyl acrylamide (DMA) (Fluka, Milwaukee, WI), diethyl ether, acryloylchloride, triethylamine, and 2-mercaptoethanol (MEO) (Aldrich, Milwaukee, WI) were purified by distillation under reduced pressure. 2,2'-azobisbutyronitrile (AIBN) (J. T. Baker, Phillipsburg, NJ) was recrystallized from methanol. Ethanol, dimethylformamide (DMF), tetrahydrofuran (THF), methylene chloride, potassium ter-butoxide, divinyl sulfone (DVS), 5,5'-thiobis

(2-nitrobenzoic acid) (DTNB), ethylenediaminetetraacetic acid (EDTA) (Aldrich, Milwaukee, WI), and cysteine hydrochloride (Pierce, Rockford, IL), were used as received. All other reagents were of analytical grade.

2.2.2 METHODS

2.2.2.1 Synthesis of Photo-Responsive Monomers

We synthesized two kinds of photo-responsive monomers, N-4-phenylazophenyl acrylamide (AZAAm) and 4-phenylazophenyl acrylate (AZAA), which have different linkages between the azobenzene and the polymerizable group (Figure 2.1). 4-Aminoazobenzene or 4-hydroxyazobenzene (0.2 mol) and triethylamine (0.26 mol) were dissolved in diethyl ether (200 ml). Acryloylchloride (0.24 mol) dissolved in 80 ml of diethyl ether was added dropwise at 0 °C under nitrogen atmosphere with stirring. The reaction mixture was allowed to come to room temperature and stirred for 4 h. The reaction solution was filtered to remove triethylammonium chloride, washed with water and evaporated. The product was recrystallized from an ethanol-water mixture and dried *in vacuo*. The structures were confirmed by ¹H-NMR (Spectrospin & Bruker, dpx200) in d-DMSO. AZAAm: δ = 5.7 - 6.7 (m, 3H), 7.4 - 7.8 (m, 5H), 7.8 - 8.2 (m, 4H); AZAA: δ = 6.1 - 6.7 (m, 3H), 7.3 - 7.7 (m, 5H), 7.8 - 8.2 (m, 4H).

2.2.2.2 Synthesis of Photo-Responsive Polymers

Two kinds of photo-responsive polymers with hydroxyl termini, DMAAm and DMAA, were synthesized by free-radical copolymerization of DMA with AZAAm or AZAA in DMF at 60 °C for 20 h, using MEO as a chain transfer reagent and AIBN as an initiator (monomer concentration = 2 mol/L) (Figure 2.2). The ratios of DMA and AZAAm or AZAA were varied to change the incorporated azobenzene moiety in the polymer. In addition, in order to investigate the effect of MW on the switching activity of the conjugate, the monomer / MEO / AIBN molar ratios were varied from 100 / 0.25 / 0.05 to

100 / 16.0 / 3.2 to make polymers with different MW. The products were purified by precipitation into diethyl ether three times and dried *in vacuo*.

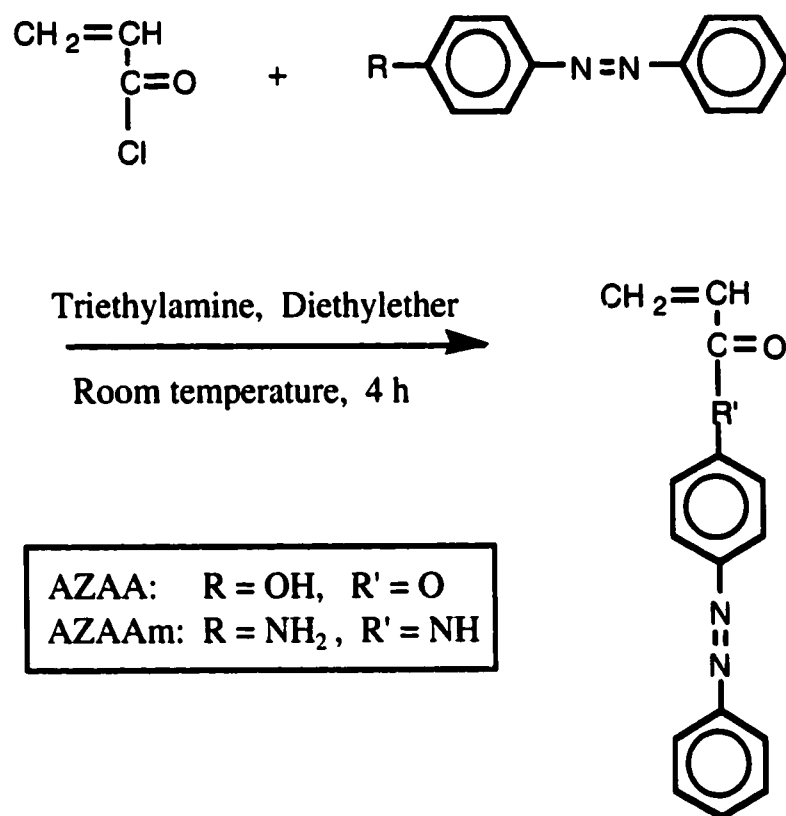


Figure 2.1. Scheme of synthesis of photo-responsive monomer (AZAA and AZAAm)

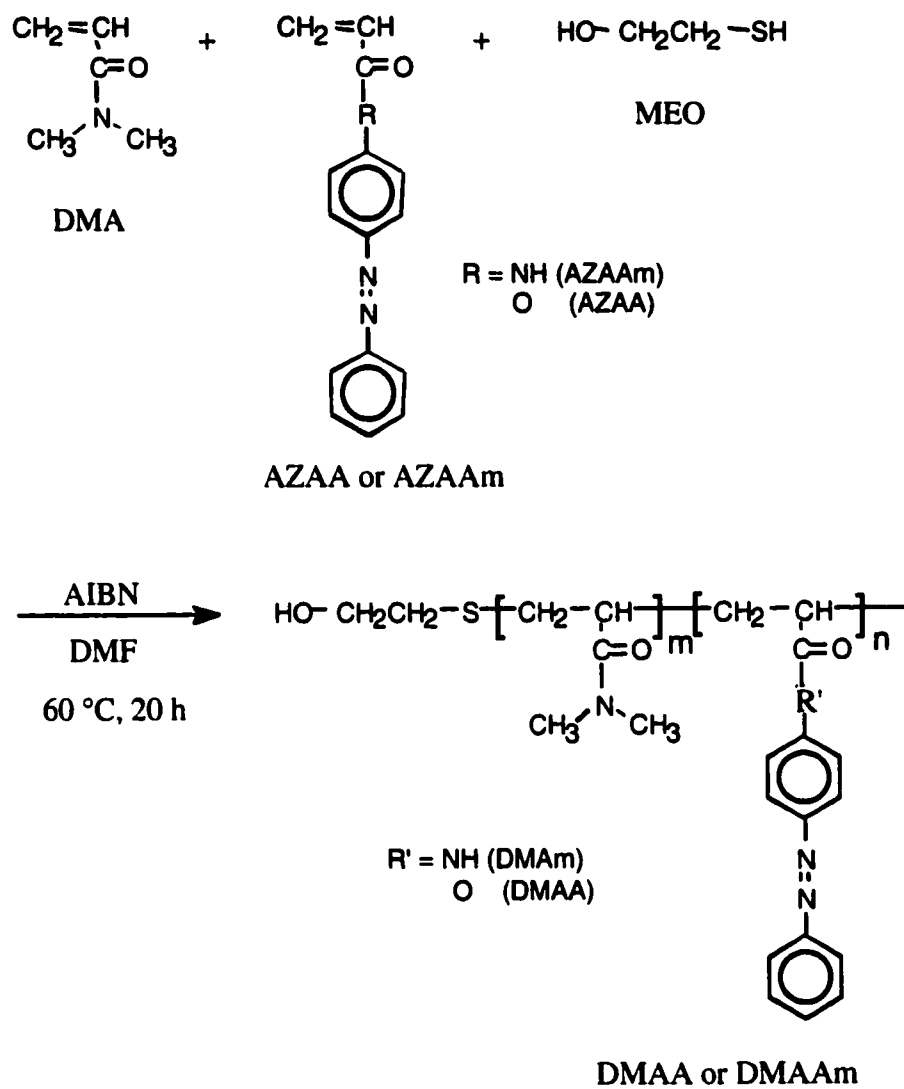


Figure 2.2. Scheme of synthesis of photo-responsive polymer (DMAA and DMAAm)

2.2.2.3 Determination of Contents of AZAAm and AZAA

The contents of AZAAm or AZAA incorporated in the copolymers were determined by ^1H -NMR (Spectrospin & Bruker, dpx200), comparing the ratio of aromatic and aliphatic hydrogens.

2.2.2.4 Determination of Molecular Weights (MWs) of the Polymers

The molecular weights (MWs) of the copolymers were determined by gel permeation chromatography (GPC), (Waters, Styragel HR3 and HR4) in THF, using polystyrene as standards.

2.2.2.5 Derivatization of End Groups of Copolymers with Vinylsulfone Groups

The hydroxyl terminus of DMAA or DMAAm was converted to vinylsulfone for conjugation to proteins (Figure 2.3). DMAA or DMAAm was dissolved in 20 ml of methylenechloride with 0.03 g of potassium tert-butoxide, and 100 μl of divinylsulfone (DVS) (DVS / OH = 10 / 1 molar ratio). The solution was stirred for 12 h at room temperature under nitrogen atmosphere. The polymers were precipitated in diethyl ether, rinsed, and dried *in vacuo*.

2.2.2.6 UV or VIS Irradiation

Two kinds of light sources, UV Cure Lamp (Thorlabs, Newton, NJ) and Fiber-Lite Illuminator (Edmund Scientific, Barrington, NJ), were used combined with two bandpass filters [UG-1 for UV, VG-1 for VIS (Edmund Scientific, Barrington, NJ)] to remove undesirable light. Thus, the UV light had a peak at 350 nm ranging from 300 to 400 nm, and the VIS light had a peak at 520 nm and light less than 420 nm was removed.

10 min of UV irradiation and 3 h of VIS irradiation were employed as standard UV or VIS irradiation times. These times were sufficient to reach saturation of the cis and trans forms of azobenzene, respectively.

2.2.2.7 LCST Measurement

The LCST was determined as the temperature that shows 10 % of the maximum absorbance at 600 nm measured by the UV-VIS spectroscope (Bausch & Lomb Spectronic 101), when raising the temperature by 0.5 °C / min. The polymer concentration was 2 mg/ml in dd-water, 100 mM sodium phosphate buffer (PB) pH 7.2, or 50 mM sodium acetate buffer (AB) pH 5.5. The LCSTs of the polymers were measured just after UV or VIS light irradiation.

2.2.2.8 Photo-Responsive Temperature Measurement

For determining the photo-responsive temperatures, the LCSTs of the polymers were measured just after UV (10 min.) or VIS (3 h) light irradiation. The photo-responsive temperature was determined as the middle temperature of the LCSTs between UV and VIS light irradiation.

2.2.2.9 Determination of VS in Polymers

The amount of active VS in the VS-terminated DMAAm (DMAAm-VS) and DMAA (DMAA-VS) copolymers was determined by reaction with cysteine. Since cysteine was detected colorimetrically by the reaction with 5,5'-thiobis (2-nitrobenzoic acid) (DTNB), the amount of VS was calculated by the amount of cysteine consumed. Briefly, 0.2 ml of polymer solution (10 mg/ml in 0.1 M PB pH 8.0) was mixed with 2 ml of cysteine solution (1.5 mM cysteine hydrochloride in 0.1 M PB pH 8.0 with 10 mM EDTA), and reacted for 4 h. 0.2 ml of the solution was mixed with DTNB solution (0.2 mg of DTNB in 2 ml of 0.1 M PB pH 8.0), and incubated for 15 min. Then, the absorbance at 412 nm was measured to calculate the amount of cysteine reacted with DTNB.

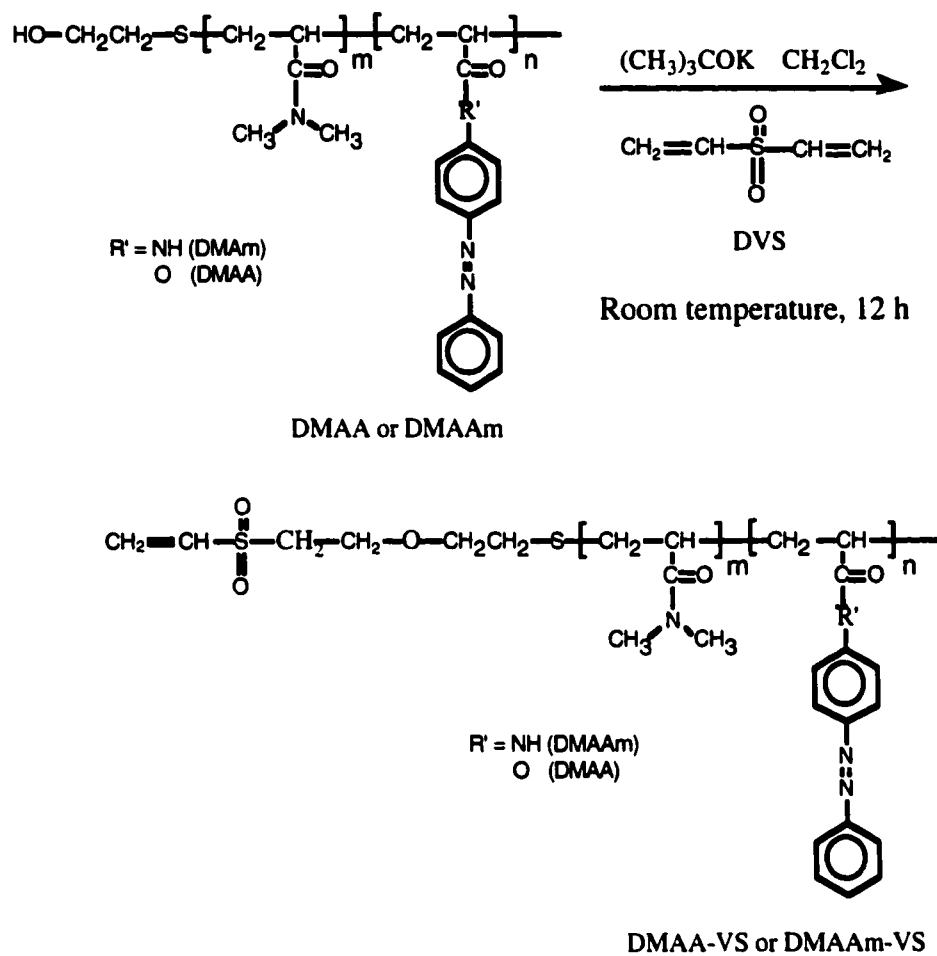


Figure 2.3. Scheme of vinylsulfonation of DMAA and DMAAm

2.3 RESULTS AND DISCUSSIONS

2.3.1 SYNTHESIS AND CHARACTERIZATION OF DMAAM AND DMAA COPOLYMERS

AZAAM and AZAA monomers were obtained from the reaction of 4-aminoazobenzene or 4-hydroxyazobenzene with acryloyl chloride. DMAAM and DMAA copolymers terminated with a hydroxyl group were synthesized by free radical copolymerization of DMA with AZAAM, and DMA with AZAA, respectively. The results of the copolymerizations varying the azobenzene monomer ratios to the amount of DMA in feed are shown in Table 2.1. The incorporated azobenzene mole fractions determined by $^1\text{H-NMR}$ were higher than the monomer contents in the feed, suggesting that azobenzene monomers might have higher reactivity than DMA in free radical polymerization. The conversions were not high (21 – 79 mol %), which might be due to the retardation effect of the azobenzene moiety on free radical polymerization [67]. DMAAM showed higher conversions and lower molecular weights than DMAA did.

2.3.2 EFFECTS OF PHOTOIRRADIATIONS ON PHASE TRANSITIONS

The UV/VIS absorbance spectra of DMAA (AZAA: 5.9 mol%) and DMAAM (AZAAM (9.6 mol%)) are shown in Figure 2.4 and 2.5. The photo-isomerization efficiency by photo-irradiation of the system was estimated by the absorbance change at 323 nm for DMAA and 353 nm for DMAAM. The peaks at these wavelengths stem from $\pi\text{-}\pi^*$ transition of the trans form of azobenzene disappeared by UV irradiation, and recovered by VIS irradiation. From these data, 10 min of UV irradiation and 3 h of VIS irradiation were employed as standard UV or VIS irradiation times, since these times were sufficient to reach saturation of the cis and trans forms of azobenzene, respectively.

Table 2.1. Characteristics of DMAAm and DMAA

Sample	AZAAm or AZAA in feed (mol %)	AZAAm or AZAA in polymer ^a (mol %)	Conversion (%)	Mn ^b (x10 ⁻⁴)
DMAAm-4.0	4.0	5.2	54.5	0.7
DMAAm-4.5	4.5	6.0	44.6	0.9
DMAAm-5.0	5.0	7.8	42.9	1.0
DMAAm-7.0	7.0	9.6	52.3	1.0
DMAAm-8.0	8.0	10.6	78.9	0.9
DMAAm-9.0	9.0	12.4	44.5	1.0
DMAAm-10.0	10.0	13.1	43.1	1.0
DMAA-3.0	3.0	2.7	41.6	1.2
DMAA-3.4	3.4	4.3	30.5	1.6
DMAA-3.6	3.6	5.0	25.1	1.7
DMAA-4.0	4.0	5.9	26.8	1.8
DMAA-4.2	4.2	6.1	24.6	1.8
DMAA-4.5	4.5	6.6	32.9	1.9
DMAA-5.0	5.0	7.3	20.6	2.0
DMAA-5.5	5.5	8.2	18.4	2.2
DMAA-6.0	6.0	9.2	22.3	2.4

^a Determined by ¹H-NMR^b Determined by GPC

Phase transitions induced by temperature changes and photo-irradiations were evaluated by turbidity development in solution at 600 nm. Figures 2.6 shows typical absorbance data for solutions of DMAA and DMAAm upon UV or VIS irradiation with increasing temperature. DMAA has a soluble-insoluble phase transition at 37 °C (10 % of maximum absorbance) under VIS light; however, it increased to 43 °C under UV irradiation. On the other hand, DMAAm has a transition at 39 °C upon VIS irradiation, which decreased to 34 °C upon UV irradiation. Therefore, these polymers showed opposite photo-responses from each other. This interesting phenomenon is discussed later.

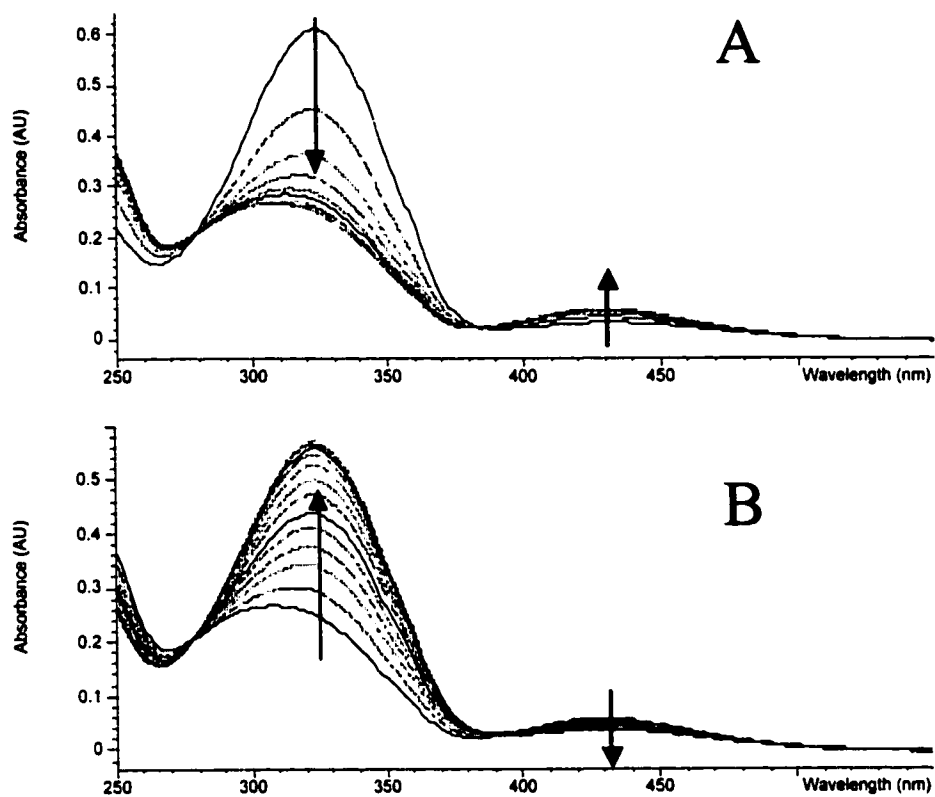


Figure 2.4. UV/VIS spectra of DMAA

The content of AZAA in the polymer was 5.9 mol%. A: UV irradiation: 0 – 9 min. B: VIS irradiation: 0 – 84 min after UV irradiation for 8 min.

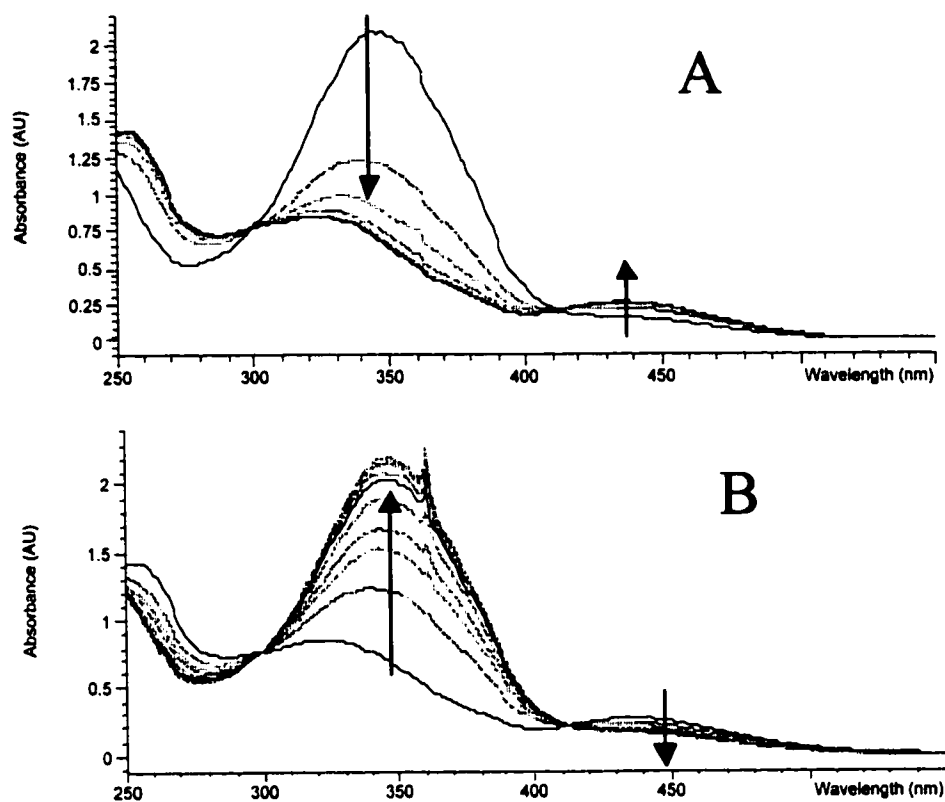


Figure 2.5. UV/VIS spectra of DMAAm

The content of AZAAm in the polymer was 9.6 mol%. A: UV irradiation: 0 – 7 min. B: VIS irradiation: 0 – 60 min after UV irradiation for 7 min.

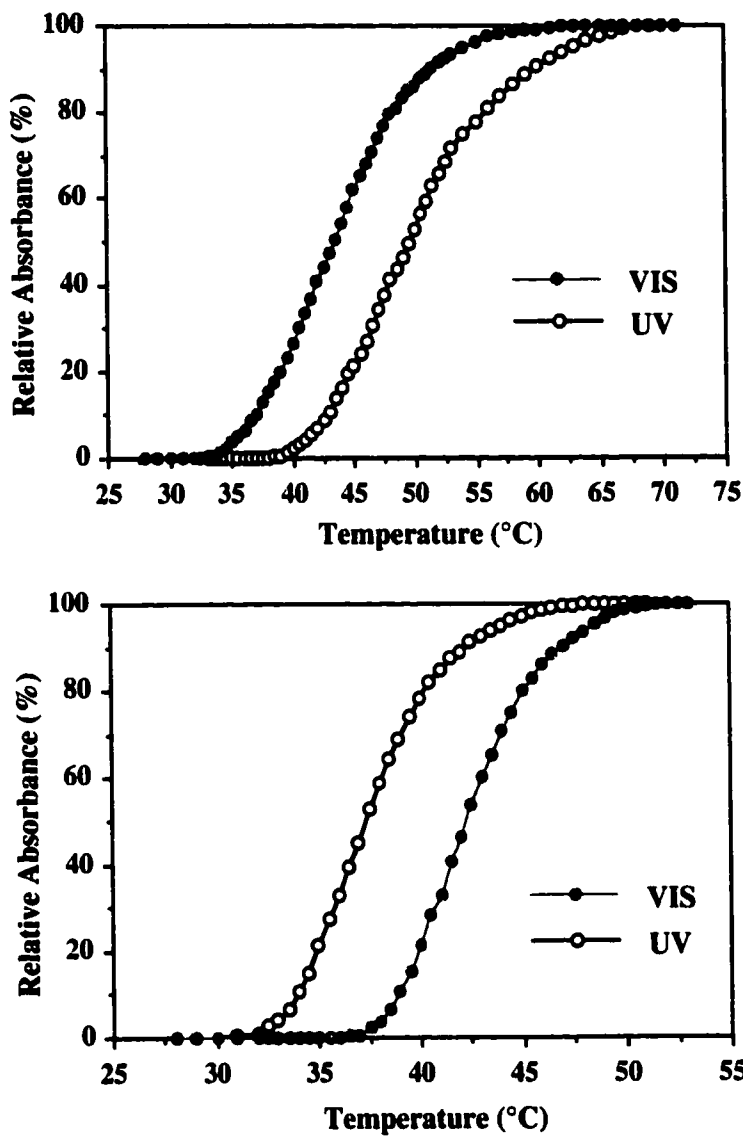


Figure 2.6. Effect of photo-irradiation on the phase transition temperature of DMAA and DMAAm

Above: DMAA (AZAA: 5.9 mol%), Below: DMAAm (AZAAm: 9.6 mol%). The absorbance was measured at 600 nm. The polymer concentration was 2 mg/ml in 100 mM PB pH7.2. The rate of heating was 0.5 °C/min. The UV and VIS light was irradiated for 10 min and 3 h, respectively, before the measurement.

2.3.3 EFFECTS OF AZOBENZENE MONOMER CONTENTS ON LCST PHASE TRANSITION

In order to elucidate the overall features of the photo-responsive properties of these polymers, we studied the effects of both the azobenzene content in the polymers and the photo-irradiations on their LCSTs in dd-water and 100 mM PB pH 7.2 (Figure 2.7). Significant decreases in the LCSTs were observed for both polymers when increasing their azobenzene monomer contents. This is probably due to the significant hydrophobic character of the azobenzene moiety.

Concerning photo-responses, DMAA copolymers demonstrated higher LCSTs under UV irradiation than VIS irradiation. In addition, the differences in the LCST between UV and VIS light irradiation in DMAA copolymers decreased gradually and disappeared at 9.2 mol % of the AZAA contents. On the contrary, DMAAm copolymers showed an interesting phenomenon. They also had higher LCSTs under UV irradiation when AZAAM was less than 6.3 mol %; however, they showed inverse photo-response above 7 mol % of AZAAM content, meaning lower LCSTs under UV irradiation than VIS irradiation.

These phenomena may be explained as shown in Figure 2.8. In the cis form, azobenzene is more polar than in the trans form, because of its higher dipole moment. Therefore, the LCST of the copolymer is expected to be higher in the cis form than in the trans form. This is the case of DMAA. However, azobenzene also has a self-assembling property. At higher contents, the trans form tends to stack together and aggregate in water, which can reduce the overall hydrophobicity of the copolymer. Thus, it is speculated that when azobenzenes are stacked, the aggregate is destroyed by photo-isomerization to the cis form (e.g. by UV irradiation), releasing the individual azobenzenes, and resulting in an increase in hydrophobicity, and reduction of the LCST of the copolymer. This might be the case of DMAAm.

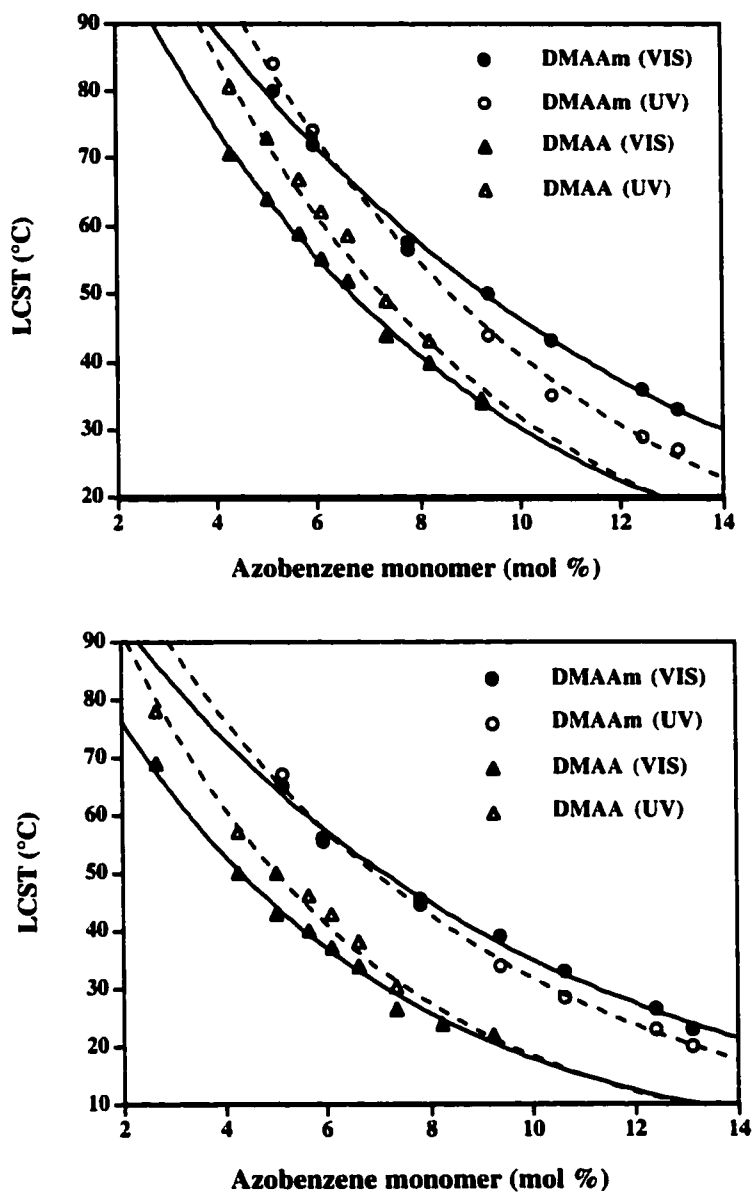


Figure 2.7. Effect of photo-irradiation and azobenzene content on the LCSTs of DMAA and DMAAm.

Polymer concentration: 2 mg/ml in dd-water (above) and 100 mM PB pH7.2 (below). The LCST was measured after UV (10 min) or VIS (3 h) irradiation.

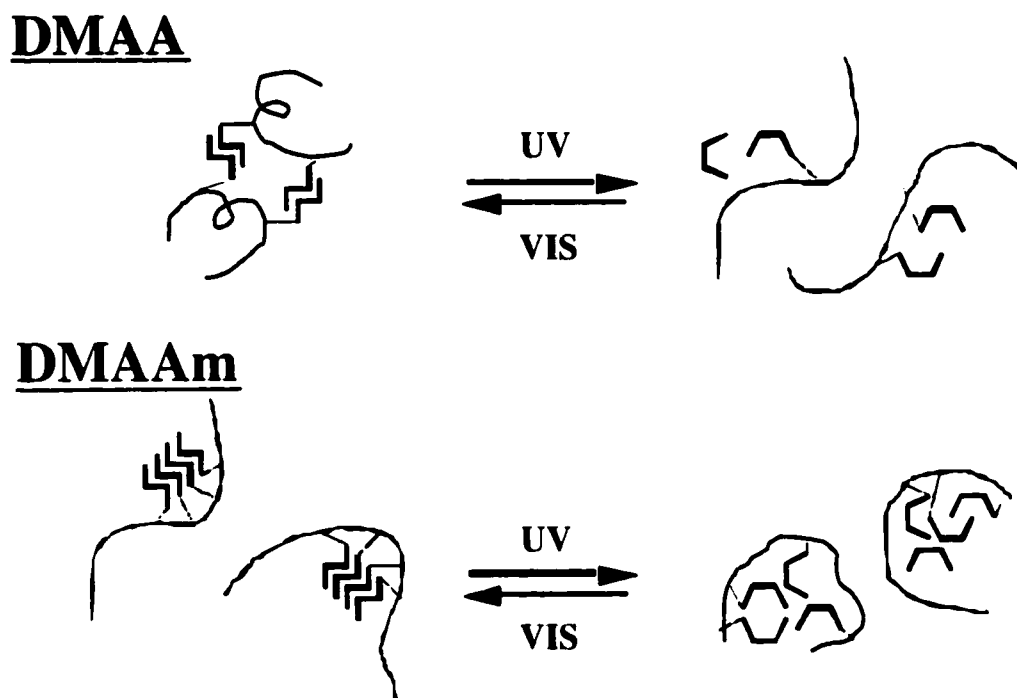


Figure 2.8. Speculated explanation of the opposite photo-responses of DMAA and DMAAm.

The critical points of the azobenzene contents, where no photo-response is detected, were observed at 6.3 mol % for DMAAm copolymers and at 9.2 mol % for DMAA copolymers. At these points, the hydrophilicity stemming from the increase of dipole moment by trans to cis photo-isomerization of azobenzene, and the hydrophobicity due to the release of azobenzene from the stacked state may just compensate each other. The data suggested that the azobenzene group of AZAAm tend to stack more easily than that of AZAA, such that the DMAAm copolymers start to show the inverse photo-response at lower azobenzene contents compared to DMAA. The only difference between AZAAm

and AZAA is the linkage between the polymer backbone and the azobenzene moiety, which is amide and ester, respectively. The data suggests that the amide bond might enhance the stacking of azobenzene in aqueous solution more than the ester bond. This may stem from the properties of the amide bond, which is rigid, planar and also capable of hydrogen bonding with each other. It is surprising that this small difference in the linkage of azobenzene to the polymer backbone changed the total photo-response of the polymer.

In addition, the AZAAm copolymers always exhibited higher LCSTs than the AZAA copolymers when in their *cis* forms (under UV irradiation), when there was no stacking effects. This might be due to the fact that the amide bond is more hydrophilic than the ester bond because of its greater hydration capacity.

In 100 mM PB, the LCSTs of the polymers were decreased and the photo-responsive temperature gaps were reduced compared with those in dd-water. However, even in PB, they still retained more than 6 °C difference in their LCSTs between UV and VIS irradiations at 40°C. This should be a suitable condition for most of the proteins including SA.

2.3.4 EFFECTS OF POLYMER AND SALT CONCENTRATIONS ON LCSTS

The effects of polymer concentration on the LCST for DMAAm and DMAA are shown in Figure 2.9. As the polymer concentration increased, the LCSTs of DMAA decreased; however, the LCSTs of DMAAm didn't change significantly. These results suggest that the precipitation of DMAA might be induced by intermolecular aggregation, while that of DMAAm might be by intramolecular aggregation. Morishima *et al.* reported that amide-linked hydrophobic moiety-bearing polymers showed intramolecular association, whereas the ester-linked amphiphilic polymers showed intermolecular association [111, 112]. These results are consistent with our results and support our assumption of the greater

stacking tendency of AZAAm compared to AZAA, because intramolecular association may occur more easily than intermolecular association even in a dilute solution.

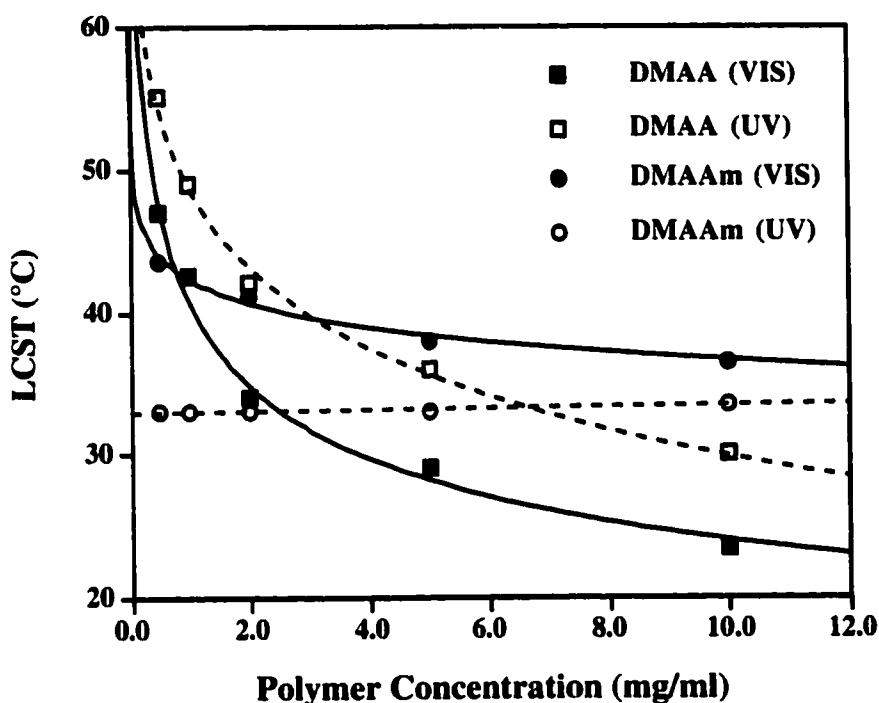


Figure 2.9. Effect of polymer concentration on the LCSTs of DMAA and DMAAm.

DMAA (AZAA: 5.9 mol%), DMAAm (AZAAm: 9.6 mol%) in 100 mM PB pH7.2. The LCST was measured after UV (10 min) or VIS (3 h) irradiation.

Figure 2.10 shows the effect of salt concentration on the LCSTs for these polymers. In this case, the LCSTs of both polymers were decreased when increasing the salt concentration. The photo-responsive temperature gap of DMAA disappeared at high salt concentration, whereas that of DMAAm still existed even at 5 M NaCl. This result suggested that the stacking effect, which might elicit the opposite photo-response of

DMAAm, is more resistant to salting-out compared to the dipole moment effect, which might induce the normal photo-response of DMAA.

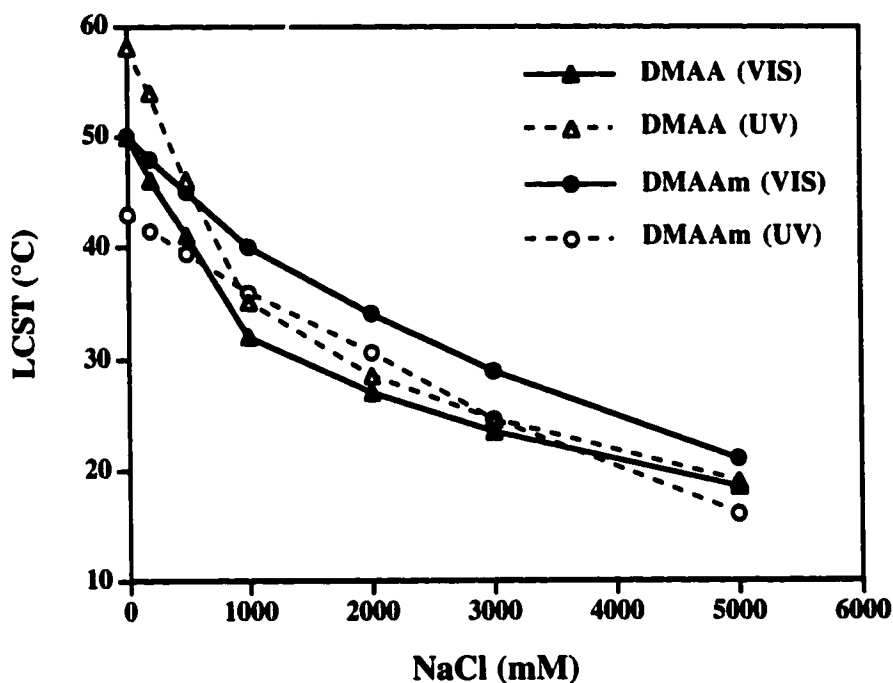


Figure 2.10. Effect of salt concentration on the LCST of DMAA and DMAAm.

The concentration of DMAA (AZAA: 5.9 mol%) and DMAAm (AZAAm: 9.6 mol%) was 2 mg/ml in 100 mM PB pH7.2. The LCST was measured after UV (10 min) or VIS (3 h) irradiation.

From these results, it was shown that both polymer concentration and salt concentration influenced the LCSTs and photo-responses for these polymers. We could estimate the photo-responsive temperatures of the conjugates using these data.

2.3.5 ISOTHERMAL PHOTO-RESPONSES

We selected two typical polymers, DMAAm with an AZAAm content of 9.6 mol %, and DMAA with an AZAA content of 5.9 mol % for investigating the isothermal photo-responses of these polymers. These copolymers showed opposite photo-responses at 37 °C to 40 °C in 100 mM PB. Figure 2.11 shows the isothermal photo-responses of these polymers. DMAA became insoluble upon VIS light and soluble upon UV light. In contrast, DMAAm became soluble upon VIS light and insoluble upon UV light. In addition, these soluble-insoluble cyclings were reversible for both polymers. Therefore, the solubilities of these polymers could be controlled by UV/VIS light irradiation. These polymers might be used as oppositely photo-regulatable materials under isothermal conditions at 37 - 40 °C.

For conjugation to SA, two kinds of photo-responsive polymers, DMAA with 5.9 mol% of AZAA and DMAAm with 9.6 mol% AZAAm, were selected, because they exhibited the photo-responsive phase transitions around 40 °C in 100 mM PB pH 7.4, which is used for SA / biotin binding assay.

2.3.6 DESIGN AND SYNTHESIS OF END-REACTIVE PHOTO-RESPONSIVE POLYMERS FOR CONJUGATION TO EG III

Photo-responsive polymers for conjugation to EG III were designed and synthesized. The photo-responsive temperature (PT) of DMAA and DMAAm was dependent on the condition of the buffer solution. The optimum buffer solution for activity assay of EG III is 50 mM sodium acetate buffer (AB) pH 5.5. Figure 2.12 shows the effect of azobenzene (AZ) content and UV/VIS photo-irradiation on the LCSTs of the polymers in 50 mM AB pH5.5. In this buffer, the LCSTs of the polymers were higher than those in 100 mM PB pH7.2 for the same AZ contents (Figure 2.7). To adjust the PT to 40 °C in 50 mM AB, more AZAA or AZAAm have to be incorporated in the polymer.

In addition, to investigate the effect of the MW of the conjugated polymer on the switching activity of EG III, DMAA and DMAAm with different MWs were synthesized keeping the PT at 40 °C in 50 mM AB.

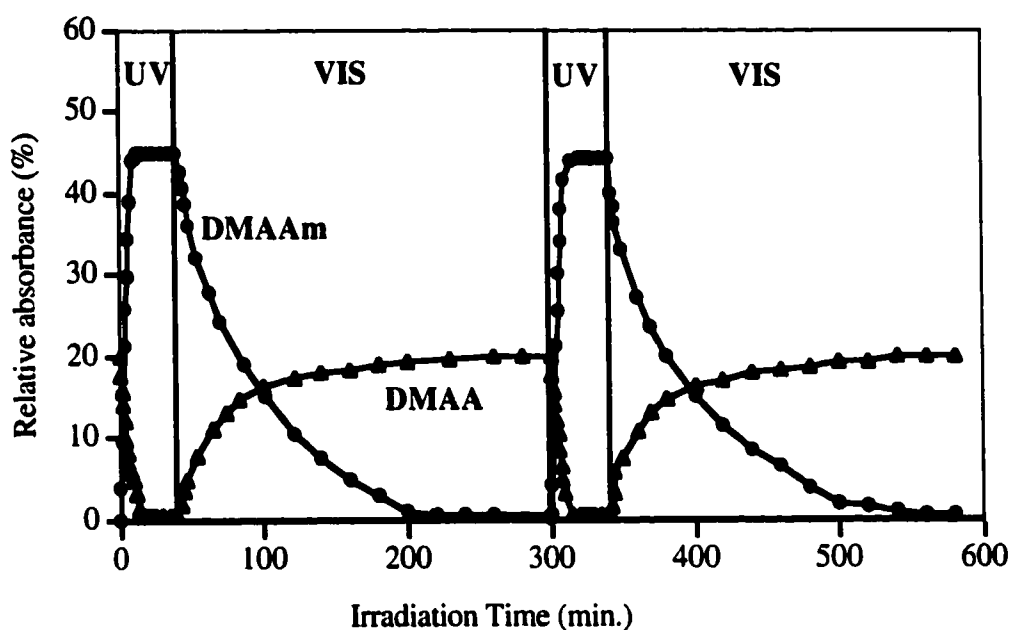


Figure 2.11. Photo-induced phase transition of DMAA and DMAAm.

The absorbance at 600 nm was measured as a function of UV and VIS irradiation time for DMAA (AZAA: 5.9 mol%) and DMAAm (AZAAm: 9.6 mol%) under isothermal condition (DMAA: 39 °C, DMAAm: 37 °C). The polymer concentration was 2 mg/ml in 100 mM PB pH7.2.

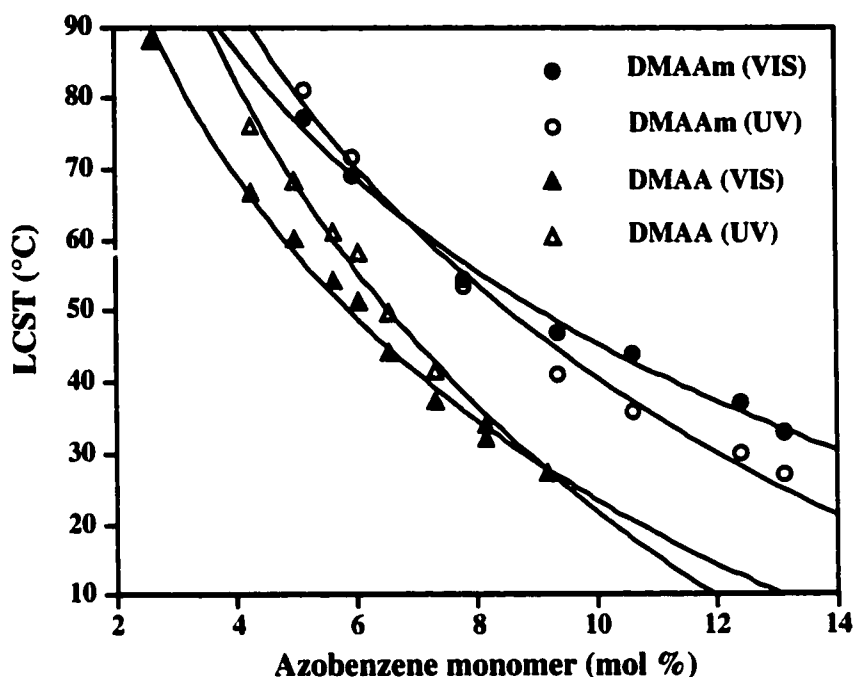


Figure 2.12. Effect of photo-irradiation and azobenzene content on the LCSTs of DMAA and DMAAm in the EG III buffer.

Polymer concentration: 2 mg/ml in 50 mM sodium acetate buffer pH5.5. The LCST was measured after UV (10 min) or VIS (3 h) irradiation.

Figure 2.13 shows the relationship among PT, AZ and MW of DMAA and DMAAm, when polymerized with constant azobenzene monomer ratio in the feed. The MW was changed by varying the feed ratio of MEO to the total monomer content. With increasing MEO in feed, the MW was decreased, but the PT was increased. The $^1\text{H-NMR}$ analysis proved that this is due to less AZ incorporated in the lower MW polymer in spite of using the same AZ content in the feed. This indicated that more azobenzene monomer had to be added to the feed to synthesize polymers with lower MW while keeping the same PT .

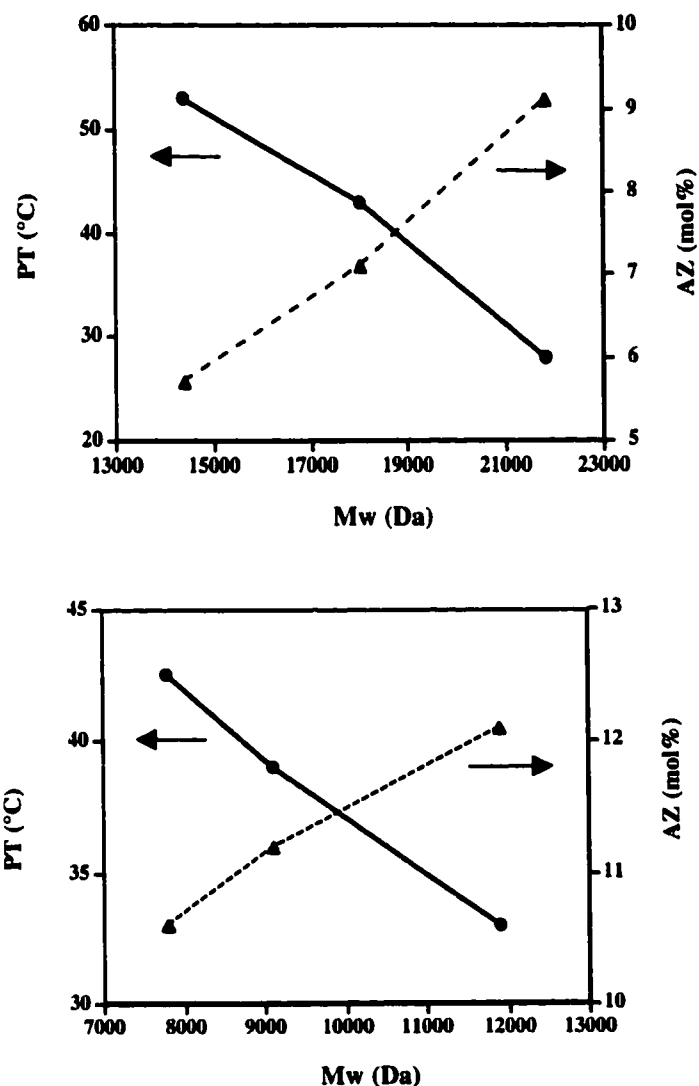


Figure 2.13. Effect of Mw (molecular weight) on PT (photo-responsive temperature) and AZ (azobenzene content) of DMAA and DMAAm

Above: DMAA. Below: DMAAm. The polymer concentration to measure the PT was 2 mg/ml in 50 mM AB pH5.5. The AZ was determined by $^1\text{H-NMR}$. The Mw was varied by changing the feed ratio of MEO from 0.5 to 2.0 mol%, with keeping the feed ratio of AZAA monomer as 5 mol% for DMAA, and AZAAm monomer as 8 mol% for DMAAm constant, and determined by GPC.

Figure 2.14 shows the relationship among the PT, the AZ and the MW of DMAA and DMAAm. The AZ was changed by varying the feed ratio of AZAA or AZAAm to DMA, while keeping the same feed ratios of MEO and AIBN. For DMAAm, as the AZ increased, the PT was decreased, but the MW didn't change. Thus, we can change the PT and the AZ independently for DMAAm. However, DMAA shows strong dependence of the MW on the AZ. When the AZ was increased, the MW was also increased, suggesting that it is difficult to change the MW independently of the AZ.

The results of polymerization of DMAA and DMAAm for conjugation to EG III are summarized in Table 2.2. Three kinds of DMAAm with different MWs and the same PT (around 40 °C) were successfully synthesized (DMAAm 4-4, 1-2, and 3-2). However, even though the feed ratios of MEO and AZAA were varied drastically, DMAA with the same PT (40 °C) always has a similar MW (see DMAA 2-3, 2-5, 5-1).

Therefore, we decided to use four polymers, DMAAm 4-4 (Mw/Mn: 15/10 kDa), DMAAm 1-2 (9/6 kDa), DMAAm 3-2 (6/3 kDa), and DMAA 2-5 (20/11 kDa), for conjugation to EG III.

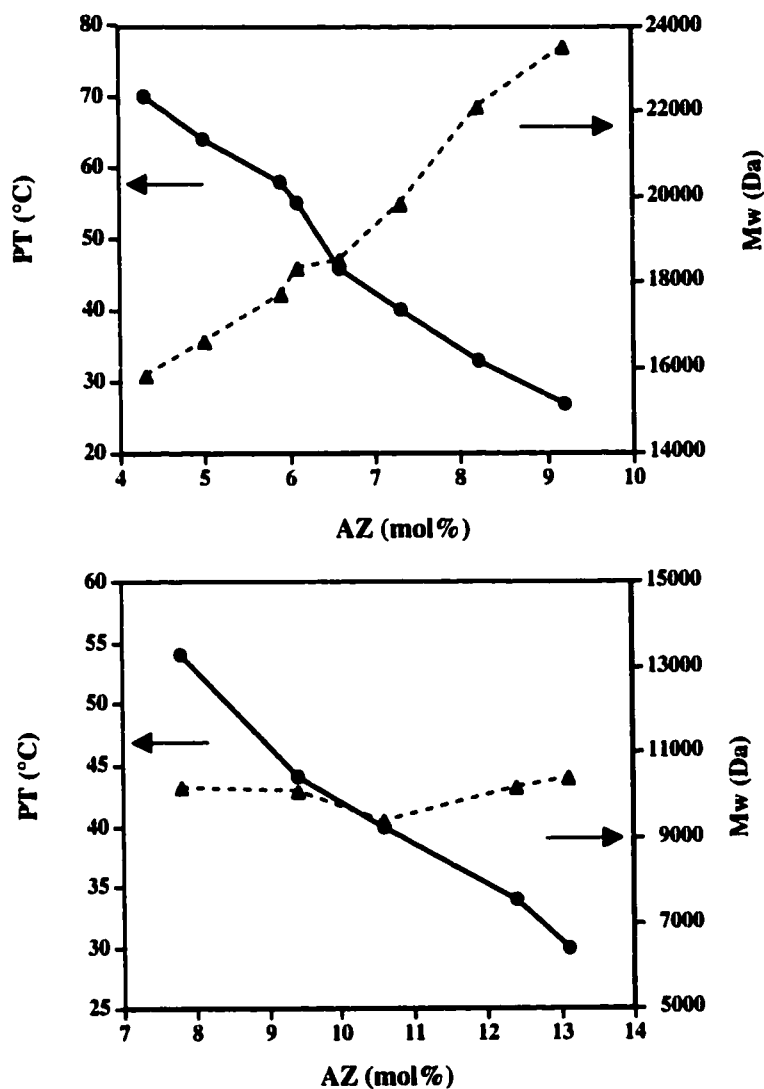


Figure 2.14. Effect of AZ (azobenzene content) on PT (photo-responsive temperature) and Mw (molecular weight) of DMAA and DMAAm.

Above: DMAA. Below: DMAAm. The polymer concentration to measure the PT was 2 mg/ml in 50 mM AB pH5.5. The Mw was determined by GPC. The AZ was determined by $^1\text{H-NMR}$. The AZ was varied by changing the feed ratio of AZAA or AZAAm, keeping the feed ratios of MEO (1.0 mol%) and AIBN (0.2 mol%) constant.

Table 2.2. Characteristics of DMAA and DMAAm for Conjugation to EG III

Sample #	MEO ^a (mol%)	AZAAm or AZAA ^a (mol %)	Photo- responsive Temp. (°C)	Mw ^b	Mn ^b	Mw/Mn ^b	Yield (%)
DMAAm 4-4	0.25	5.5	42.0	14900	9600	1.55	31.6
DMAAm 3-1	0.25	6.0	35.0	14800	8900	1.67	27.2
DMAAm 2-1	0.5	7.0	38.5	12100	7700	1.59	38.3
DMAAm 1-1	0.5	8.0	33.0	11900	7300	1.63	27.2
DMAAm 1-2	1.0	8.0	39.0	9100	5700	1.59	48.5
DMAAm 1-3	2.0	8.0	42.5	7800	4700	1.67	60.4
DMAAm 3-2	2.0	9.0	38.5	5700	3200	1.79	74.1
DMAAm 3-3	4.0	10.0	31.0	4200	2300	1.79	67.5
DMAA 2-3	0.5	4.0	41.5	18900	11400	1.66	15.5
DMAA 2-2	0.5	4.5	35.5	20500	12400	1.65	22.1
DMAA 1-4	0.5	5.0	28.0	21800	12600	1.73	14.9
DMAA 1-5	1.0	5.0	43.0	18000	10200	1.76	21.0
DMAA 1-6	2.0	5.0	53.0	14400	8300	1.74	46.8
DMAA 2-4	2.0	5.5	50.0	16600	10200	1.63	40.0
DMAA 2-5	2.0	6.0	41.5	17600	10500	1.66	35.1
DMAA 3-4	4.0	7.0	74.0	17600	10400	2.07	54.3
DMAA 5-1	4.0	9.0	42.0	19400	11300	1.71	47.0
DMAA 5-2	4.0	11.0	27.0	23600	13200	1.78	40.7
DMAA 3-5	8.0	8.0	>80	7100	5100	1.38	60.5
DMAA 5-3	8.0	13.0	48.0	16500	9100	1.80	52.3
DMAA 3-6	16.0	9.0	>80	3300	1900	1.78	15.9
DMAA 5-4	16.0	15.0	>80	4100	3300	1.26	34.3

^a Molar ratio to total monomer in feed, ^b Determined by GPC

2.3.7 SYNTHESIS AND DETERMINATION OF REACTIVE VS CONTENT OF DMAAM-VS AND DMAA-VS

The hydroxyl termini of DMAAm and DMAA were converted to VS termini via the reaction with DVS. The active VS in DMAAm-VS and DMAA-VS, which can react with a thiol group, were assayed colorimetrically using Cys / DTNB system. The percentages

of the active VS in DMAAm-VS and DMAA-VS are listed in Table 2.3. Almost 100 % of the terminal hydroxyl groups were converted to VS. These termini were used for the conjugation with cysteines of proteins in the following chapter.

Table 2.3. Percentages of the active VS in DMAA and DMAAm

Target protein	Photo-responsive polymer	Mn (kDa)	VS (%) [#]
SA	DMAA-VS	18	98.0
SA	DMAAm-VS	10	97.5
EG III	DMAA-VS	11	96.7
EG III	DMAAm-VS	10	98.9
EG III	DMAAm-VS	6	102.3
EG III	DMAAm-VS	3	105.7
# : assuming Mn as an average MW of each polymer			

2.4 CONCLUSIONS

Photo-responsive polymers suitable for conjugation to proteins were investigated. Significant differences in the LCSTs (8-10 °C) when under UV vs. VIS irradiation were detected for DMAA and DMAAm in aqueous solutions. In addition, they showed opposite photo-responses, that is, DMAA becomes soluble (“on” state) and DMAAm

becomes insoluble (“off” state) under the same UV light irradiation. This can be useful for photo-switchable devices.

In particular, DMAAm with 9.6 mol % of AZAAm and DMAA with 5.9 mol % of AZAA demonstrated the opposite photo-responses at 37 - 40 °C in 100 mM PB pH7.2, which is appropriate condition for the SA conjugate. While, DMAAm with 5.5 mol % of AZAAm and DMAA with 6.0 mol % of AZAA demonstrated the opposite photo-responses at 37 - 40 °C in 50 mM AB pH5.5, which is suitable for EG III conjugate. DMAAm-VS with three different MW of (Mn: 3, 6, 10 kDa) were also synthesized for EG III conjugation.

In the following chapter, using these polymers, we have developed photo-switchable proteins, which can be both “on” and “off” by the same UV or VIS light stimulus, where the wavelength will not damage the proteins.

CHAPTER 3 STREPTAVIDIN-PHOTORESPONSIVE POLYMER CONJUGATES

3.1 INTRODUCTION

We have selected streptavidin (SA) as the first model protein to develop photo-switchable proteins. SA shows a remarkably high affinity for its ligand, biotin ($K_d = 10^{-13}$ M). This unusual interaction is utilized in a wide variety of biological, clinical, and diagnostic applications. On the other hand, it is very difficult to dissociate bound biotin from SA. Therefore, most applications involve only one-way irreversible bindings. However, the recovery of bound biotin or biotinylated molecules from SA is desirable for many practical and economical reasons. Photo-switching of the biotin-SA association will expand the possible applications of this high affinity pair.

We have been developing a reversible biotin-binding and releasing system using site-specific conjugation of stimuli-responsive polymers to mutant SAs [87-89]. To date, we have succeeded in controlling the binding and release of biotin or biotinylated proteins by using temperature or pH stimuli.

In this chapter, we describe new site-specific conjugates that respond to UV and VIS light irradiations. The conjugates were constructed using two kinds of end-reactive photo-responsive polymers, DMAAm-VS, and DMAA-VS, and two SA mutants, E116C and S139C, which have differing conjugation sites. DMAA and DMAAm are dual stimuli-responsive polymers (temperature and light) (chapter 2). Thus, the conjugates were expected to exhibit both thermo- and photo-responses for biotin-binding. First, we focused on the thermo-responsive properties of these conjugates, and then their photo-responsive behaviors were investigated. Using these conjugates, we have evaluated three key factors that influence the temperature- or photo-induced biotin-binding and releasing

properties of the conjugates. These factors are the conjugation site, the MW of the conjugated polymer, and the addition of free polymer to the conjugate solution.

3.2 MATERIALS AND METHODS

3.2.1 MATERIALS.

Ethylenediamine tetraacetic acid (EDTA), 4-phenylazomaleinanil (PAM) (Aldrich, Milwaukee, WI), tris(2-carboxy ethyl)-phosphine hydrochloride (TCEP) (Pierce, Rockford, IL), iminobiotin beads, cysteine hydrochloride (Pierce, Rockford, IL), Microcon-30, Centriprep-10 (Millipore, Bedford, MA), and [³H]Biotin (d-[8,9-³H(N)]-Biotin, Dupont, Wilmington, DE) were used as received. All other reagents were of analytical grade. Restriction enzymes (MscI, MluI, and HindIII) and T4 DNA Ligase were purchased from New England Biolabs (Beverly, MA). Qiaex II kit for extracting DNA was purchased from Qiagen (Santa Clarita, CA). pET21a vector was obtained from Novagen (Madison, WI).

3.2.2 GENETIC ENGINEERING OF SA.

The SA mutant E116C and S139C were constructed by site-directed, cassette mutagenesis, using a synthetic 'core' SA gene previously designed and constructed for protein expression in *Escherichia coli* [85]. Oligonucleotides were designed to substitute cysteine for the glutamic acid at position 116 or the serine at position 139. The following sense and anti-sense oligonucleotides were obtained from Integrated DNA Technologies (Coralville, IA). (The underlined bold-face type indicates amino acid changes):

E116C:

5'CCAGTACGTTGGTGGTGCTGAAGCTCGTATCAACACCCAGTGGTTGTTGAC
CTCCGGCACCACCTTGCGCTAA-3'

3'GGTCATGCAACCACCACGACTTCGAGCATAGTTGTGGGTCACCAACAACCTG
GAGGCCGTGGTGGACGCGATTGCGC-5'

S139C:

5'CGCGTGGAATCCACCCTGGTTGGTCACGACACCTTCACCAAAGTTAAACC
GTCCGCTGCTTGCTAAATAAA3'

3'ACCTTTAGGTGGGACCAACCAGTGCTGTGGAAGTGTC AATTTGGCAGGCGA
CGAACGATTATTTTCGA5'

The SA gene in pUC18 was digested with MscI and MluI restriction enzymes for E116C, and MluI and HindIII for S139C, isolated on a 1.2 percent agarose gel, extracted and purified using Qiaex II kit. The synthetic oligonucleotides, designed with the same restriction enzymes, were annealed and ligated into the pUC18/SA vector using T4 DNA Ligase. The DNA sequence of the mutant gene was confirmed using automated dye-deoxy sequencing (PE Applied Biosystems, Foster City, CA). The SA mutant gene was subsequently subcloned into pET21a for expression in *E.coli* strain BL21(DE3). The protein was expressed and refolded using established protocols [85]. Analysis of the SA mutant included SDS-PAGE, mass spectrometry, and biotin binding studies.

3.2.3 CONJUGATION OF POLYMER TO SA.

The DMAA-VS and DMAAm-VS synthesized for SA conjugation in chapter 2 were used as temperature- and photo-responsive polymers. Conjugation of the polymer to the SA mutant (E116C or S139C) was carried out in 100 mM sodium tetraborate buffer, pH 8.0, containing 50 mM sodium chloride and 5 mM EDTA (Figure 3.1). Cysteine residues in

E116C or S139C form disulfide bonds during storage. In order to reduce disulfide bonds to sulfhydryl groups, TCEP at 50-fold molar excess to the mutants was added into the solution, which was then rotated at room temperature for 20 min. Then, DMAA-VS or DMAAm-VS was added in 50-fold molar excess to the mutants to obtain high conjugation efficiency, and reacted for 1 h at room temperature. The reaction was then continued for 24 h at 4 °C.

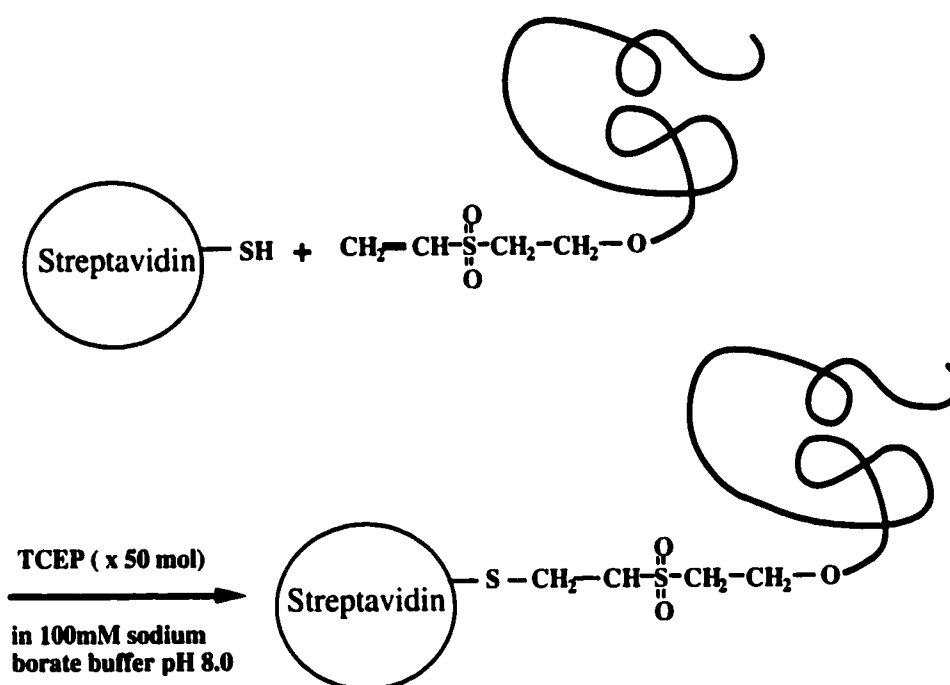


Figure 3.1. Specific conjugation of a photo-responsive polymer to a streptavidin (SA).

The conjugates were separated from the unconjugated mutants by thermally-induced precipitation, i.e., centrifuging the mixture at 15000 rpm (31000g) for 15 min at 52 °C (Figure 3.2). The unconjugated mutants were retained in the supernatant. The thermally-induced precipitation was repeated three times.

Further purification was carried out using an iminobiotin column to remove the conjugates from the free polymers. Iminobiotin has been used for purifying SA and avidin due to its reversible binding to these proteins at different pHs (Figure 3.2). The conjugates were bound to iminobiotin beads in binding buffer (50 mM sodium carbonate buffer, 500 mM sodium chloride, pH 11) at room temperature, and the free polymers were washed off under these conditions. Then, bound conjugates were eluted in elution buffer (100 mM acetic acid, pH 2.6) at room temperature. The purified conjugates were condensed by a Centriprep-10 (MW cut off: 10 kDa) to 30 – 300 µg/ml.

3.2.4 CONJUGATION OF AZOBENZENE TO SA.

As a control, azobenzene (AZ) was directly conjugated to SA (E116C) site-specifically. 4-phenylazomaleinanil (PAM) was reacted with the cysteine in E116C (Figure 3.3). Maleimide groups react with thiols of cysteines specifically at pH 7.0. To reduce disulfide bonds formed between E116Cs to thiol groups, TCEP at 50-fold molar excess to E116C was added into the E116C solution (100 mM sodium phosphate buffer, pH 7.0, containing 5 mM EDTA) and rotated at room temperature for 20 min. PAM in 50-fold molar excess to E116C was dissolved in DMF (10 % volume of the EG III solution), and mixed with the E116C solution. The reaction proceeded for 1 h at room temperature with rotation, followed by the rotation overnight at 4 °C. The conjugate was purified from the unreacted PAM by ultrafiltration using Centriprep-10. The conjugation was confirmed by

the absorbance at 350 nm (due to azobenzene conjugated to E116C), and also by electrospray ionization mass spectrometry (ESI-MS).

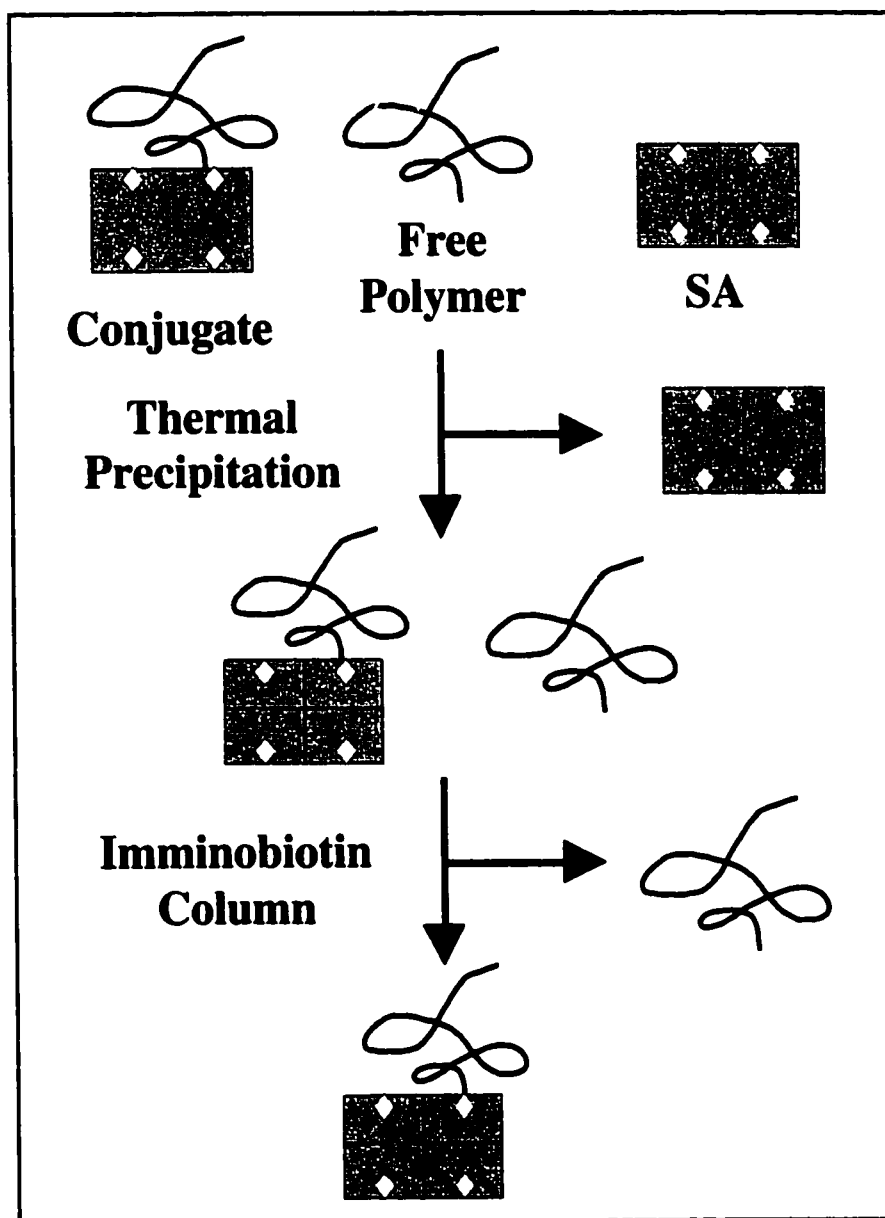


Figure 3.2. Scheme of purification of the conjugate.

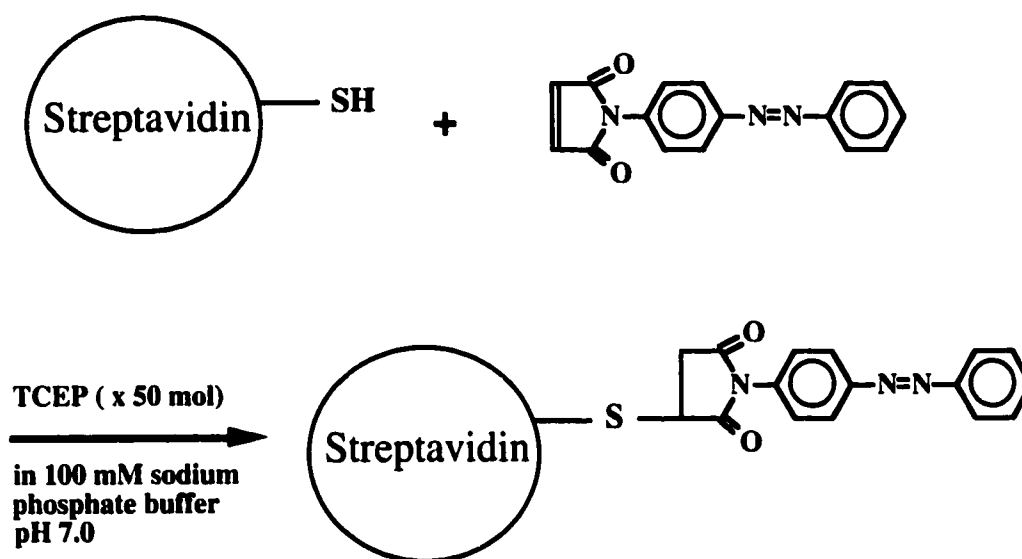


Figure 3.3. Specific conjugation of an azobenzene to a streptavidin (SA).

3.2.5 PHOTO-IRRADIATION.

The same method as described in chapter 2 was employed.

3.2.6 TEMPERATURE-RESPONSIVE BIOTIN-BINDING ASSAY

[³H]Biotin was employed to quantitate biotin binding. The procedure is schematically shown in Figure 3.4. A 10 µg sample of the conjugate was suspended in 0.9 ml of 100 mM sodium phosphate buffer (pH7.4) containing 50 mM sodium chloride and 5 mM of EDTA. A 100 µl mixture of ³H-biotin and unlabeled biotin (1 % of ³H-biotin) was added to the conjugate solution after incubation at 52 °C for 1 h. The ratio of total biotin/biotin binding sites was 1.5 (molar ratio). The solution was incubated at the temperature for the

assay, and a 100 μ l aliquot was taken at the end of each incubation. The unbound biotin was separated from the bound biotin by ultrafiltration of the aliquot using a Microcon-30 (MW cutoff: 30 kDa) at the incubation temperature of the solution. A 30 μ l aliquot of the filtrate that contained unbound biotin was counted in a β -counter (LS7000 Liquid scintillation system, Beckman Instruments, Inc. Fullerton, CA) to determine the unbound biotin. The biotin binding could be quantitated by the depletion of free biotin in the solution.

3.2.7 PHOTO-RESPONSIVE BIOTIN-BINDING ASSAY

The procedure is schematically shown in Figure 3.5. A 10 μ g sample of the conjugate was suspended in 1.2 ml of 100 mM sodium phosphate buffer (pH7.4) containing 50 mM NaCl and 5 mM EDTA. A 100 μ l mixture of 3 H-biotin and unlabeled biotin was added to the conjugate solution after incubation at 40 $^{\circ}$ C for 1 h. The ratio of total biotin/biotin binding sites was 1.5 (molar ratio). A 50 μ l aliquot was taken in the time course of the sampling. The unbound biotin was separated from the bound biotin by ultrafiltration of the aliquot using a Microcon-30 (Mw cut off: 30 kD) at 40 $^{\circ}$ C. A 30 μ l aliquot of the filtrate that contained unbound biotin was submitted to a β -counter (LS7000 Liquid scintillation system, Beckman Instruments, Inc. Fullerton, CA) to determine the unbound biotin. The biotin binding could be quantitated by the depletion of free biotin in the solution. For the photo-irradiation, VIS light was irradiated continuously, while UV light was irradiated continuously for the first 10 min to saturate the cis form of azobenzene, then periodically for 1 min every 10 min to keep azobenzene in the cis form.

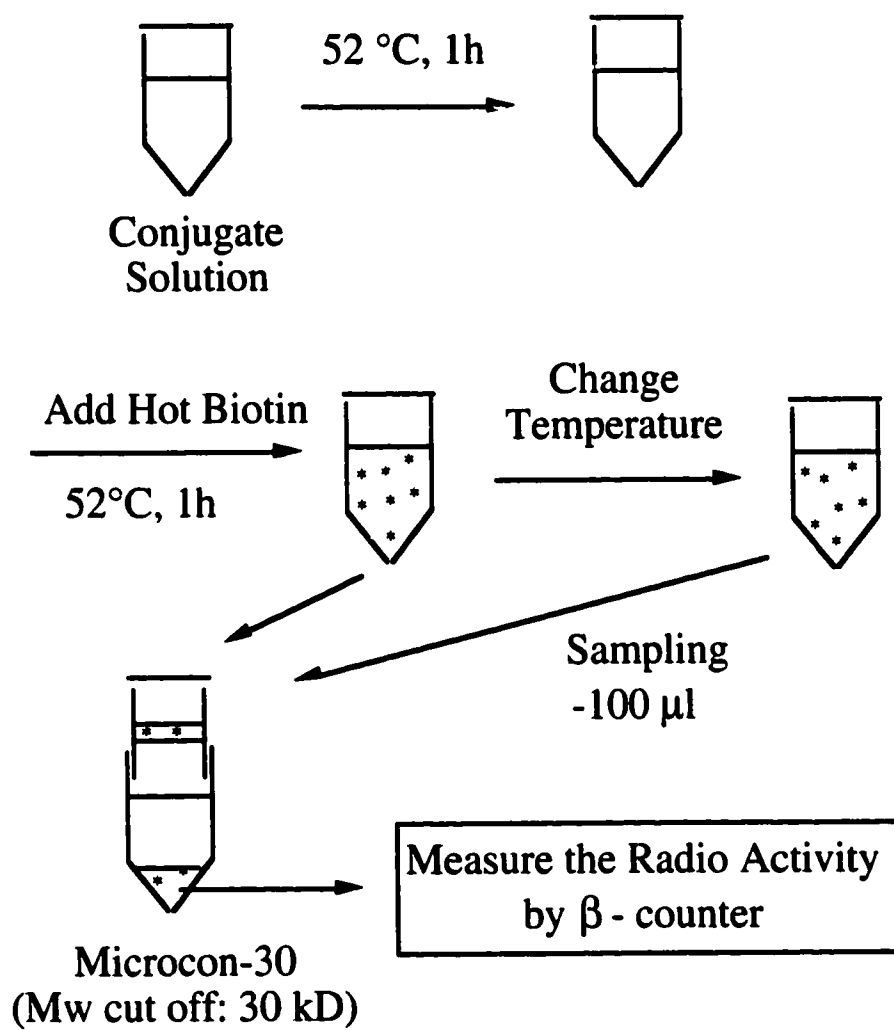


Figure 3.4. Temperature responsive biotin-binding assay.

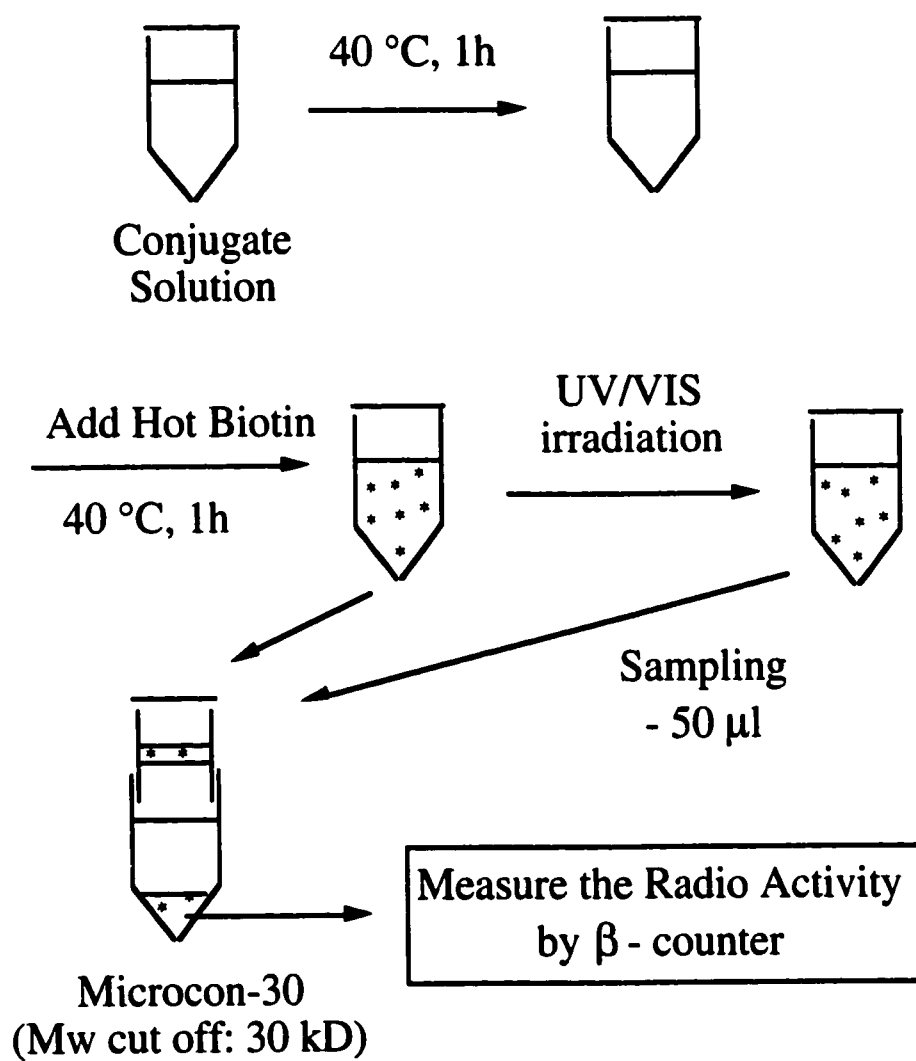


Figure 3.5. Photo-responsive biotin-binding assay

3.3 RESULTS AND DISCUSSION

3.3.1 PREPARATION OF SA MUTANTS

We have used cassette site-directed mutagenesis to create the SA mutants, E116C and S139C. Figure 3.6 shows the 3-D structure of SA. Each subunit of E116C has only one cysteine residue that replaces the glutamic acid at position 116. Trp120 is one of the key residues which interacts with the biotin via van der Waals forces. Near the Trp120, residue 116 may have a significant impact on the binding of biotin. S139C has a cysteine at the 139 position, which is the C-terminus of SA, and is not involved in biotin-binding activity. Therefore, using these mutants, we can elucidate the effect of the conjugation position on the biotin binding ability.

3.3.2 SA-DMAA OR DMAAM CONJUGATION

The polymers were conjugated to SA site-specifically by reaction of the VS group at the end of the polymer with the sulfhydryl groups of the protein. The conjugate was separated from the unreacted SA by thermally induced precipitation of the polymer, and then separated from the free polymer by imino-biotin column purification.

The ratio of polymer/SA of the conjugates were evaluated by UV/VIS absorbance of the purified conjugates. The absorbance at 280 nm, 325 nm, and 335 nm were used as the representative absorbance of SA, DMAA, and DMAAm respectively. The absorbance at 280 nm from the polymer was subtracted from the absorbance of the conjugate solution to determine the concentration of SA in the conjugate. The ratios of polymer/SA determined are shown in Table 3.1. The ratios were almost two. Thus, two binding pockets out of four pockets of SA were conjugated to the polymers, and the other two sites were not conjugated. This might be reasonable, since when one polymer is conjugated, the adjacent conjugation site might be blocked by the polymer. This results in two polymers conjugated to one SA.

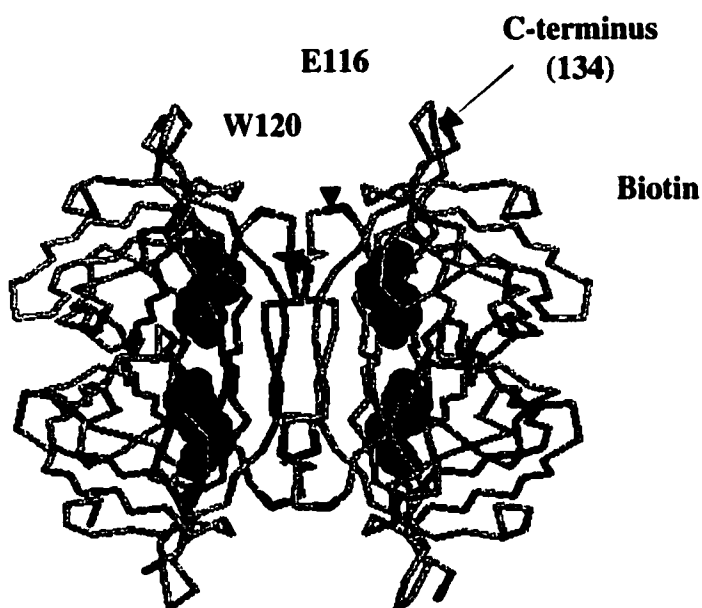


Figure 3.6. 3-D molecular structure model of streptavidin (SA)

3.3.3 SA-AZ CONJUGATION

The conjugation of azobenzene to E116C was confirmed by the absorbance at 350 nm from the azobenzene. The Mw of the conjugate was determined to be 13523 Da by ESI-MS, which corresponds to one azobenzene conjugated to one monomer of E116C. In addition, there was almost no unconjugated E116C detected by ESI-MS. Thus, we can conclude that this conjugation was site-specific and the yield of the conjugation was very high.

Table 3.1. Polymer/streptavidin (SA) ratios of the purified conjugates.

The ratios were determined by UV/VIS spectra using OD₂₈₀ for SA, OD₃₂₃ for DMAA and OD₃₃₅ for DMAAm polymer.

Conjugate	Polymer/SA ratio
E116C-DMAA	2.03
E116C-DMAAm	1.89
S139C-DMAA	2.11
S139C-DMAAm	1.93

3.3.4 TEMPERATURE-RESPONSIVE BIOTIN-BINDING

Figure 3.7 shows the biotin-binding activity changes of E116C conjugates as a function of temperature. The biotin-binding activity represents the percentage change in biotin-binding capacity of the conjugates, assuming 100 % binding at 4 °C and 0 % binding at 52 °C. The LCST of the conjugate was determined as the temperature that gave 10 % of maximum biotin-binding. The LCST of the DMAA conjugate was 35 °C, and that of the DMAAm conjugate was 40 °C, which were close to the original LCST of DMAA and DMAAm, 37 °C and 39 °C respectively.

Figure 3.8 - 3.10 show the effect of incubation time and temperature on the binding and releasing properties of biotin for the E116C conjugates and the E116C control. The biotin-binding capacity is determined assuming 100 % binding at 4 °C after 1 h incubation. For the conjugates, the biotin-binding capacity was plotted as the percentage of conjugated sites using the polymer/SA ratios in Table 3.1. Although E116C didn't exhibit any thermal response on biotin-binding, both conjugates showed biotin-blocking ability after the first incubation at 52 °C. Biotin bound completely within 1 h at 4 °C.

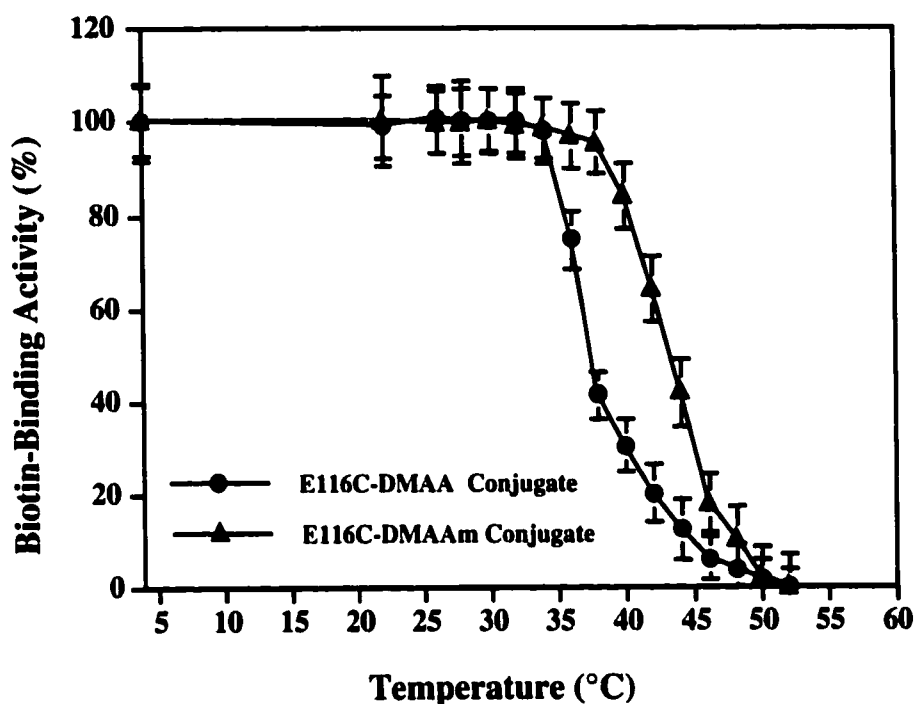


Figure 3.7. Effect of temperature on biotin-binding activity of E116C-DMAA and E116C-DMAAm conjugates containing free polymers.

Biotin-binding activity was measured in 100 mM sodium phosphate buffer pH7.4. The solution temperature was reduced from 52 °C to 4 °C stepwise, incubating for 15 min at each temperature. The biotin-binding activity represents the percentage change in biotin-binding capacity of the conjugates, assuming 100 % binding at 4 °C and 0 % binding at 52 °C.

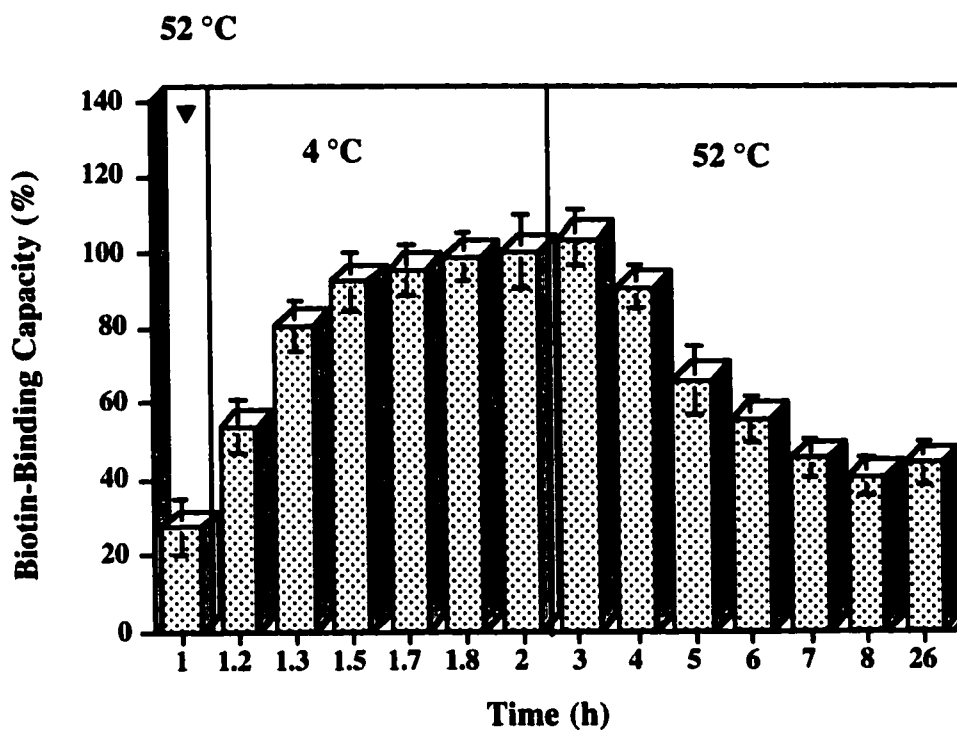


Figure 3.8. Effect of incubation time and temperature on biotin-binding capacity of E116C-DMAA conjugate containing free polymer.

The biotin-binding capacity was measured in 100 mM sodium phosphate buffer pH7.4. The biotin-binding capacity is determined assuming 100 % binding at 4 °C after 1 h incubation. The biotin-binding capacity was plotted as the percentage of conjugated sites using the polymer/SA ratios in Table 3.1.

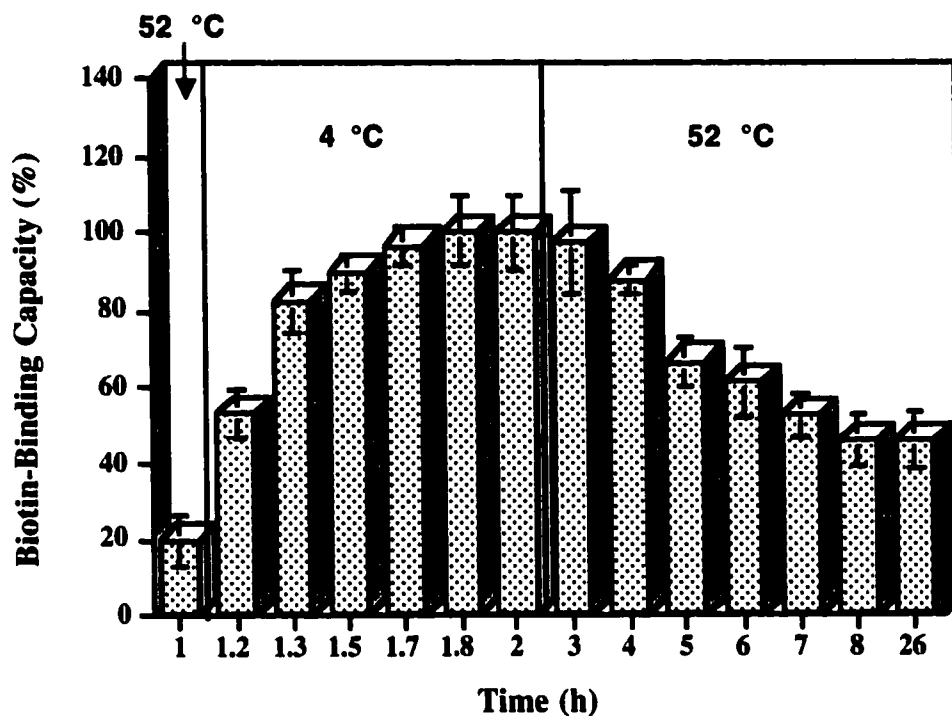


Figure 3.9. Effect of incubation time and temperature on biotin-binding capacity of E116C-DMAAm conjugate containing free polymer.

The biotin-binding capacity was measured in 100 mM sodium phosphate buffer pH7.4. The biotin-binding capacity is determined assuming 100 % binding at 4 °C after 1 h incubation. The biotin-binding capacity was plotted as the percentage of conjugated sites using the polymer/SA ratios in Table 3.1.

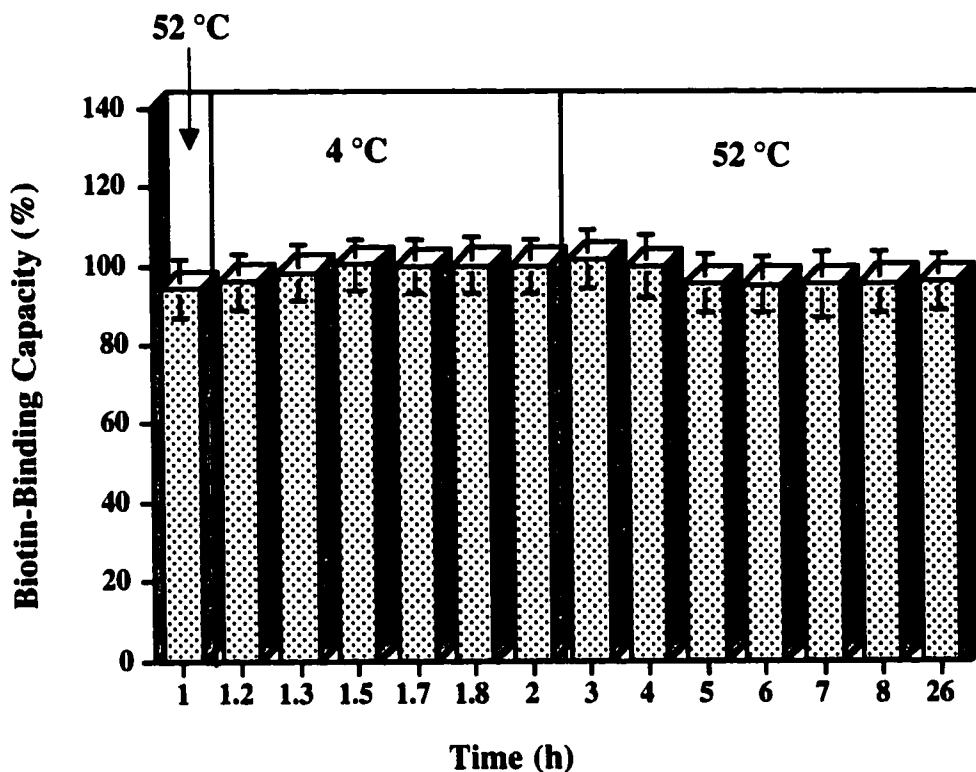


Figure 3.10. Effect of incubation time and temperature on biotin-binding capacity of E116C.

The biotin-binding capacity was measured in 100 mM sodium phosphate buffer pH7.4. The biotin-binding capacity is determined assuming 100 % binding at 4 °C after 1 h incubation.

However, the bound biotin was released gradually after the second incubation at 52 °C. The release of the bound biotin took 6 h to complete. From these data, the off rate of the bound biotin was calculated as $1.6 \times 10^{-4} \text{ sec}^{-1}$ for the E116C-DMAA conjugate, and $1.4 \times 10^{-4} \text{ sec}^{-1}$ for the E116C-DMAAm conjugate, assuming simple first order kinetics.

These values are very close to the off rate of wild type SA at 52 °C ($3.0 \times 10^{-4} \text{ sec}^{-1}$). Therefore, the release of biotin may be derived from blocking biotin from rebinding after being thermodynamically released by the phase transition of the conjugated polymer. Thus, the gradual rate of release may be due to the small off rate of the bound biotin.

Figures 3.11 and 3.12 show the thermal cycling responses for the biotin binding and release of E116C and S139C conjugates, physical mixtures of the SA and the polymers, and mutants as controls. The temperature was cycled between 4 °C and 52 °C three times. For the conjugates, the biotin-binding capacity was plotted as the percentage of conjugated sites using the polymer/SA ratios in Table 3.1. The E116C conjugate displayed a striking thermally-dependent biotin binding capacity that translated into biotin blocking and releasing activities. Moving the conjugation site away from the biotin binding site had a large effect on the switching ability, as the S139C conjugate did not display a thermal dependence above the controls of protein alone and protein/polymer physical mixtures. These results demonstrate that the switching activity is strongly dependent on the location of the conjugation site, consistent with the need for the polymer to be near the binding site. As for the S139C conjugates, the DMAA conjugate exhibited more thermal response than the DMAAm conjugate. This might be explained by the differences in MW of the conjugated polymers. Since DMAA has a larger MW (18 kDa) than DMAAm (10 kDa), the DMAA conjugate might be able to block and release the biotin more effectively.

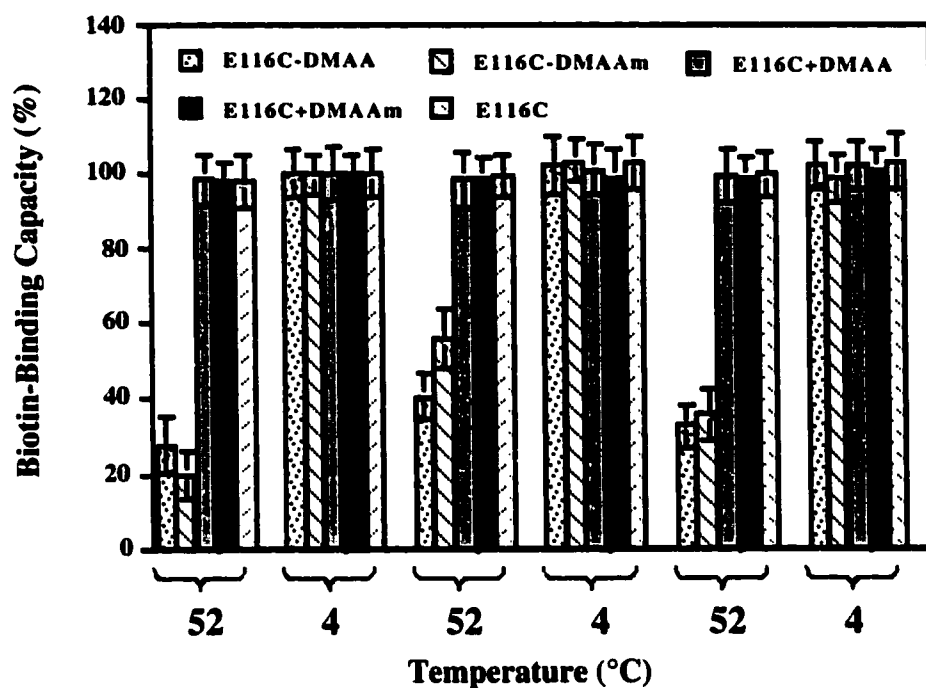


Figure 3.11. Effect of thermal cycling on biotin-binding capacity of E116C conjugates containing free polymer.

The effect of thermal cycling on the biotin-binding capacity of the E116C conjugates, physical mixtures of E116C and the polymers, and E116C in 100 mM sodium phosphate buffer at pH7.4. The biotin-binding capacity was determined assuming 100 % binding at 4 °C after 1 h incubation. The incubation times at 4 °C and 52 °C were 1 h and 6 h, respectively. For the conjugates, the biotin-binding capacity was plotted as the percentage of conjugated sites.

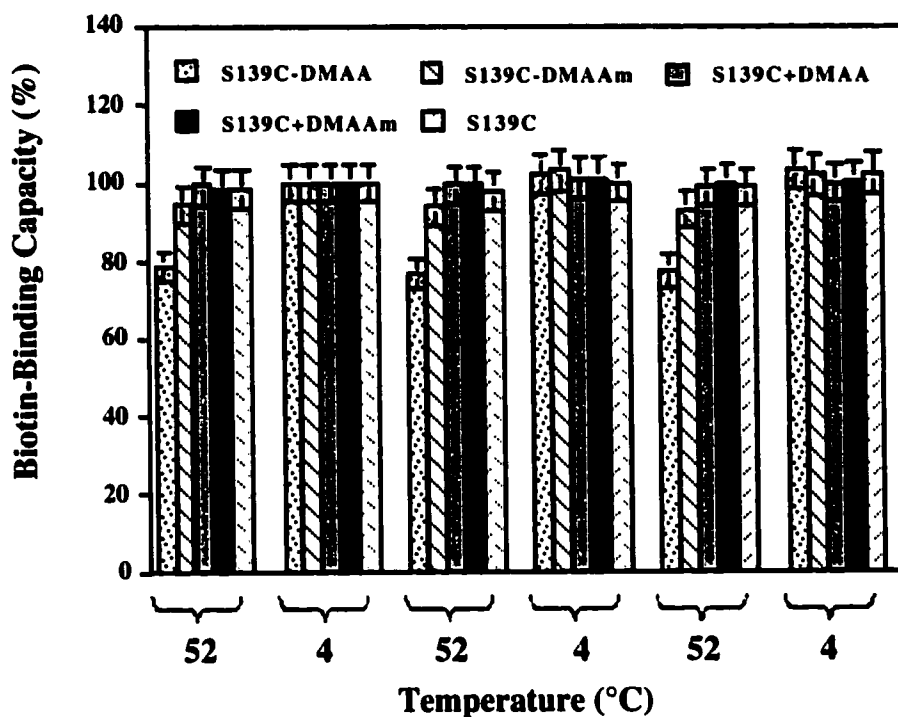


Figure 3.12. Effect of thermal cycling on biotin-binding capacity of S139C conjugates containing free polymer.

The effect of thermal cycling on the biotin-binding capacity for the S139C conjugates, physical mixtures of S139C and the polymers, and S139C in 100 mM sodium phosphate buffer at pH7.4. The biotin-binding capacity was determined assuming 100 % binding at 4 °C after 1 h incubation. The incubation times at 4 °C and 52 °C were 1 h and 6 h, respectively. For the conjugates, the biotin-binding capacity was plotted as the percentage of conjugated sites.

Iminobiotin affinity chromatography was used to purify the conjugates from free polymer. This purification allowed the study of the role of free polymer in the blocking and release switching activity. Figure 3.13 shows the effect of thermal cycling on biotin-binding of the E116C conjugates purified from the free polymers. Although the purified

conjugates showed reversible thermal responses for biotin binding, they exhibited less cycling responses than the unpurified conjugates (Figure 3.11). This suggests that the free polymer might enhance the response.

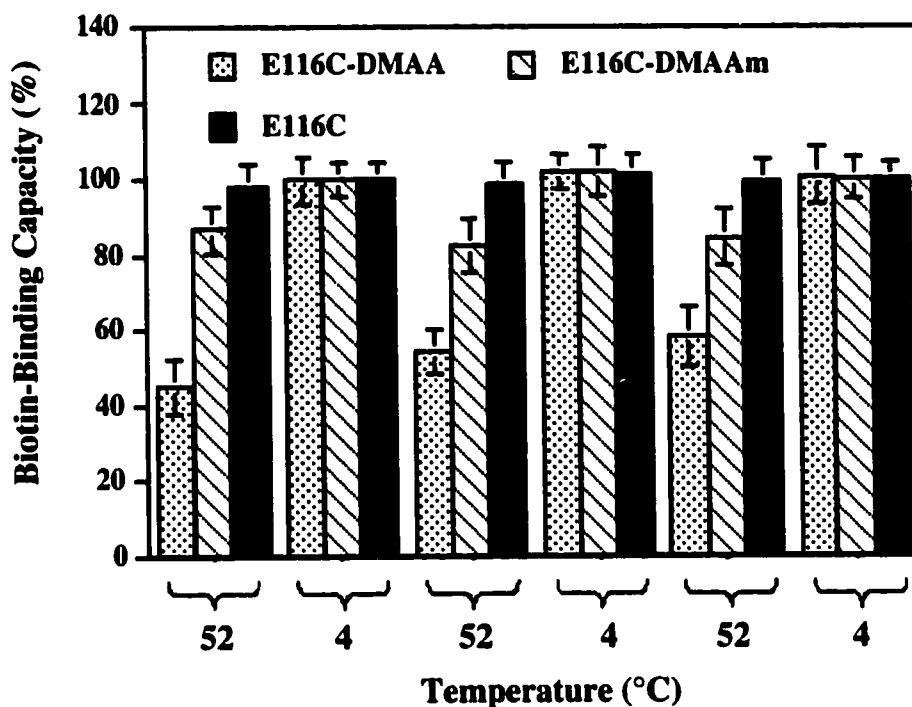


Figure 3.13. Effect of thermal cycling on biotin-binding capacity of the purified E116C conjugates.

The effect of thermal cycling on the biotin-binding capacity for the E116C conjugates purified from the free polymers, and E116C in 100 mM sodium phosphate buffer at pH7.4. The biotin-binding capacity was determined assuming 100 % binding at 4 °C after 1 h incubation. The incubation times at 4 °C and 52 °C were 1 h and 6 h, respectively. For the conjugates, the biotin-binding capacity was plotted as the percentage of conjugated sites.

The effect of free polymer addition to the purified conjugates on the thermal responses is shown in Figure 3.14. The responses increased in magnitude as more of the free polymer

was added, approaching the same level as the unpurified conjugates. This effect was clarified by characterizing the S139C conjugates. The purified S139C conjugates did not display any switching capability, and the addition of free polymer led to only a small increase in activity. Taken together with the E116C conjugates results, this suggests that the free polymer is likely aggregating with the conjugated polymer in the collapsed state. When directed to a site near the binding pocket, as with the E116C mutant, this polymer aggregate more effectively blocks biotin association. But the aggregation effect is insignificant if the free polymer is directed toward a conjugation site that is too distant from the binding site. In addition, after comparing the DMAA and DMAAm conjugates, DMAA conjugates exhibited more blocking than DMAAm conjugates. These findings confirm that the conjugation site and the MW of the conjugated polymer provide important avenues for engineering the molecular switch activity.

3.3.5 PHOTO-RESPONSIVE BIOTIN-BINDING

Since the E116C conjugates exhibited the most effective thermal switching activity for biotin-binding, the photo-switching activity of the E116C conjugates was investigated. Figure 3.15 and 3.16 show the effects of temperature and UV/VIS photo-irradiation on the biotin-binding activity of E116C-DMAA and E116C-DMAAm conjugate. A temperature of 52 °C was chosen as the maximum temperature, because the polymers collapsed completely at 52 °C. The transition temperature of biotin-binding activity of the E116C-DMAA conjugate was shifted to higher temperature upon UV irradiation. On the contrary, the transition temperature of the E116C-DMAAm conjugate was decreased upon the same UV irradiation. Between these transition temperature gaps, the conjugates were expected to exhibit photo-responsive biotin-binding. Thus, photo-responsive biotin binding assays for the conjugates were carried out under isothermal conditions at 40 °C. As a control, an azobenzene (AZ) was directly conjugated to E116C site-specifically (SA-AZ conjugate).

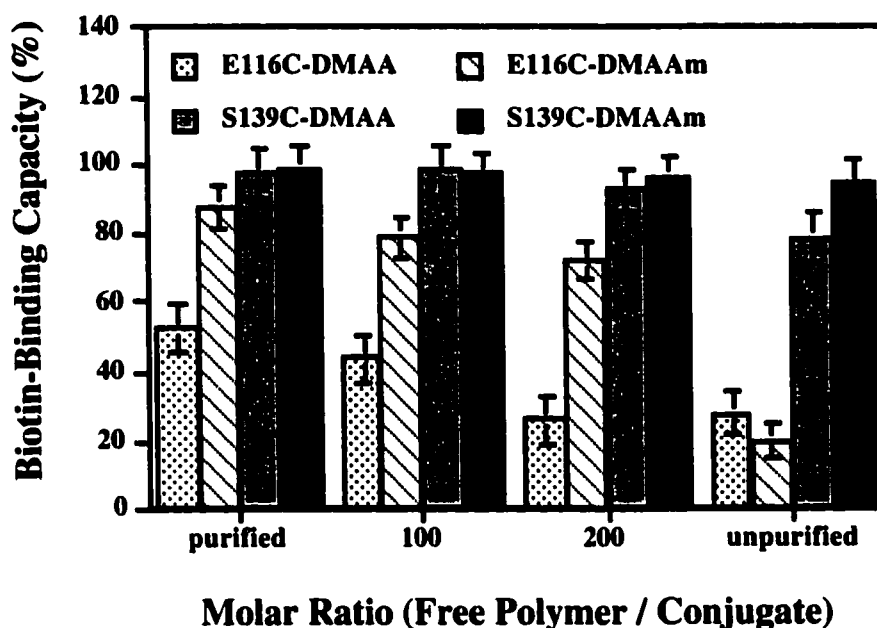


Figure 3.14. Effect of addition of free polymer on biotin-binding capacity of the purified conjugates.

The effect of adding free polymer on the biotin-binding capacity at 52 °C for E116C conjugates and S139C conjugates in 100 mM sodium phosphate buffer pH7.4. The unpurified samples were those isolated by thermal precipitation from the conjugation reaction. The biotin-binding capacity was determined assuming 100 % binding at 4 °C after 1 h incubation. The capacity was measured after incubation at 52 °C for 6 h. For the conjugates, the biotin-binding capacity was plotted as the percentage of conjugated sites. The molar ratios of free polymer/conjugate in the unpurified states were calculated as 1430 for E116C-DMAA, 385 for E116C-DMAAm, 1150 for S139C-DMAA and 364 for S139C-DMAAm conjugates by use of the conjugation conversions.

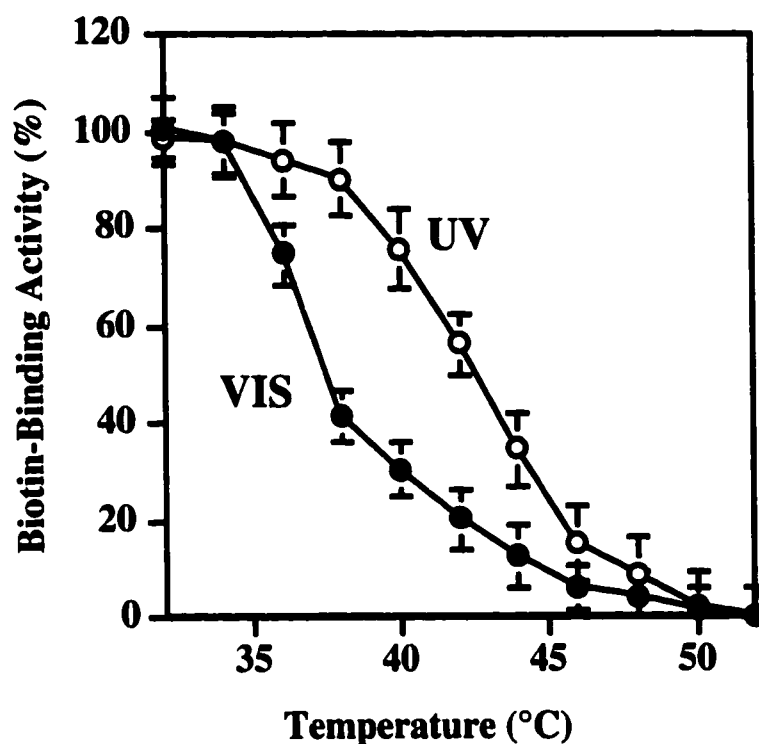


Figure 3.15. Effect of temperature and photo-irradiation on biotin-binding activity of E116C-DMAA conjugate containing free polymer.

The biotin-binding activity as a function of the solution temperature of E116C-DMAA conjugate under UV and VIS irradiation in 100 mM sodium phosphate buffer pH 7.4. The solution temperature was reduced from 52 °C to 4 °C stepwise, incubating for 15 min at each temperature under UV or VIS irradiation. VIS light was irradiated continuously. UV light was irradiated continuously for the first 10 min to saturate the cis form of azobenzene, then periodically for 1 min in every 10 min to keep the cis form. The biotin-binding activity represents the percentage change in the biotin-binding capacity of the conjugates from 4 °C to 52 °C, assuming 100 % binding at 4 °C and 0% binding at 52 °C.

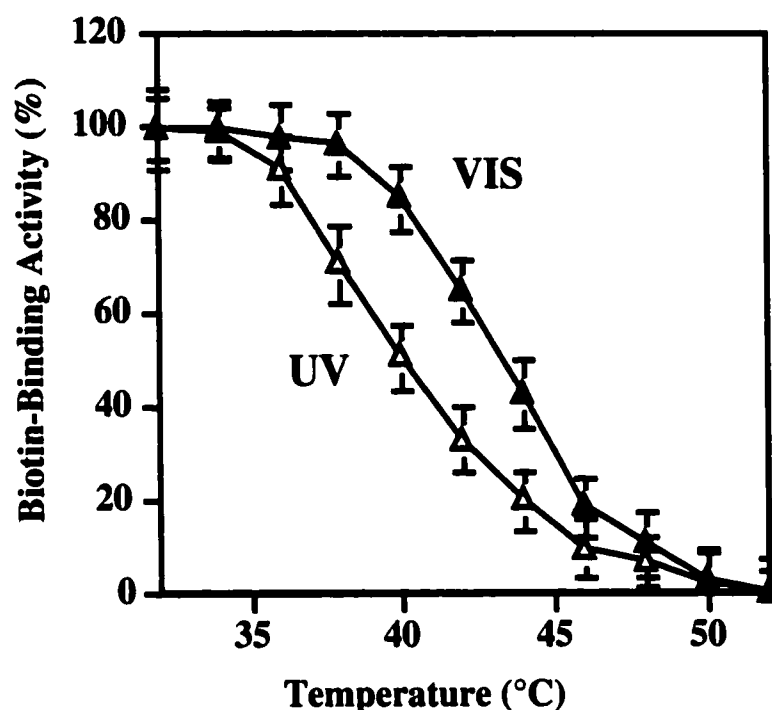


Figure 3.16. Effect of temperature and photo-irradiation on biotin-binding activity of E116C-DMAAm conjugate containing free polymer.

The biotin-binding activity as a function of the solution temperature of E116C-DMAAm conjugate under UV and VIS irradiation in 100 mM sodium phosphate buffer pH 7.4. The solution temperature was reduced from 52 °C to 4 °C stepwise, incubating for 15 min at each temperature under UV or VIS irradiation. VIS light was irradiated continuously. UV light was irradiated continuously for the first 10 min to saturate the cis form of azobenzene, then periodically for 1 min in every 10 min to keep the cis form. The biotin-binding activity represents the percentage change in the biotin-binding capacity of the conjugates from 4 °C to 52 °C, assuming 100 % binding at 4 °C and 0% binding at 52 °C.

Figure 3.17 and 3.18 show the effect of UV/VIS photo-cycling on biotin-binding to these conjugates and their physical mixtures under isothermal conditions at 40 °C. E116C-AZ conjugate and E116C were used as controls. While E116C or physical mixtures of E116C and the polymers didn't show any significant photo-responses, the E116C-DMAA conjugate exhibited a 47 % greater effect on biotin-blocking or release with VIS light than with UV light. On the contrary, the E116C-DMAAm conjugate showed a 38 % greater effect on biotin-blocking or release with UV light than with VIS light. These opposite photo-responsive phenomena agree with the photo-responsive phase transitions of the original polymers; DMAA becomes insoluble under VIS light, while DMAAm becomes insoluble under UV light. Therefore, the photo-induced biotin-blocking may be caused by the photo-induced collapse of the conjugated polymers.

The release of the bound biotin was slower than the binding step. The off-rate of the bound biotin from the biotin-SA complex was calculated from Figure 3.17 and 3.18 as $1.7 \times 10^{-4} \text{ sec}^{-1}$ for the SA-DMAA conjugate, and $1.5 \times 10^{-4} \text{ sec}^{-1}$ for the SA-DMAAm conjugate, assuming simple first order kinetics. These values are only 3.2-3.6 times larger than the off-rate of wild type SA at 40 °C ($4.7 \times 10^{-5} \text{ sec}^{-1}$). Therefore, the release of biotin may be mainly due to the inhibition of the re-binding of the released biotin due to either physical blocking by the collapsed polymer or to conformational changes in the Trp120 region of the conjugate. The slow release (e.g. over 8 hrs) of biotin may be due to the high affinity of the bound biotin. Moreover, from the observation that SA-AZ conjugate didn't show any effect of irradiation, we can conclude that the effect of the conjugated polymer is significant for controlling the biotin-binding and release from SA by photo-irradiation.

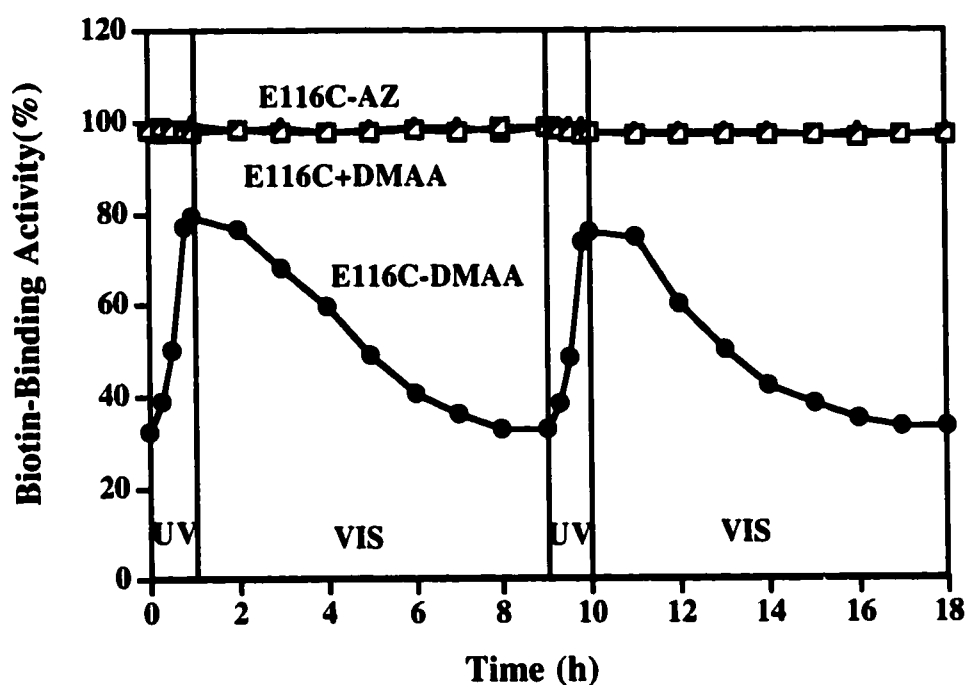


Figure 3.17. Photo-cycling effect on biotin-binding activity of E116C-DMAA conjugate containing free polymer.

Photo-responsive biotin-binding activity of E116C-DMAA conjugates, their physical mixture, and E116C-AZ conjugate in response to UV/VIS cyclic irradiation under isothermal conditions at 40 °C. VIS light was irradiated continuously. UV light was irradiated continuously for the first 10 min to saturate the cis form of azobenzene, then periodically for 1 min in every 10 min to keep the cis form. The biotin-binding activity represents the percentage change in the biotin-binding capacity of the conjugates from 4 °C to 52 °C, assuming 100 % binding at 4 °C and 0% binding at 52 °C.

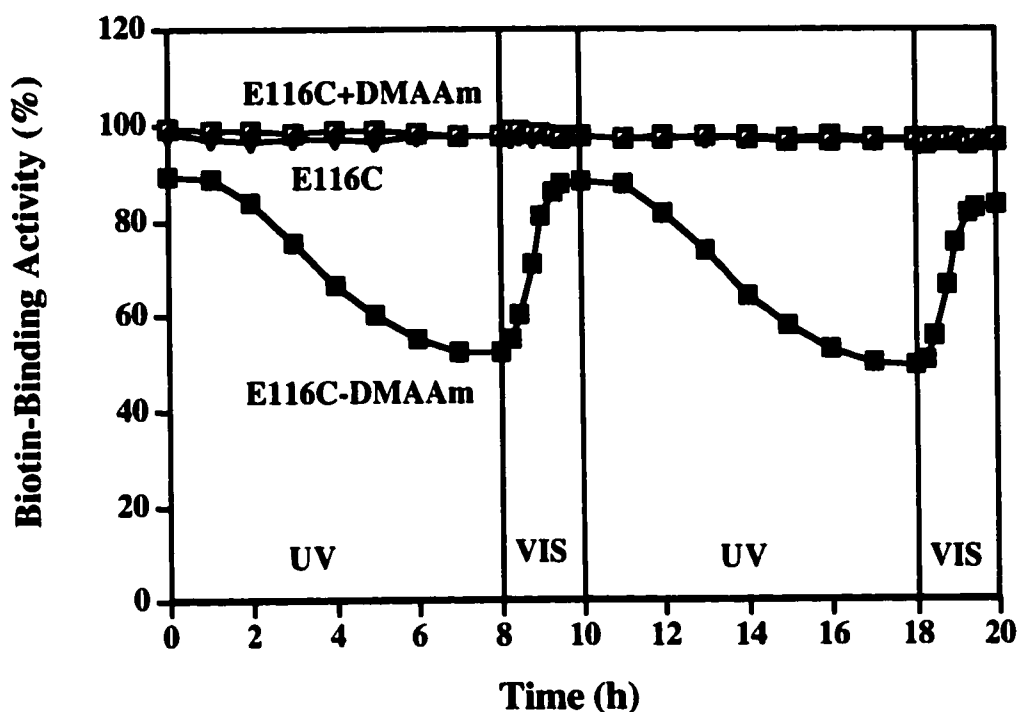


Figure 3.18. Photo-cycling effect on biotin-binding activity of E116C-DMAAm conjugate containing free polymer.

Photo-responsive biotin-binding activity of E116C-DMAAm conjugates, their physical mixture, and E116C in response to UV/VIS cyclic irradiation under isothermal conditions at 40 °C. VIS light was irradiated continuously. UV light was irradiated continuously for the first 10 min to saturate the cis form of azobenzene, then periodically for 1 min in every 10 min to keep the cis form. The biotin-binding activity represents the percentage change in the biotin-binding capacity of the conjugates from 4 °C to 52 °C, assuming 100 % binding at 4 °C and 0% binding at 52 °C.

3.4 CONCLUSIONS

We have investigated new site-specific conjugates of mutant SAs, E116C and S139C, with end-reactive temperature- and photo-responsive polymers, DMAA and DMAAm. The conjugates of E116C with DMAA or DMAAm exhibited reversible switching of biotin binding between 52 °C and 4 °C, while the conjugates with S139C did not. The E116C conjugates bound biotin at 4°C, where the polymer was hydrated, and released biotin completely at 52 °C, where the polymer was collapsed. The off rate of the conjugate in the shrunken state of the polymer was almost the same as that of wild type SA. This suggests that the release of biotin may be due to the blocking of the open binding site after biotin is released. Three key factors to improve the thermal switching property of the conjugate have been elucidated. They are the position of the conjugation, the MW of the conjugated polymer, and the addition of free polymer. When the conjugation position is close to the binding site, when the MW of the polymer is high, and when free polymer is added to the conjugate solution, the thermal response will be maximized.

The photo-responses of these conjugates for biotin binding and release were investigated upon UV/VIS light cyclic irradiation under isothermal conditions at 40 °C. The conjugates demonstrated reversible blocking and release of biotin in response to UV/VIS cycling. In addition, they exhibited the opposite photo-responses. From the biotin release data, the photo-induced biotin off rates of the conjugates were only three times larger than the off rate of wild type SA at 40 °C, suggesting that the photo-induced release of biotin from the conjugates might be due to the blocking of thermodynamically released biotin, similar to the temperature-induced release of biotin.

The site-specific conjugation of such photo-responsive polymers to genetically-engineered proteins could provide a general approach to the design and development of photo-switchable proteins, where the specific molecular recognition and binding process are controlled by external light signals.

CHAPTER 4 SITE-DIRECTED MUTAGENESIS OF EG III

4.1 INTRODUCTION

In order to create a photo-switchable enzyme, we have selected EG III as a model enzyme. EGIII has been industrially used in textile processing. One of the problems encountered using cellulase in textile application is fiber strength loss. Thus, fine control of the cellulase activity is desired. Photo-switchable EGIII will be preferable in this application.

Genencor International Inc. has cloned EG III, and established the expression systems for EGIII using *T. reesei*. and *A. niger*. These fungi have been used for industrial enzyme production for many years and are well-characterized production systems. Genencor International Inc. has provided the cloned WT EG III gene to us.

We have constructed four kinds of site-directed mutant EGIII genes, S25C, N107C, N55C and N151C. These positions were selected, based on structure-function relationship using the 3-D structure of EG III, as candidates for conjugation sites to control the catalytic activity associated with the phase transition of the conjugated polymer. These mutants were expressed, purified and characterized.

4.2 MATERIALS AND METHODS

4.2.1 MATERIALS

Restriction enzymes, XbaI and BglII, were purchased from New England Biolabs (Beverly, MA). QIA Prep Spin Plasmid Kit (QIAGEN, Santa Clarita, CA) and Quikchange Site-Directed Mutagenesis Kit (Stratagene, La Jolla, CA) were used as received. The cloned EG III gene ligated in a plasmid pGPT-pyrG1 and endoglycosidase

H were kindly provided by Genencor International Co. Butyl sepharose (Pharmacia, Piscataway, NJ), 4-phenylazomaleinanil (PAM) (Aldrich, Milwaukee, WI), bis-tris propane, ammonium sulfate, o-nitrophenyl- β -D-cellobioside (ONPC) (Sigma, St. Louis, MO), hydroxyethyl cellulose (HEC) medium Viscosity (Fluka, Ronkonkome, NY), tris(2-carboxyethyl)-phosphine hydrochloride (TCEP), BCA protein assay kit (Pierce, Rockford, IL), Ultrafree Biomax (Millipore, Bedford, MA), Precast gel (Novex, San Diego, CA), Kaleidoscope MW marker, Econo-pac 10PG (Biorad, Hercules, CA) and Fluorescein-5-maleimide (Molecular Probes, Eugene, OR) were used as received. All other reagents were of analytical grade.

4.2.2 CONFIRMATION OF EG III GENE IN THE PLASMID

The cloned EGIII gene was supplied from Genencor in a plasmid pGPT-pyrG1, which has two unique cloning sites, XbaI and BglII. The EGIII gene was inserted between these restriction sites, and was located just after the glucoamilase promoter, which is a strong promoter for transcription.

The plasmid was transformed into E.coli. (Top10⁺ (HB101)), and the transformed cell was selected from the agar plate with carbonicillin. The plasmids were isolated using a miniprep method [QIA prep spin plasmid kit (QIAGEN)]. The existence of the EG III gene was confirmed by restriction digestion by BglII and XbaI, followed by gel electrophoresis.

4.2.3 SITE-DIRECTED MUTATION OF EG III

The EG III mutant genes S25C, N107C, N55C, and N151C were constructed by site-directed PCR mutagenesis using Quikchange (Stratagene, CA), in which pfu DNA polymerase polymerizes the circular plasmid DNA completely. Then, 20 ng of the plasmid was mixed with 125 ng of the mutant primers (sense and antisense) and amplified by PCR using pfu polymerase. The product was digested by Dpn I and

transformed into Top10F'. The transformed cell was selected from the agar plate with carbenicillin, and grown in LB medium. The mutated plasmid was collected by mini-prep (QIAprep, QIAGEN).

The following primers (Integrated DNA Technologies Inc., Coralville, IA) were used for the four kinds of mutagenesis with the plasmid sent from Genencor as a template. The underlined bold sequences were the mutated portions.

1. S25C (36 bases, 58 % GC, T_m = 81 °C)

5'-p-CAACCTTTGGGGAGCAT**TGT**GCCGGCTCTGGATTTGG-3'

5'-p-CCAAATCCAGAGCCGGC**ACA**TGCTCCCCAAAGGTTG-3'

2. N107C (35 bases, 63 %GC, T_m = 82 °C)

5'-p-CACCGCAGCCAACCCG**TGT**CATGTCACGTACTCGG-3'

5'-p-CCGAGTACGTGACATG**ACA**CGGGTTGGCTGCGGTG-3'

3. N55C (35 bases, 65 %GC, T_m = 83 °C)

5'-p-GTGGTCCGGCGGCCAG**TGC**AACGTCAAGTCGTACC-3'

5'-p-GGTACGACTTGACGTT**GCA**CTGGCCGCCGGACCAC-3'

4. N151C (35 bases, 57 %GC, T_m = 80 °C)

5'-p-CGCTCTACTATGGCTACT**TGCG**GAGCCATGCAAGTC-3'

5'-p-GACTTGCAATGGCTCC**GCA**GTAGCCATAGTAGAGCG-3'

4.2.4 DETERMINATION OF DNA CONCENTRATION.

The concentration of DNA was determined from the absorbance at 260 nm by using an extinction coefficient of 50 µg ds-DNA/ml and 25 µg ss-DNA/ml .

4.2.5 DNA SEQUENCING.

ABI DNA sequencing method was used to confirm the site-directed mutations.

4.2.6 GEL ELECTROPHORESIS FOR DNA

The plasmids were digested by restriction enzymes, Bgl II, Xba I, and Sal I, and run in an agarose gel (1.2 wt % agarose) under 100 mA constant current at room temperature. The DNA was stained using ethidium bromide.

4.2.7 EXPRESSION OF THE MUTANT EG IIIS

Plasmid pGPTpyrG I was used to express EG III in *A. niger*. In the plasmid, the *T. reesei* genomic clone of EG III was placed after the strong glucoamylase (GAM) promoter for *A. niger*. The vector was transformed into an *A. niger* strain, dgr246p2. Transformants were selected on media lacking uridine and then screened for high remazol brilliant blue carboxymethylcellulose (RBB-CMC) activity in shake flask culture. The best producers in shake flasks were grown in 15 liter fermentors.

4.2.8 PURIFICATION OF THE MUTANT EG IIIS

Fermentation broths were treated by Endoglycosidase H (Endo H) to break heterogeneous glycosylation. EndoH (9 mg/ml) was added into the fermentation broth to a final dilution of 50 to 1 and incubated at 37 °C overnight. Ammonium sulfate (AS) was added to a concentration of 0.5 M, and centrifuged for 10 min. The pellet was discarded. A 20 ml sample of butyl sepharose beads in a drip column was equilibrated with 0.5 M AS in 50 mM Bis-Tris Propane, pH 5.5. A 15 ml volume of the enzyme solution

(supernatant) was loaded and washed with 3 volumes of the equilibration solution. The EG III was eluted from the beads by 50 mM bis-tris propane pH 5.5 without AS. The fractions that had absorbance at 280 nm were collected. The buffer was exchanged to 50 mM sodium acetate buffer (AB) pH 5.5 and condensed to 1 mg/ml concentration by using an ultracentrifuge membrane (Ultrafree, MW cut off; 5 kDa).

4.2.9 DETERMINATION OF THE MUTANT EG IIIS

To determine the correct expression of the site-directed mutant EG IIIs, SDS-PAGE, ESI-MS, N-terminal sequencing (University of Oregon) and peptide mapping methods (Genencor International Inc.) were used.

4.2.10 DETERMINATION OF PURITY OF THE MUTANT EG IIIS

The purity of the mutant was evaluated from the SDS-PAGE gel. The SDS-PAGE gel for the mutants with 10 mM DTT were stained by coomassie brilliant blue (CBB). The gel was scanned and the CBB density was quantitated by Image Quant (Molecular Dynamics). The area of each peak was integrated and the percentage of the EG III mutant peak was calculated.

4.2.11 CONJUGATION OF FLUORESCEIN-5-MALEIMIDE (F-MI) TO EG III MUTANTS

To determine the reactivity of the genetically introduced Cys, the mutant EG III was conjugated to F-MI in 100 mM sodium phosphate buffer pH 7.0 (c.f. Figure 3.2). Briefly, 200 µg of EG III mutant in 100 mM sodium phosphate buffer (pH 7.0) was prepared by exchanging the buffer using Ultrafree (MW cut off : 5 kDa). A 10-fold molar excess of TCEP was added to the EG III solution to reduce disulfide bonds to sulfhydryl groups. A 50-fold excess of F-MI was dissolved in DMF (10% volume of the total conjugation solution), and mixed with the EG III solution (EG III / TCEP / F-MI = 1 / 10 / 50 molar ratio). The reaction solution was rotated at 4 °C overnight. After the reaction, the buffer

was exchanged to 50 mM AB pH5.5. The conjugate was separated from unconjugated F-MI by a polyacrylamide desalting column (Econopac 10PG, Biorad).

4.2.12 CATALYTIC ACTIVITY ASSAY

We have used two kinds of substrates, ONPC and HEC, for the activity assay of EG III in order to investigate the effect of the size of the substrate on the activity. The substrate concentration and the incubation time were varied. The kinetic parameters, Michaelis constant (K_m) and turnover number (k_{cat}), were determined by a Lineweaver-Burk plot assuming Michaelis-Menten kinetics, and were compared with those of WT EG III.

4.2.12.1 ONPC Assay

ONPC is a chromogenic substrate. ONPC is hydrolyzed by EG III to generate a dye (nitrophenol), which is detected at 405 nm absorption (Figure 4.1). The activity of EG III was measured in 50 mM sodium acetate buffer pH 5.5. A 900 μ l sample of ONPC (2 – 10 mM) and a 100 μ l sample of EG III (1 μ M) solutions were pre-incubated at 40 °C and 52 °C. The reaction was initiated by addition of ONPC into the EG III solution in a total volume of 1 ml, and was incubated at each temperature. A 100 μ l aliquot was taken from the reaction solution, and the reaction was terminated with the addition of 50 μ l of 200 mM glycine buffer, pH10. Samples were taken at 8 – 10 different time points in order to produce reliable values for the initial velocities. The absorbance at 405 nm was measured in a microtiter plate reader (Benchmark, BioRad). The concentration of nitrophenol was calculated using the extinction coefficient at 405 nm.

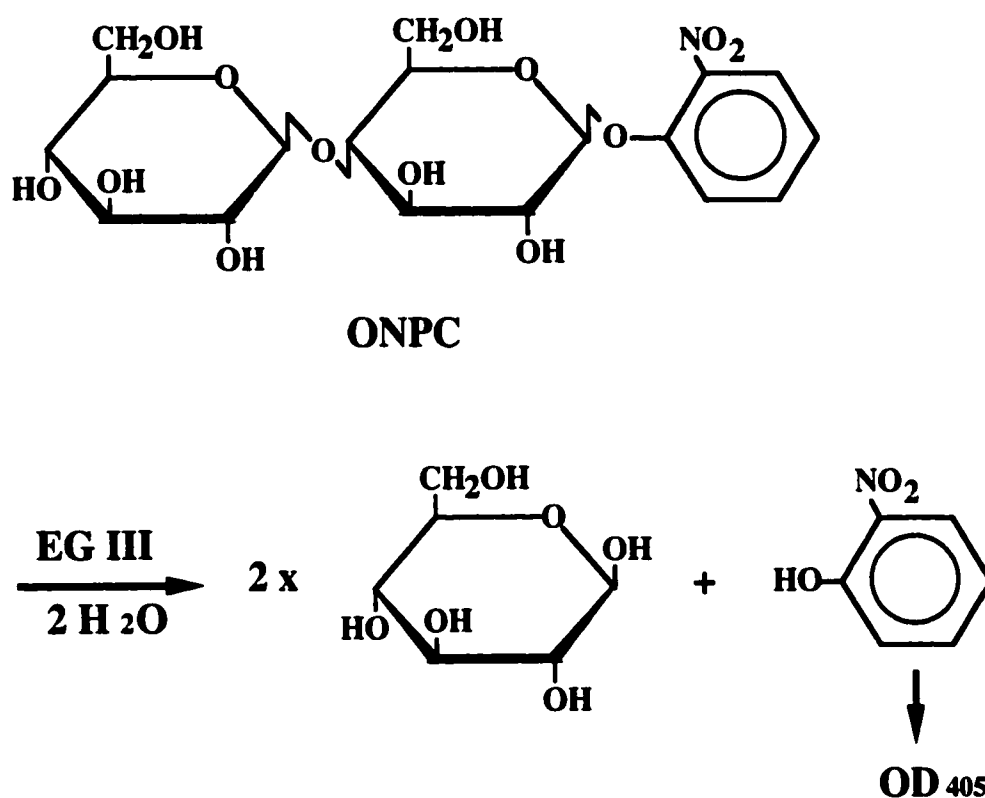


Figure 4.1. Catalytic activity assay of EG III using o-nitrophenyl- β -D-cellobioside (ONPC) as a substrate.

4.2.12.2 HEC Assay

HEC is a soluble cellulose derivative, which is hydrolyzed by EG III, and generates hydroxyethyl glucose. The activity of EG III was evaluated by measuring the amount of

produced glucose amount, which was quantitated by p-hydroxybenzoic acid hydrazide (PHBAH) reagent. PHBAH reacts with glucose producing glucosazone, which is detectable at 405 nm. (Figure 4.2). Briefly, A 100 μ l sample of EG III (1 μ M) and a 900 μ l sample of HEC (Cellulose WP-40, Fluka-BioChemika) (0.25 - 2 w/v %) solutions in 50 mM sodium acetate buffer (pH 5.5) was pre-incubated in a microtube at each temperature. The reaction was initiated by addition of HEC into EG III solution in a total volume of 1 ml, and was incubated at 40 °C or 52 °C. A 100 μ l aliquot was taken from the reaction solution, and the reaction was stopped by the addition of 50 μ l of 2 % NaOH solution. Samples were taken at 8 – 10 different time points in order to produce reliable values for the initial velocities. In order to quantitate the glucose amount, 20 μ l of the reaction solution was mixed with 400 μ l of PHBAH solution (1 w/v % in 0.3 N NaOH) in a microtube. The top of the cap of the microtube was punctured with a syringe needle. Then, the tube was placed in boiling water for 10 min (for steam treatment). The solution was cooled and 200 μ l of the solution was placed into microtiter wells. The absorbance at 405 nm was measured. The glucose concentration was calculated from a standard curve produced from a series of glucose concentrations.

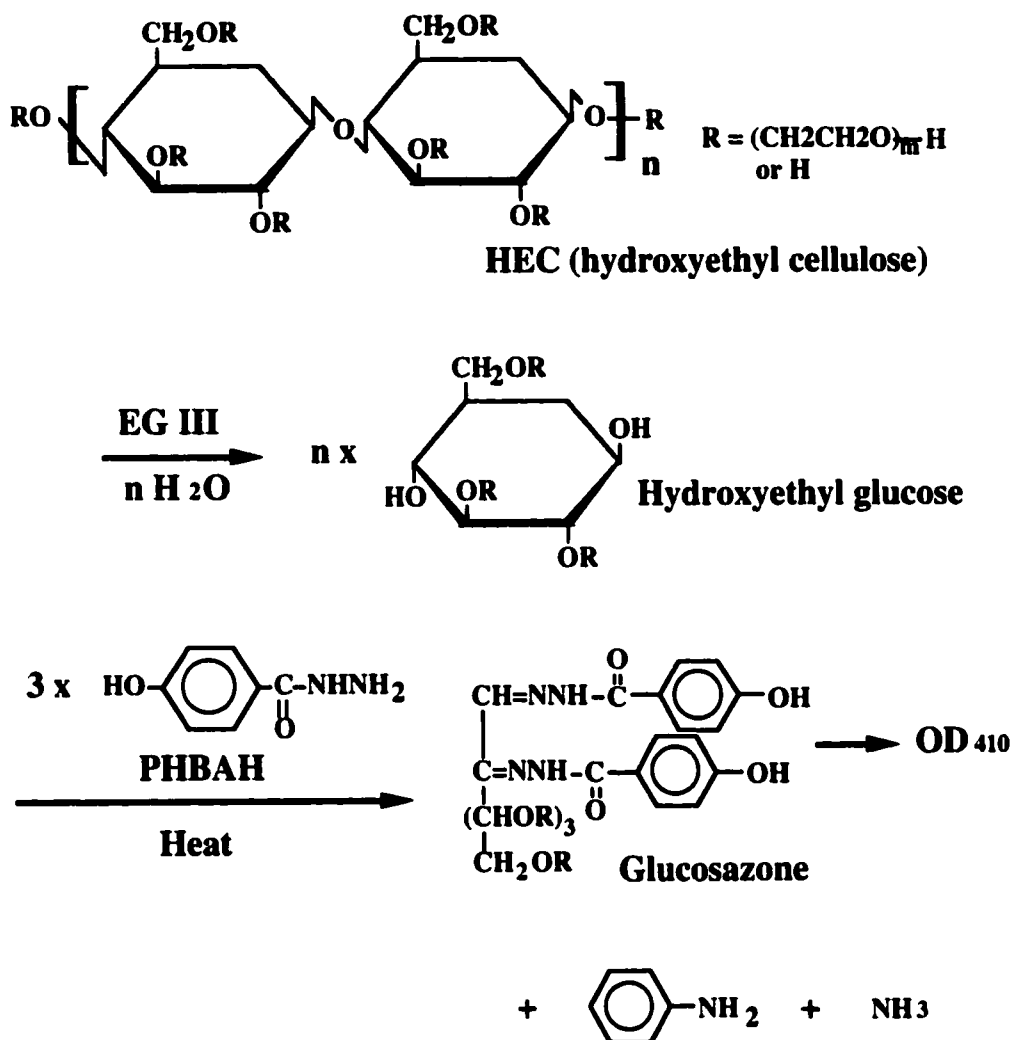


Figure 4.2. Catalytic activity assay of EG III using hydroxyethyl cellulose (HEC) as a substrate.

4.3 RESULTS AND DISCUSSION

4.3.1 STRUCTURE AND PROPERTY OF WT EG III

WT EGIII has a Mw of 23.5 kDa and a near-neutral pI of 7.4. The optimum pH is pH 5.5 and the optimum temperature is between 40 °C and 55 °C. Thus, the catalytic activity assay was performed in 50 mM AB pH 5.5 at 40 °C and 52 °C. EG III consists of 218 amino acid residues with two cysteines at positions 4 and 32, which form an inner disulfide linkage to stabilize the protein, and two putative N-linked glycosylation sites (NTT, NYS), however it was reported that the specific activity is unaffected by glycosylation by Genencor International Inc. The secondary structure of EG III is composed of three β -sheets and a small α -helix.

The conjugation site should be located at a position close enough to the catalytic active site to influence the activity when the polymer is collapsed; however, it should not influence the activity when the polymer is hydrated and expanded. We have selected four positions to be mutated to a cysteine for site-specific conjugations with photo-responsive polymers. They are S25, N107, N55, and N151. Figure 4.3 shows a 3-D schematic structure of EG III, showing the site-directed mutation positions we selected, catalytic active site (E116, E200, D99), the N-term (Q1), and the C-term (N218) (PDB was provided by Genencor International Inc.). N55 and N151 are located at positions closer to the active site than S25 and N107. Using these mutants, we can compare the effect of conjugation position on the switching activity.

4.3.2 SITE-DIRECTED MUTATION OF EG III

A site-directed mutagenesis method (Quikchange, Stratagene, CA) was used to construct the EG III mutants. The plasmid pGPT-pyrG1 provided by Genencor was transformed to *E.coli*. (Top10⁺ (HB101)). The transformed *E.coli*. was selected from the agar plate with carbonicillin and grown. The plasmid was isolated by using a miniprep method (QIA prep spin plasmid kit (QIAGEN)). The existence of EG III gene was confirmed by

restriction digestion by BglII and XbaI, followed by gel electrophoresis. We used the plasmid as a template, and eight kinds of primers listed in 4.2.3 for the site-directed mutations. The side-directed mutations were confirmed by ABI DNA sequencing method.

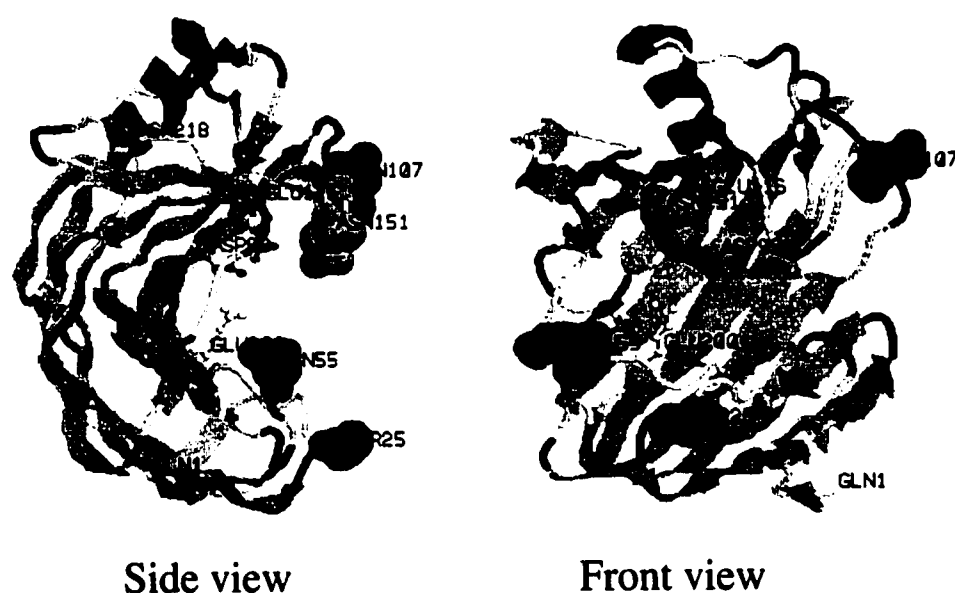


Figure 4.3. Molecular model of endoglucanase III (EG III).

The positions of mutations (S25, N55, N107, N155), possible catalytic active sites (D99, E116, E200), N-terminus (Q1) and C-terminus (N218) are shown.

4.3.3 EXPRESSION, PURIFICATION AND EVALUATION OF THE SITE-DIRECTED MUTANTS OF EG IIIS

The four kinds of EG III mutant genes were transformed into and expressed by *A. niger*. The secreted EG IIIs were purified from their fermentation broths using hydrophobic interaction chromatography.

The expression yields of the mutants are summarized in Table 4.1. There were large differences in the yields among them. N55C showed the highest yield, followed by S25C. The results of SDS-PAGE for the mutants are shown in Figure 4.4. S25C and N55C have a major band at 25 kDa, which correspond to EG III (MW: 23.5 kDa), but N107C and N151C have a major band at 180 kDa, which is not EG III. There is no dimerization detected by SDS-PAGE for any of the mutants. Figure 4.5 shows the catalytic activities of these mutants toward ONPC as a substrate. S25C and N55C exhibited the cellulolytic activities at the same level as WT, but N107C and N151C did not show any activity. These results suggested that S25C and N55C mutants were expressed successfully; however, N107C and N155C were not.

Table 4.1. Expression yields of the endoglucanase III (EG III) mutants.

The yields were calculated using the extinction coefficient of 72000 at OD₂₈₀.

Mutant	Yield (mg/ ml broth)
S25C	0.44
N55C	1.43
N107C	0.08
N151C	0.26

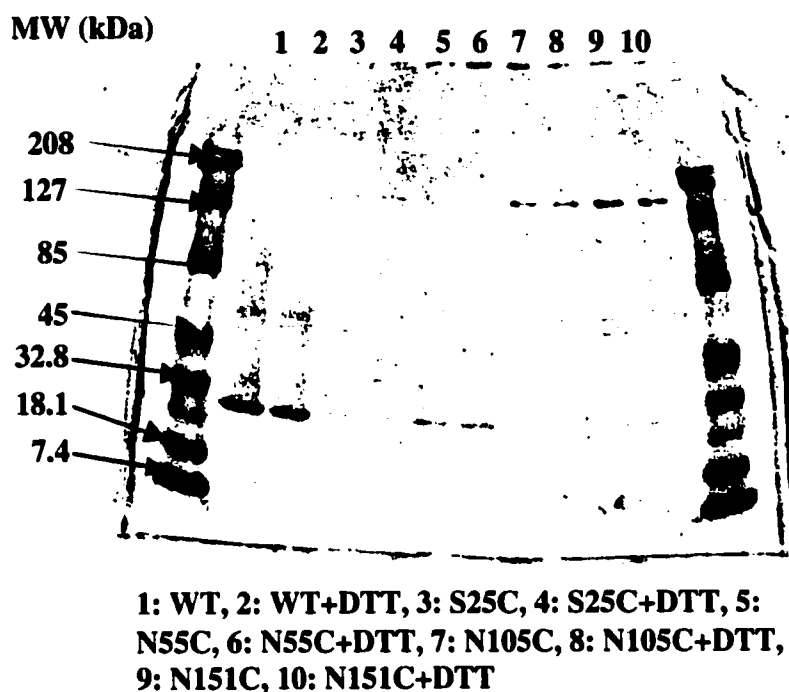


Figure 4.4. SDS-PAGE of wild type (WT) endoglucanase III (EG III) and the mutants.

The site-specific mutations of S25C and N55C in the protein level were confirmed by Genencor International Inc. using a peptide mapping method, in which the proteins were hydrolyzed by specific proteases, and the fragments analyzed by LC-MS. The results of the LC-MS for WT, S25C and N55C EG IIIs showed that only the mutated fragment had different MW from that of WT, and the difference of the MW agreed with the theoretical difference of the site-directed mutation.

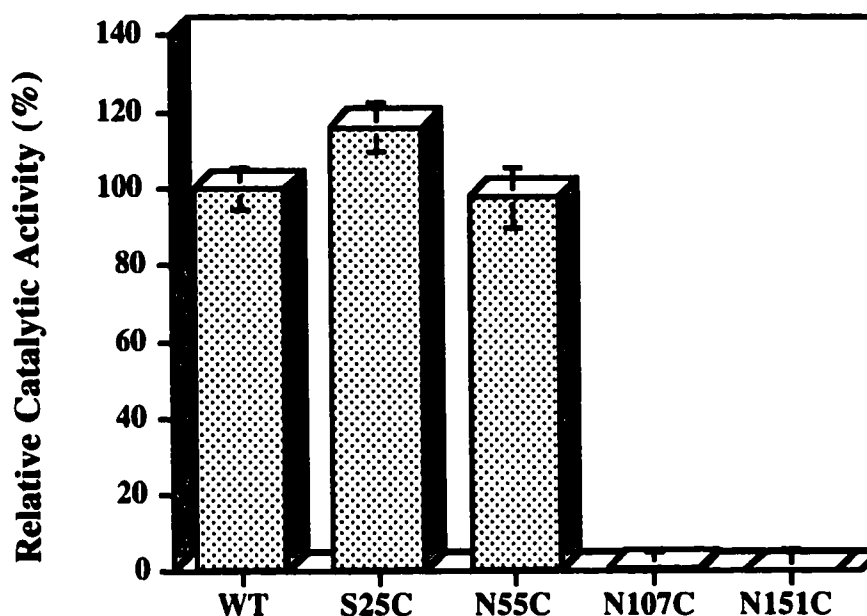


Figure 4.5. Comparison of catalytic activities of EG III mutants.

The activity was measured for 100 nM EG III toward 8 mM ONPC at 40 °C in 50 mM sodium acetate buffer pH5.5, and normalized to the activity of wild type (WT) EG III.

The reactivity of the genetically introduced Cys was confirmed by conjugating these mutants to fluorescein-5-maleimide (F-MI). The WT EG III was also conjugated to F-MI as a control. Figure 4.6 shows the results of SDS-PAGE stained by CBB (A) and the fluorescence upon UV light irradiation without staining (B). The S25C-F and the N55C-F conjugates showed a dense fluorescent band at the EG III position in the SDS-PAGE gel. This indicates that the conjugates have extra cysteines. Figure 4.7 shows the UV/VIS spectra of the EG III-F conjugates. The S25C-F and the N55C-F had a significant absorption at 478 nm stemming from fluorescein in the UV/VIS spectra, while the WT-F did not. The molar ratio of fluorescein to EG III calculated from the absorbance data at

280 nm for EG III and at 478 nm for fluorescein were determined to be 0.18 for WT, 0.78 for S25C, and 0.64 for N55C. This result also suggests the presence of the extra cysteines in S25C and N55C.

Therefore, we can conclude that S25C and N55C mutant EG IIIs were expressed successfully and they contain a reactive cysteine.

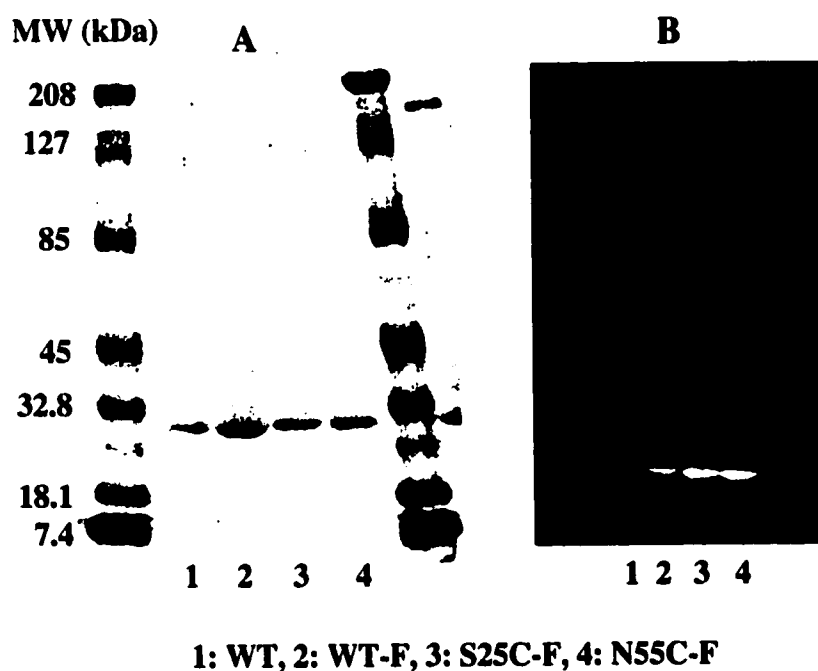


Figure 4.6. SDS-PAGE of EF III-F (fluorescein) conjugates.

(A): stained by CBB, (B): fluorescence upon UV irradiation without staining.

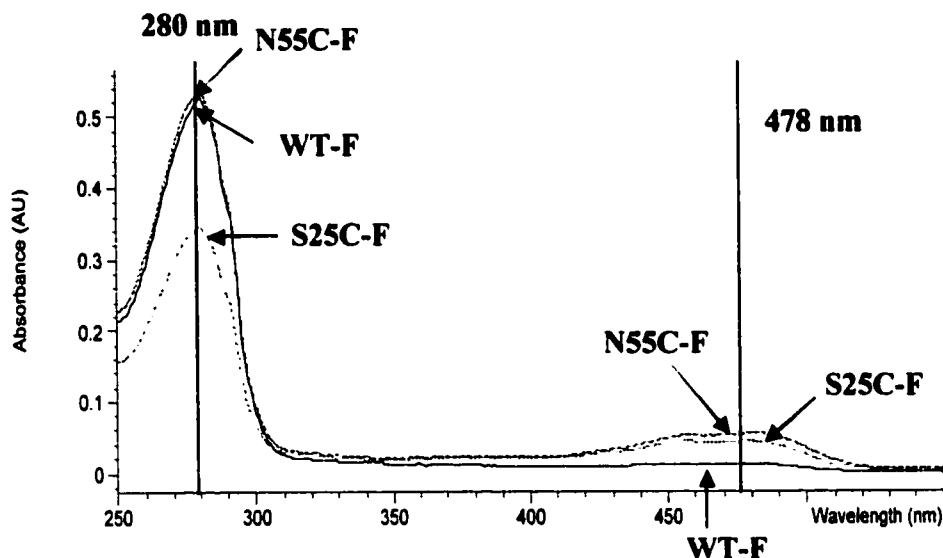
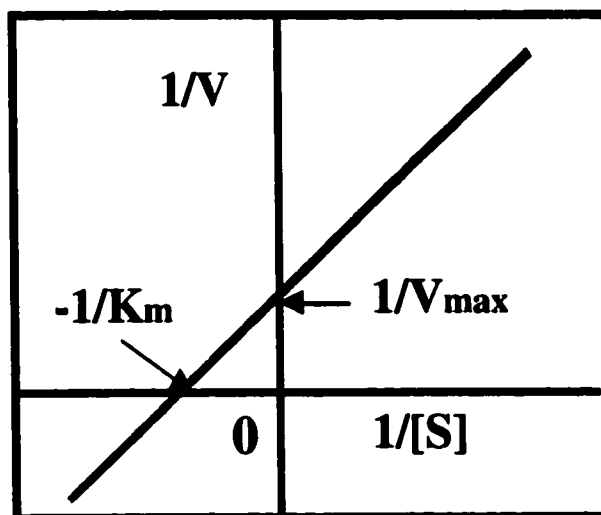


Figure 4.7. UV/VIS spectra of EG III-F conjugates.

The absorbance at 280 nm is due to EG III, and that at 478 nm is due to fluorescein.

4.3.4 DETERMINATION OF THE KINETIC PARAMETERS OF CATALYTIC ACTIVITY OF WT AND MUTANT EG IIIS BY ONPC ASSAY

The kinetic parameters, K_m , k_{cat} , and k_{cat}/K_m , of WT and mutant EG IIIs were evaluated with ONPC as a substrate. The time course of ONP production by WT, S25C and N55C EG IIIs for various concentrations of ONPC were measured at 52 °C. The kinetic parameters were determined from a Lineweaver-Burk plot assuming Michaelis-Menten kinetics (Figure 4.8).



$$1/V = K_m/V_{\max}(1/[S]) + 1/V_{\max}$$

Figure 4.8. Lineweaver-Burk plot

The kinetic parameters for the hydrolysis of ONPC are summarized in Table 4.2. To calculate accurate k_{cat} values (V_{\max} / enzyme concentration), the purity of the mutants were evaluated by CBB density on a SDS-PAGE gel of the mutant EG IIIs run with DTT. The purity of S25C and N55C were determined to be 88.4 % and 94.0 %, respectively. N55C exhibited a higher K_m value than WT and S25C, suggesting that the mutation at the 55 position weakened the affinity between cellobioside and EG III. However, the k_{cat} values of the mutants are similar to that of WT. This indicates that the 25 and the 55 residues don't participate in the catalytic event. Combining these two, the specific parameter, k_{cat}/K_m of N55C was slightly lower than those of S25C and WT.

Table 4.2. Comparison of kinetic parameters of EG III mutants toward o-nitrophenyl- β -D-cellobioside (ONPC).

The activity was measured for 100 nM EG III at 52 °C in 50 mM sodium acetate buffer pH5.5.

EG III	K_m (mM)	k_{cat} (sec ⁻¹)	k_{cat}/K_m (sec ⁻¹ mM ⁻¹)
WT	19.5	12.8	0.656
S25C	20.8	14.5	0.697
N55C	33.9	13.6	0.401

4.3.5 DETERMINATION OF THE KINETIC PARAMETERS OF CATALYTIC ACTIVITY OF WT AND MUTANT EG IIIS BY HEC ASSAY

To investigate the effect of the size of the substrate on the activity, HEC was used as a large substrate. The product, glucose, was determined by PHBAH. The reaction of PHBAH-glucose produces a significant absorbance increase in the 400 to 450 nm range, and the absorbance at 405 nm is proportional to the concentration of glucose. The kinetic parameters of EG III mutants toward HEC are summarized in Table 4.3. The K_m values of S25C and N55C were found to be higher than that of WT. This suggests that the affinity of the mutants to HEC was lowered by the mutations at the 25 or 55 position. In addition, from the finding that the mutation at the 25 position did not influence the affinity with a small substrate, ONPC, the 25 residue must only influence the binding to the large substrate, HEC. The similar k_{cat} values of the mutants to that of WT indicate that the 25 and 55 residues do not significantly participate in the catalytic event toward HEC. The k_{cat}/K_m values showed that both mutants had slightly lower specific activities toward HEC than the WT EG III.

Table 4.3. Comparison of kinetic parameters of EG III mutants toward hydroxyethyl cellulose (HEC).

The activity was measured for 100 nM EG III at 52 °C in 50 mM sodium acetate buffer pH5.5.

EG III	K_m (mg/ml)	k_{cat} (sec ⁻¹)	k_{cat}/K_m (ml/mg sec ⁻¹)
WT	19.9	10.4	0.523
S25C	27.2	13.4	0.493
N55C	29.2	12.7	0.435

4.4 CONCLUSIONS

We have constructed four kinds of site-directed mutant EG III genes, S25C, N55C, N107C and N151C. They were transformed into and expressed in a fungus, *A. niger*, and purified from their fermentation broths using hydrophobic interaction chromatography. The activity measurements, SDS-PAGE and peptide mapping for these mutants have shown that S25C and N55C were expressed successfully, but N107C and N151C were not. The reactivity of the genetically engineered Cys of S25C and N55C were confirmed by the conjugations of these mutants to F-MI.

The kinetic parameters of the catalytic activity of WT and the mutant EG IIIs were evaluated by ONPC and HEC assay. The N55C mutant exhibited a higher K_m value but a similar k_{cat} value to WT and S25C. These results indicate that the 55 residue is involved in the binding of ONPC but does not participate in the catalytic event. The S25C mutant showed a higher K_m value only for HEC, but not for ONPC, suggesting the 25 residue does not influence the binding of the small substrate, but does for the large substrate.

These mutants are conjugated to DMAA or DMAAm, and the kinetic values of the conjugates are compared to those of the mutants in Chapter 5.

CHAPTER 5 EG III – PHOTO-RESPONSIVE POLYMER CONJUGATES

5.1 INTRODUCTION

In the previous chapters, EG III mutants, S25C and N55C, and photo-responsive polymers, DMAA and DMAA, with different MWs were prepared. In this chapter, the polymers have been conjugated to the mutant EG IIIs site-specifically.

Using these conjugates, the following five factors have been examined for their effects on the thermo- and photo-switching activity.

- 1: Position of the conjugation.
- 2: Mw of the conjugated polymer.
- 3: Size of the substrate.
- 4: Conjugation of the opposite photo-responsive polymer
- 5: Addition of free polymer.

ONPC and HEC were used for the activity assay to elucidate the effect of the size of the substrate on the switching activity. To elucidate the “polymer” effect on the photo-responsive activities, an azobenzene was directly conjugated to the mutant EG IIIs site-specifically, and the switching activity was compared with that of the polymer conjugate. The conjugates were immobilized onto magnetic beads to investigate the switching activity of the purified state without the free polymers. Thermo- and photo-cycling effects on the activity were investigated to estimate the response rate and durability of the

conjugates as a molecular switch. The mechanism of the stimuli-responsive switching was elucidated by kinetics studies of the conjugates. Finally, the possibility of a practical application was investigated using cotton cloth as a substrate.

These investigations will lead to the elucidation of the mechanism of the stimuli-responsive activity changes, and the establishment of a general strategy for designing and developing novel photo-switchable enzymes.

5.2 MATERIALS AND METHODS

5.2.1 MATERIALS

4-phenylazomaleinanil (PAM) (Aldrich, Milwaukee, WI), bis-tris propane, ammonium sulfate, o-nitrophenyl- β -D-cellobioside (ONPC) (Sigma, St. Louis, MO), hydroxyethyl cellulose (HEC) medium Viscosity (Fluka, Ronkonkome, NY), tris(2-carboxyethyl)-phosphine hydrochloride (TCEP), BCA protein assay kit, streptavidin magnetic beads, EZ-Link sulfo-NHS-LC-LC-biotin, 4'-hydroxyazobenzene-2-carboxylic acid (HABA), Magna Bind Streptavidin (Pierce, Rockford, IL), Ultrafree Biomax (Millipore, Bedford, MA), Precast gel (Novex, San Diego, CA), Kaleidoscope MW marker, Econo-pac 10PG (Biorad, Hercules, CA) and cotton cloth (gauze) were used as received. All other reagents were of analytical grade.

5.2.2 DERIVATIZATION OF END GROUPS OF COPOLYMERS WITH ACRYLATE GROUPS

To improve the conversion of the conjugation, another chemical reaction, acrylate-thiol, was examined. The hydroxyl terminus of DMAA or DMAAm was converted to acrylate groups to prepare acrylate-terminated DMAA (DMAA-AA) and DMAAm (DMAAm-AA) (Figure 5.1). Approximately, 2 g of DMAA or DMAAm were dissolved in 20 ml of DMF with triethylamine (TEA). Acryloylchloride (AC) was added dropwise into the

solution at 0 °C under a nitrogen atmosphere with stirring (polymer / AC / TEA = 1 / 10 / 13 molar ratio). The reaction mixture was allowed to come to room temperature and was stirred for 4 h. The polymers were precipitated in diethyl ether, washed, and dried *in vacuo*.

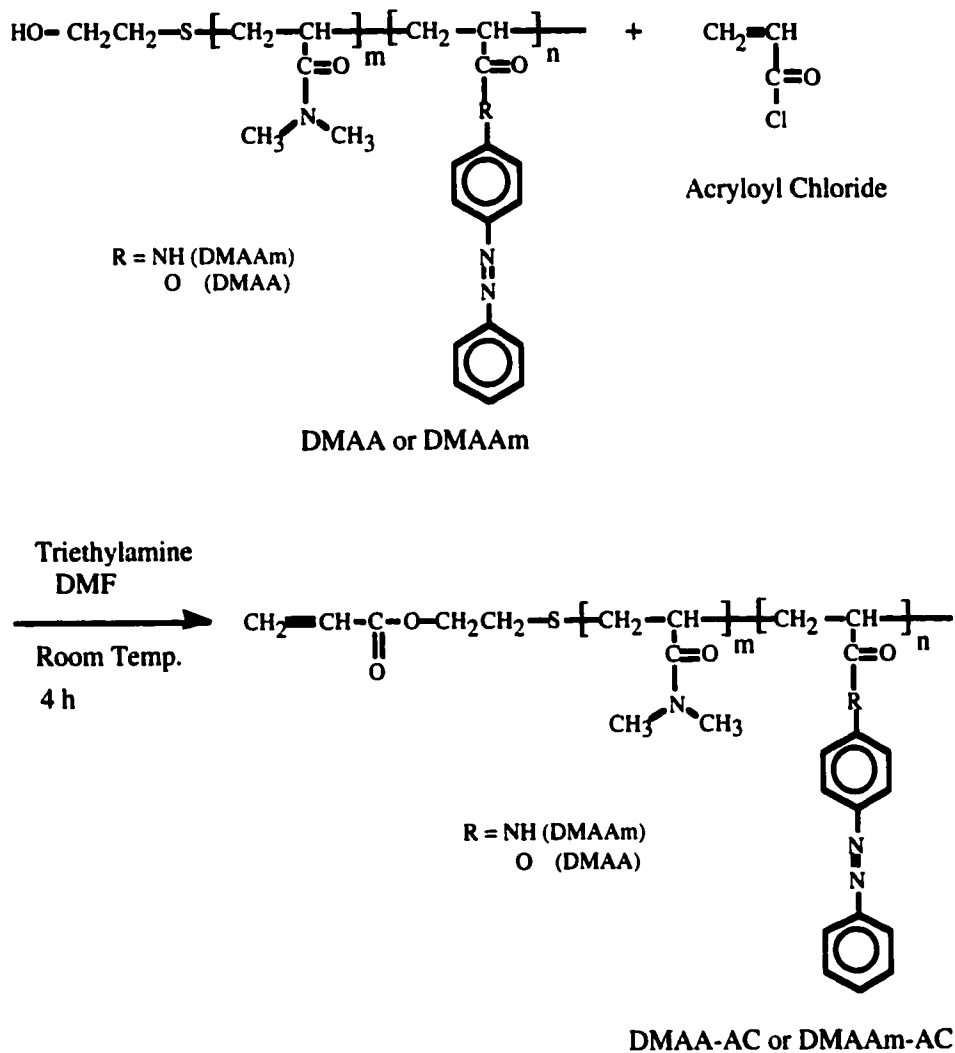


Figure 5.1. Scheme of synthesis of DMAA-AA and DMAAm-AA.

5.2.3 CONJUGATION OF PHOTO-RESPONSIVE POLYMERS TO EG III MUTANTS

Site-specific conjugations of EG III mutants to DMAA-VS, DMAAm-VS, DMAA-AA or DMAAm-AA with different Mw were carried out by reacting the VS group or the AA group of the polymer with the sulfhydryl group of EG III mutant in 100 mM PB, pH 7.0 or 8.0 (Figure 5.2 and 5.3). Cysteine residues in the EG III mutants form disulfide bonds during storage. To reduce disulfide bonds to sulfhydryl groups, TCEP at a 10-fold molar excess to the mutant was added into the solution and it was rotated for 20 min at room temperature. Then, a 50-fold molar excess of the polymer to the mutant was added to obtain high conjugation efficiency. The reaction proceeded overnight at 4 °C. The buffer was exchanged to 50 mM AB (pH 5.5) at 4 °C using an ultrafiltration membrane (Ultrafree, Millipore) to stabilize the conjugate. Then, the conjugates were separated from the unconjugated mutants by thermally induced precipitation at 52 °C. The unconjugated mutants were retained in the supernatant. The precipitates were resuspended in 50 mM AB pH 5.5. The thermally induced precipitation was repeated three times to remove the unconjugated mutants completely.

The conjugates were determined by SDS-PAGE. The conversion of the conjugates was quantitated using the BCA protein assay method (Pierce).

5.2.4 IMMOBILIZATION OF THE CONJUGATES ON MAGNETIC BEADS

The conjugates were biotinylated by reacting with sulfo-NHS-LC-LC-biotin as shown in Figure 5.4. The conjugate was dissolved in 100 mM sodium phosphate buffer, pH 7.4 at 4 °C, at a concentration of 200 µg/ml. A 10-fold molar excess of Sulfo-NHS-LC-LC-Biotin, dissolved in de-ionized water immediately prior to use, was added to the solution at room temperature. The solution was gently rotated at 4 °C for 5 h. The biotinylated conjugate was purified from the unconjugated biotin by ultrafiltration using Biomax-5 (MW cut off: 5 kDa), followed by thermal precipitation at 52 °C.

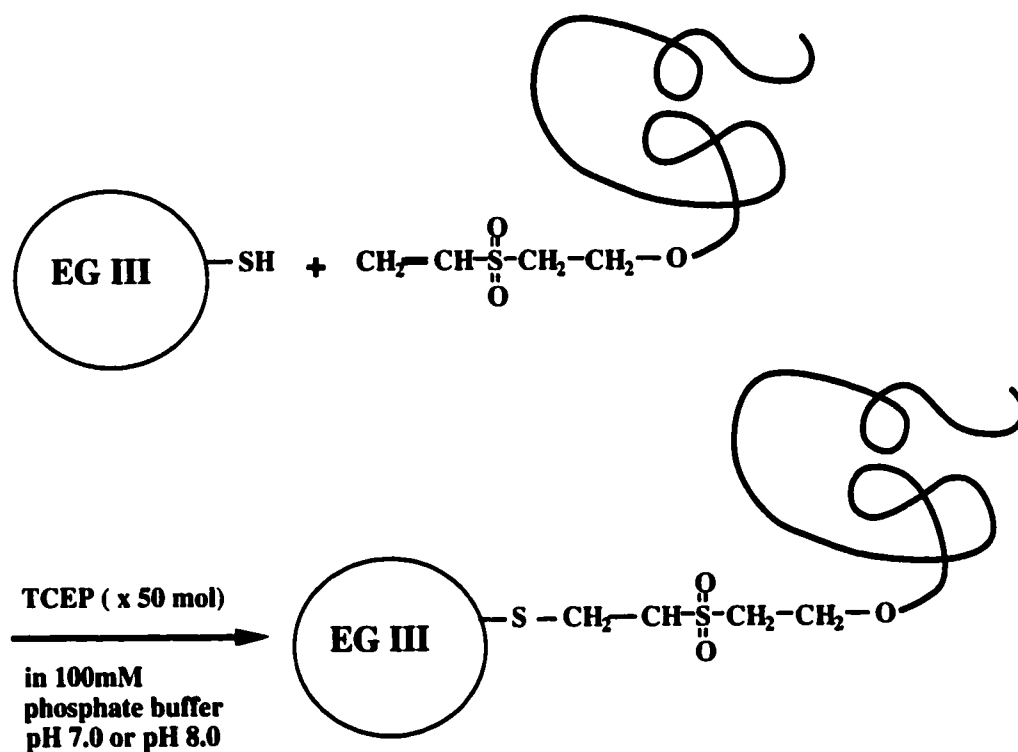


Figure 5.2. Specific conjugation of a VS-terminated polymer to an EG III mutant.

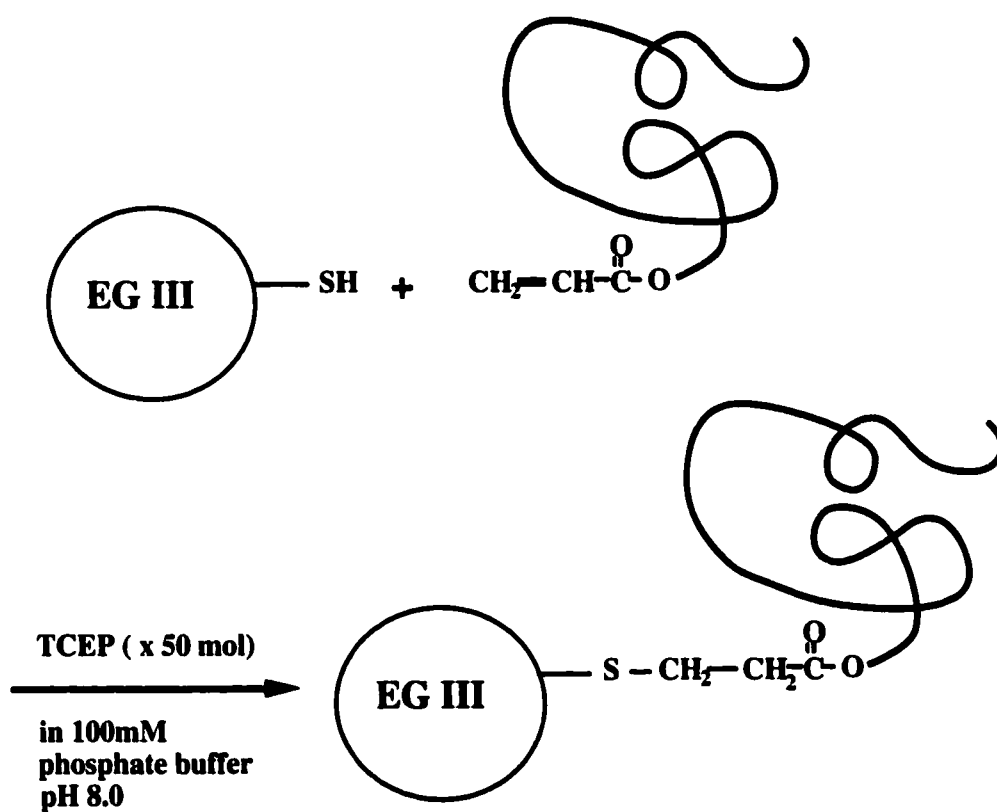


Figure 5.3. Specific conjugation of an AA-terminated polymer to an EG III mutant.

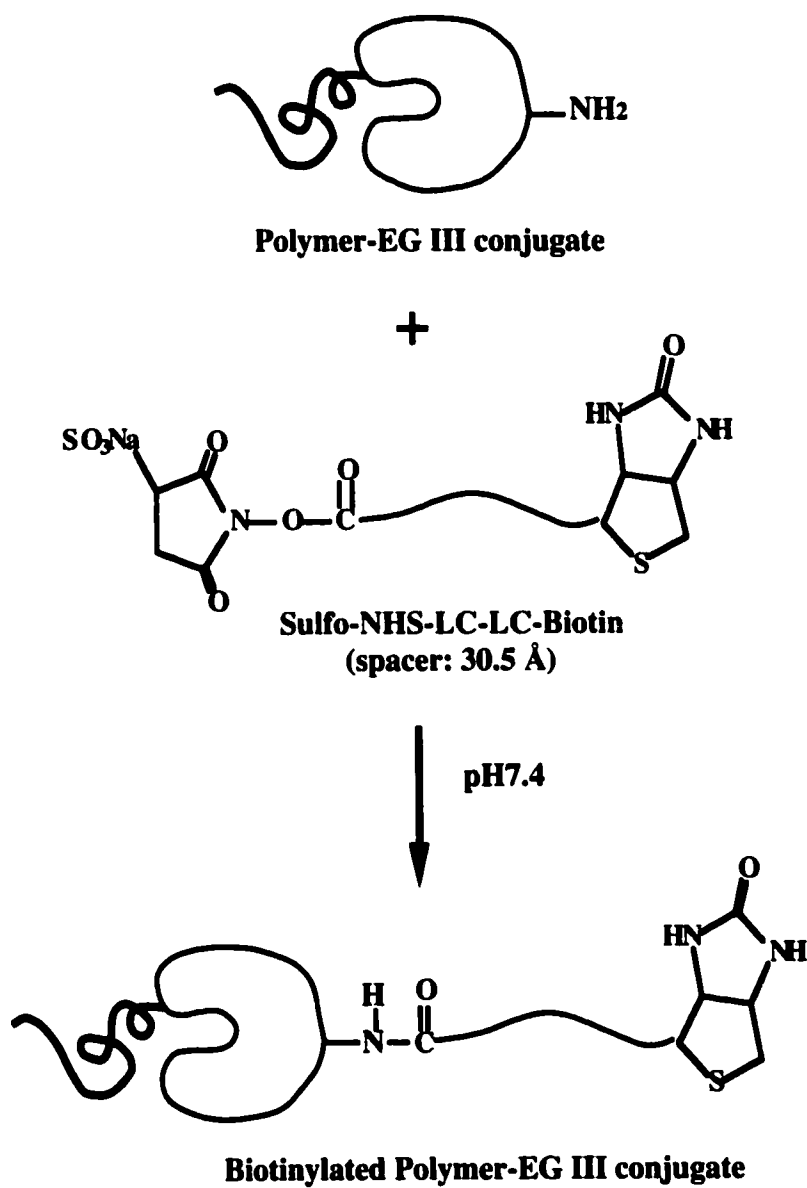


Figure 5.4. Biotinylation of Polymer-EG III conjugate.

The degree of biotinylation was determined using a HABA assay. Briefly, 0.5 ml of a mixture of avidin (20 μ M) and HABA (600 μ M) was added to a quartz cuvette. The absorbance at 500 nm was measured on a UV-VIS spectroscope. To this solution, 50 μ l of biotinylated conjugate solution was added. The absorbance at 500 nm was recorded 30 min after the addition of the biotinylated conjugate solution. The concentration of biotin in the biotinylated protein solution was determined from the calibration curve of a known concentration of biotin solution.

The biotinylated conjugate was immobilized on streptavidin magnetic beads. A 1 mg sample of magnetic beads was mixed with 20 μ g of conjugate in 1 ml of 50 mM AB (pH5.5) containing 50 mM NaCl, 5 mM EDTA and 0.2 wt.% of BSA. The amount of the immobilized conjugate was determined by depletion of the conjugate from the supernatant. The immobilized conjugates were separated from free polymer by washing the beads ten times with 1 ml of 50 mM AB pH5.5.

5.2.5 CONJUGATION OF 4-PHENYLAZOMALEINANIL (AZ-MI) TO EG III MUTANTS

To investigate the polymer effect on the photo-switching activity, an azobenzene was directly conjugated to the mutants as a control. The mutant EG III was conjugated with AZ-MI in 100 mM sodium phosphate buffer (PB) pH 7.0 (c.f. Figure 3.2). Briefly, a 200 μ g sample of EG III mutant in 100 mM sodium phosphate buffer pH 7.0 was prepared by exchanging the buffer using Ultrafree (Millipore). A 10-fold molar excess of TCEP was added to the EG III solution to reduce the disulfide bonds to sulfhydryl groups. A 50-fold excess of AZ-MI was dissolved in DMF (10% volume of the total conjugation solution), and mixed with the EG III solution (EG III / TCEP / AZ-MI = 1 / 10 / 50). The conjugation was carried out at 4°C overnight with gentle rotation. After the reaction, the buffer was exchanged with 50 mM AB pH5.5. The conjugate was separated from the unconjugated AZ-MI by a polyacrylamide desalting column (Econopac 10PG, Biorad).

5.2.6 CONJUGATION OF PHOTO-RESPONSIVE POLYMERS TO WILD TYPE EG III

As a control to investigate the effect of the position of conjugation on the switching activity, DMAAm (10 kDa) was conjugated to WT EG III via the reaction of primary amino groups of EG III and VS group of the DMAAm in 100 mM sodium borate buffer pH9.0. Although there are five lysines, three arginines and one N-terminus in WT EG III as primary amino groups, the N-term amino group is most likely reactive to VS at pH9.0 because it is exposed on the surface and has the lowest pK_a of 9.1. Briefly, a 50-fold molar excess of the polymer to the WT EG III was added to obtain high conjugation efficiency. The reaction proceeded overnight at 4 °C. The buffer was exchanged to 50 mM AB (pH 5.5) at 4 °C using an ultrafiltration membrane (Ultrafree, Millipore) to stabilize the conjugate. Then, the conjugates were separated from the unconjugated WT EG III by thermally induced precipitation at 52 °C. The unconjugated WT EG III was retained in the supernatant. The precipitates were resuspended in 50 mM AB pH 5.5. The thermally induced precipitation was repeated three times to remove the unconjugated WT EG III completely.

5.2.7 CATALYTIC ACTIVITY ASSAY OF THE CONJUGATES

5.2.7.1 Substrates

ONPC and HEC were used for the activity assay of the conjugates to elucidate the effect of the size of the substrate on the switching activity. The assay method for each substrate is the same as described in Chapter 4. To investigate the practical possibility of the conjugates, cotton cloth was used as a substrate. The activity was determined by measuring the product (glucose) concentration by PHBAH assay described in Chapter 4.

5.2.7.2 Thermo-Responsive Activity Assay of the Conjugates

Since the enzyme activity is highly dependent on temperature, each mutant EG III was used as a control to compare the effect of temperature on the activity of the conjugates. The catalytic activity of the EG III conjugates was measured at 32 °C and 52 °C by an endpoint assay, using 8 mM ONPC or 20 mg/ml HEC as substrates for 100 nM conjugates.

5.2.7.3 Photo-Responsive Activity Assay of the Conjugates

To investigate the photo-switching activity, the photo-responsive temperature was determined. The catalytic activity upon UV or VIS irradiation was measured as a function of temperature, and the temperature, at which a difference in activity was observed between UV and VIS irradiation, was determined as the photo-responsive temperature. The photo-responsive activity was measured under the isothermal condition at the photo-responsive temperature upon UV or VIS irradiation.

5.2.7.4 Activity Assay for the Immobilized Conjugates

The thermo- and photo-responsive activity changes of the immobilized conjugates were measured using the same protocol as that of the conjugates in solution for 100 nM conjugates immobilized onto the magnetic beads. The activity of the immobilized WT EG III was used as a control.

5.2.7.5 Cyclic Activity Assay

The effects of thermo- and photo-cycling on the activity of the conjugates were examined by measuring the activity changes in response to the temperature cycling between 32 and 52 °C upon VIS irradiation, or the light irradiation cycling of UV and VIS light at the photo-responsive temperature (45 °C). The response rate and the durability for the on-off switching were evaluated.

5.2.7.6 Kinetic Studies of the Conjugates

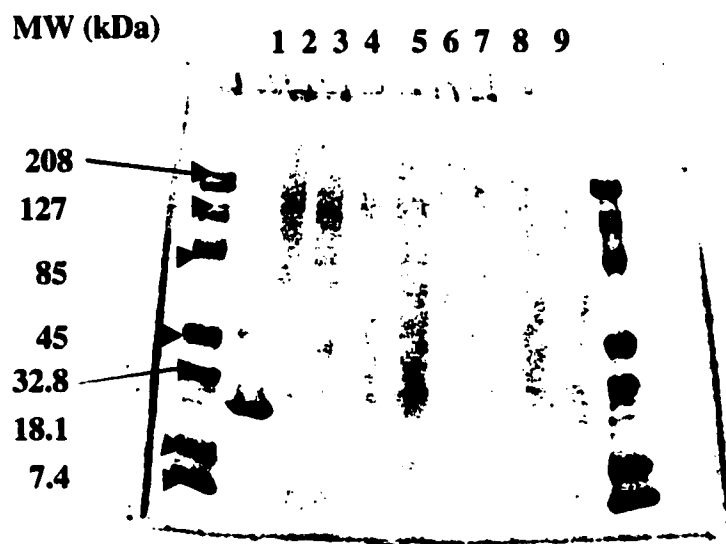
To elucidate the mechanism of the stimuli-responses, the kinetics parameters of the conjugates were determined as functions of temperature and photo-irradiation. The substrate concentration and the incubation time were varied, and the activity was measured by endpoint assay. The kinetic parameters, K_m and k_{cat} , were determined by a Lineweaver-Burke plot assuming Michaelis-Menten kinetics. The assay method for each substrate is the same as described in Chapter 4.

5.3 RESULTS AND DISCUSSIONS

5.3.1 CONJUGATIONS OF MUTANT EG IIIS TO THE PHOTO-RESPONSIVE POLYMERS

The EG III mutants, S25C and N55C, were conjugated to DMAA-VS, DMAAm -VS, DMAA-AA or DMAAm-AA in the presence of TCEP (10-fold molar excess) in 50 mM PB pH7.0 or pH8.0. The native EG III has one internal disulfide bond between position 4 and 32. Since this bond is necessary to stabilize the tertiary structure (7 kcal/mol) [94], it is important to note that this low amount of TCEP does not reduce internal disulfide bonds, only external ones. The conjugates were separated from the unconjugated mutants by thermally induced precipitation at 52 °C. A BCA protein assay method (Pierce) was employed to estimate the amounts of the conjugates in the precipitates.

Figure 5.5 shows the results of SDS-PAGE of the precipitates of the conjugate solutions. The precipitates did not have the EG III band at 23.5 kDa. This indicates that the unconjugated EG III was separated completely from the conjugates by thermal precipitation. They have a smeared band stemming from the conjugates in the higher MW region.



1: WT, 2: S25C-DMAA (11 kDa), 3: S25C-DMAAm (10kDa), 4: S25C-DMAAm (6kDa), 5: S25C-DMAAm (3kDa), 6: N55C-DMAA (11kDa), 7: N55C-DMAAm (10kDa), 8: N55C-DMAAm (6kDa), 9: N55C-DMAAm (3kDa).

Figure 5.5. SDS-PAGE of EG III-DMAA and EG III-DMAAm conjugates.

Table 5.1. Conversion of EG III-DMAA or DMAAm Conjugate

The amount of conjugate was determined by BCA protein assay. AA represents acrylate-terminated polymer.

Conjugate	pH 7.0		pH 8.0	
	μg	mol %	μg	mol %
S25C-DMAA (11 kDa)	13.5	1.6	136.3	16.2
S25C-DMAAm (10 kDa)	24.1	2.9	198.1	23.5
S25C-DMAAm (6 kDa)	28.2	3.4	291.9	34.6
S25C-DMAAm (3 kDa)	23.1	2.8	167.3	19.8
N55C-DMAA (11 kDa)	11.8	1.6	78.5	10.8
N55C-DMAAm (10 kDa)	22.5	3.1	141.4	19.4
N55C-DMAAm (6 kDa)	24.3	3.3	148.3	20.3
N55C-DMAAm (3 kDa)	23.2	3.2	144.2	19.8
N55C-DMAA (AA) (11 kDa)	-	-	68.0	9.3
N55C-DMAAm (AA) (10 kDa)	-	-	119.0	16.3
N55C-DMAAm (AA) (6 kDa)	-	-	123.0	16.9
N55C-DMAAm (AA) (3 kDa)	-	-	92.4	12.6
WT + DMAA(11 kDa)	0.1	0.0	0.2	0.0
WT + DMAAm (10 kDa)	0.2	0.0	0.2	0.0

Table 5.1 shows the conversions of the conjugates detected by the BCA assay. Physical mixtures of WT EG III and the polymers did not have any EG III in the precipitates. For the specific reaction of the VS or AA to the thiol group, the reaction pH should be between 7.0 and 8.5. The higher pH is necessary to maximize the yield. On the contrary, EG III becomes unstable at alkalic pH. Thus, the conjugation at pH7.0 and pH8.0 were compared. The conversions of the conjugates at pH8.0 are much higher than that at pH7.0, and no aggregation was observed during the conjugation at pH8.0. The S25C conjugates showed higher conversions than the N55C conjugates, suggesting that the 25 position is more accessible than the 55 position. The conversions of the conjugates with AA terminated polymers were less than those with VS terminated polymers. Thus, we decided to use the pH8.0 condition and the VS terminated polymers for the conjugation.

5.3.2 THERMO-RESPONSIVE ACTIVITY CHANGES OF THE CONJUGATES

Figure 5.6 shows the temperature-induced phase transition behaviors of the polymers used for the conjugation. All polymers exhibited LCSTs at 37 °C- 43 °C. Since they were completely soluble at 32 °C, and insoluble at 52 °C, these two temperatures were used for the investigation of thermo-switching activity changes of the conjugates.

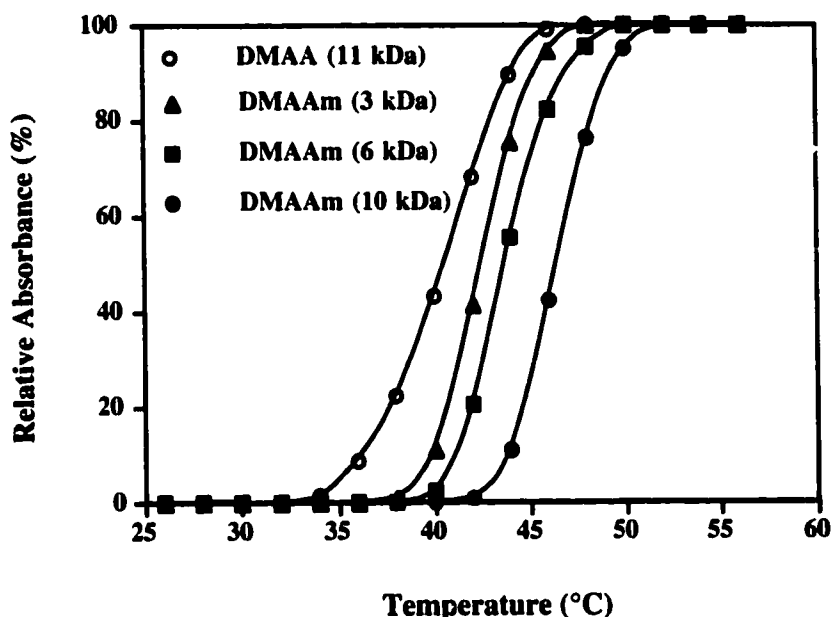


Figure 5.6. The LCSTs of DMAA and DMAAm.

The relative absorbance changes at 600 nm was measured to show the turbidity of the polymer solution (2 mg/ml) in 50 mM sodium acetate buffer pH5.5. The heating rate was 0.5 °C/min.

Figure 5.7 shows the thermo-responsive relative activity changes of the S55C and S25C conjugates toward ONPC at 32 °C and 52 °C. The activities of the conjugates were normalized to that of the mutant at each temperature. The physical mixtures of the mutants and the polymers were used as controls. While the physical mixtures did not show activity changes, the conjugates exhibited shut-off of catalytic activity at 52 °C. In particular, the conjugates with high MW polymers, N55C-DMAA (11 kDa) and N55C-DMAAm (10 kDa), showed complete shut-off of the activity at 52 °C. In addition, as the

MW of the conjugated polymer was decreased, the shut-off effect was weakened. For the S25C conjugates, no complete shut off effect was observed, even for the conjugate with high MW (11 kDa) polymer. These results indicate that both the MW and the position of conjugation are crucial for the activity switching.

The effect of the size of the substrate on the switching activity was investigated by using HEC as a substrate. Figure 5.8 shows the thermo-responsive relative activity changes using HEC as a substrate for N55C and S25C conjugates. Even at 32 °C, the activities were much lower than the unconjugated mutants, while they were almost the same for ONPC. This suggests that the conjugated polymer interfered with the binding of HEC to EG III even in the expanded state. A similar phenomenon was reported by Oupicky *et al.* [130]. The conjugates of poly[N-(2-hydroxypropyl)methacrylamide] to α -chymotrypsin was active to a small tripeptide substrate; however, the activity was decreased to Poly(ethylene glycol)-based synthetic substrate, and disappeared to bovine serum albumin. Thus, the sterical hindrance of the conjugated polymer might prevent the access of a large substrate to the active site. When the temperature was increased to 52 °C, the conjugates showed shut-off effect on the activity. For HEC, even the N55C-DMAAm (6 kDa) exhibited the complete shut-off of the activity, unlike the situation with ONPC. This indicates that a low MW polymer could shut off the activity completely for a larger substrate. Similar to the ONPC assay, S25C conjugates did not show complete shut-off of the activity. Thus, the importance of the position of the conjugation for regulating the activity is shown for HEC as well as ONPC.

Since the conjugates were aggregated and precipitated at 52 °C, the shut-off effect might be due to the simple physical shielding of the substrate by the aggregation of the polymers. Thus, we conjugated DMAAm (10 kDa) to the N-terminus of WT EG III to investigate the effect of conjugation position on the switching activity, since the N-terminus of EG III is located far from the active site. The VS-terminated DMAAm was conjugated to primary amino group of WT EG III in 100 mM sodium borate buffer

pH9.0. In this condition, the N-terminus of WT EG III was preferentially conjugated to the VS group. Figure 5.9 shows comparison of the thermo-switching activities of the DMAAm conjugates to three different positions of EG III. The WT-DMAAm conjugate exhibited lower shut-off activity at 52 °C than the mutant conjugates for both substrates. The remoter the conjugation position was located to the active site, the weaker the shut-off effect became. Therefore, the switching was induced not only by simple shielding of the polymer aggregation, but also by the physical blocking of the active site by the conjugated polymers.

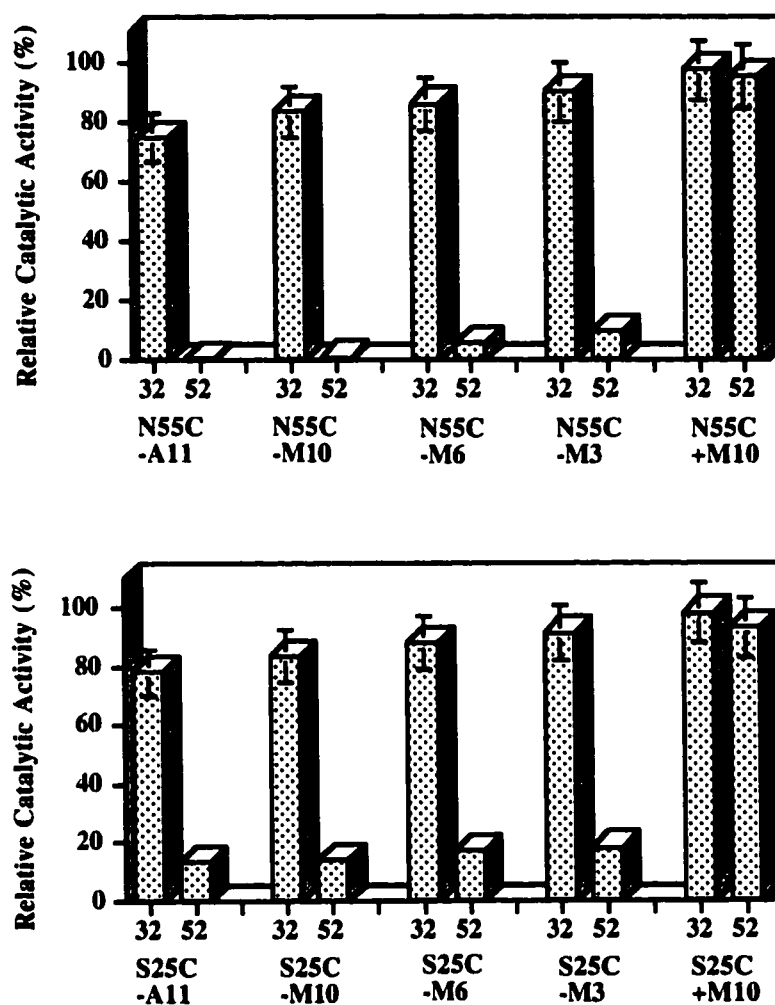


Figure 5.7. Thermo-responsive activity changes of the conjugates.

The activities were measured for 100 nM conjugates with free polymer using ONPC (8mM) as a substrate, and normalized to the activity of N55C or S25C as 100 % at each temperature. A11: DMAA (11 kDa), M10: DMAAm (10 kDa), M6: DMAAm (6 kDa), M3: DMAAm (3 kDa).

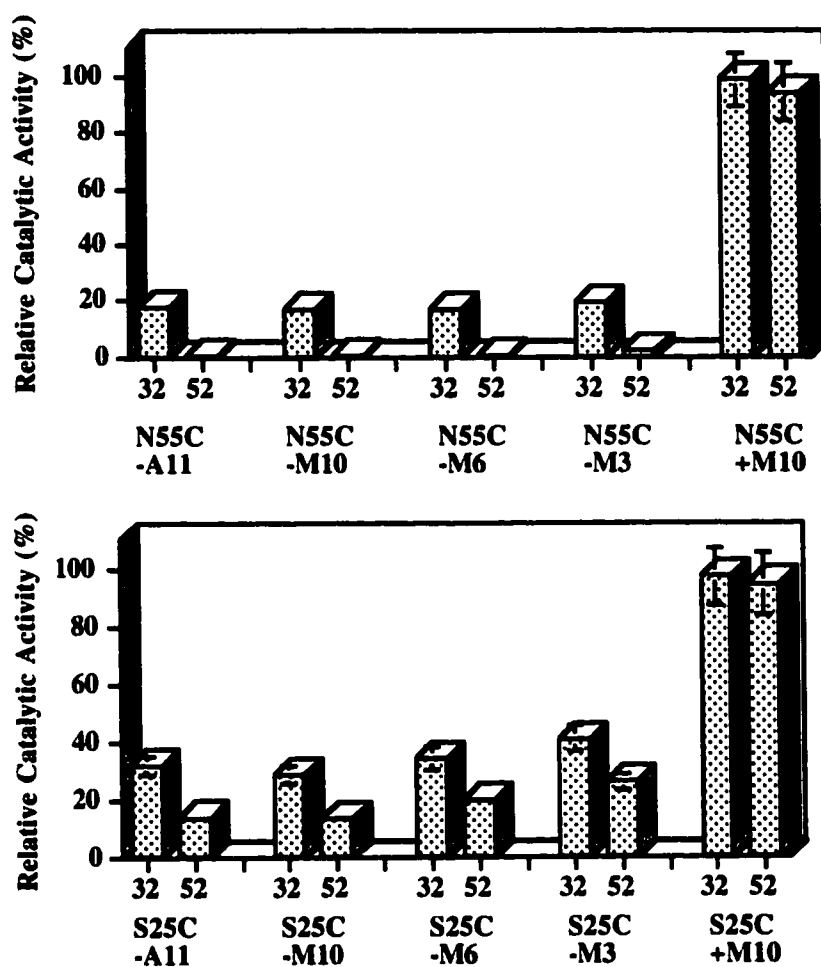


Figure 5.8. Thermo-responsive activity changes of the conjugates.

The activities were measured for 100 nM conjugates with free polymer using HEC (20 mg/ml) as a substrate, and normalized to the activity of N55C or S25C as 100 % at each temperature. A11: DMAA (11 kDa), M10: DMAAm (10 kDa), M6: DMAAm (6 kDa), M3: DMAAm (3 kDa).

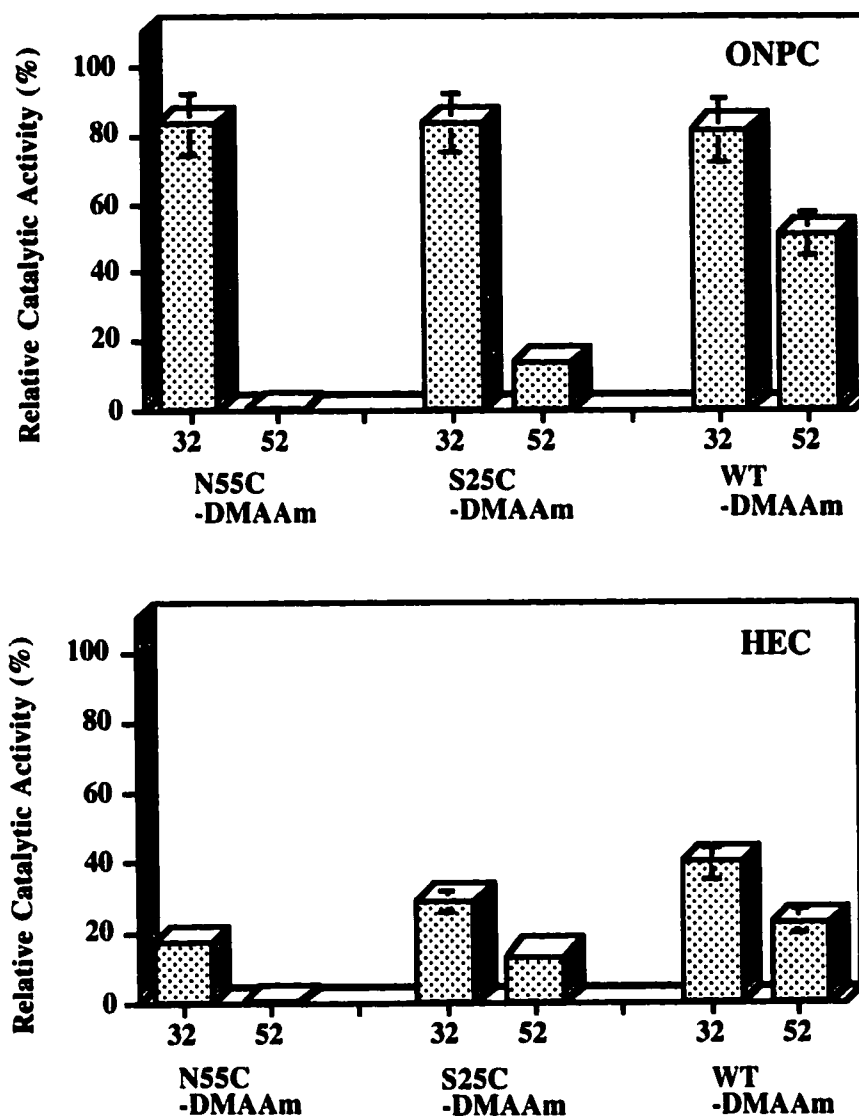


Figure 5.9. Thermo-responsive activity changes of the conjugates.

The activities were measured for 100 nM DMAAm (10 kDa) conjugates (to S25C, N55C or WT EG III) with free polymer using ONPC (8 mM) or HEC (20 mg/ml) as a substrate, and normalized to the activity of N55C, S25C or WT EG III as 100 % at each temperature.

5.3.3 PHOTO-RESPONSIVE ACTIVITY CHANGES OF THE CONJUGATES

Figure 5.10 shows the effect of UV or VIS irradiation on the phase transition temperature of DMAA (11 kDa) and DMAAm (10 kDa) polymers in 50 mM AB pH5.5. Upon the same UV irradiation, the LCST of DMAA increased from 37 °C to 43 °C, while that of DMAAm decreased from 44 °C to 35 °C. Thus, they exhibited opposite photo-responses.

Figure 5.11 and 5.12 show the effects of temperature and UV or VIS irradiation on the activities of N55C, N55C-DMAA (11 kDa), and N55C-DMAAm (10 kDa) conjugates toward ONPC. The activity of the N55C increased with increasing temperature, and UV or VIS irradiation did not influence the activity. The activities of the conjugates were shut off completely at 52 °C. The shut-off temperature of the DMAA conjugate was increased, while that of DMAAm conjugate was decreased by the same UV light irradiation. In addition, this opposite photo-responsive activity is in agreement with the opposite photo-induced phase transition of the conjugated polymers (c.f. Figure 5.9). The temperature ranges of the activity transition agreed with the ranges of phase transition of the conjugated polymers (shown as LCST). This result suggests that the shrinkage of the polymer has induced the shut-off of the catalytic activity.

Figure 5.13 and 5.14 show the results of the same experiments for the conjugates toward HEC. Similar to the results for ONPC, the activities of the conjugates for HEC were shut off completely at 52 °C, and they exhibited opposite photo-responses. The activity shut-off was associated with the phase transition of the conjugated polymers. However, the activity for HEC is much lower than that for ONPC. This may be due to the size exclusion effect of the conjugated polymers against a large substrate.

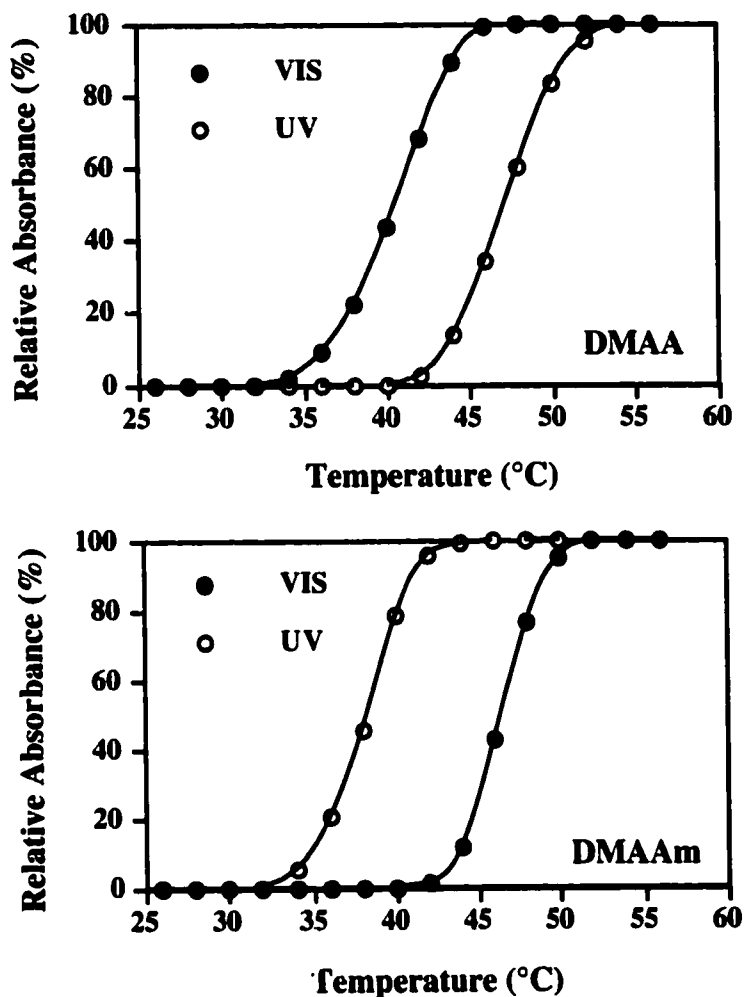


Figure 5.10. Photo-responsive LCST changes of DMAA and DMAAm.

Relative absorbance at 600 nm was measured for DMAA (11 kDa) (above) and DMAAm (10 kDa) (below) solutions. The polymer concentration was 2 mg/ml in 50 mM sodium acetate buffer pH5.5. The heat rate was 0.5 °C/min. The UV and VIS light was irradiated for 10 min and 3 h, respectively, before the measurement.

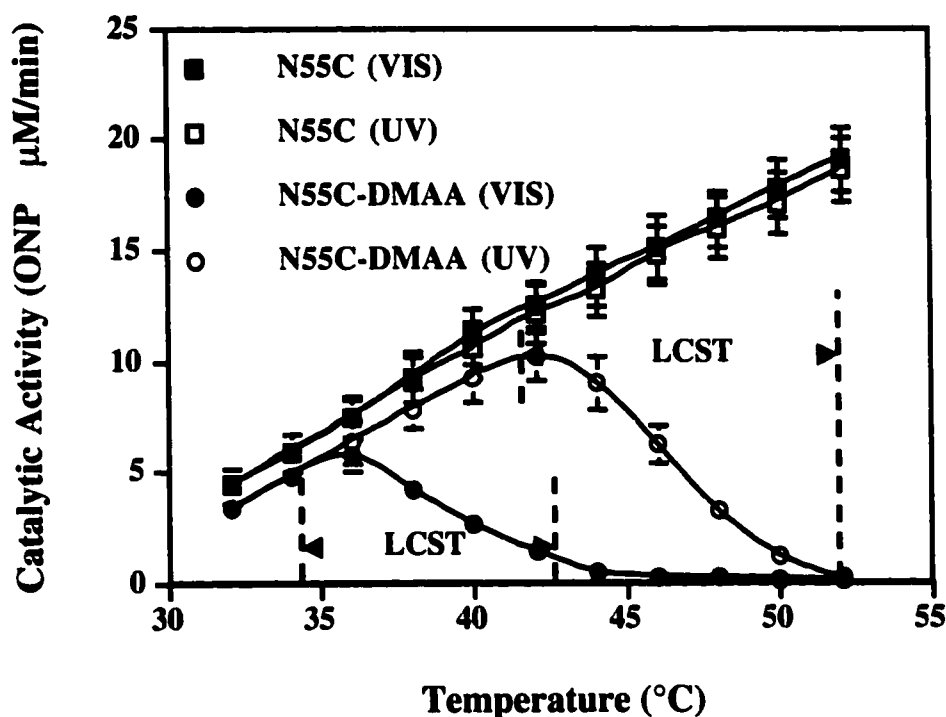


Figure 5.11. Effects of temperature and photo-irradiation on catalytic activity of N55C-DMAA conjugate toward ONPC.

The activity was measured for 100 nM N55C or N55C-DMAA (11 kDa) conjugate with free polymer as an initial velocity of the product (ONP) using 8 mM ONPC as a substrate in 50 mM sodium acetate buffer pH5.5. The phase transition temperature ranges of the conjugated polymers are shown as LCST. The UV and VIS light was irradiated for 10 min and 3 h, respectively, before the measurement.

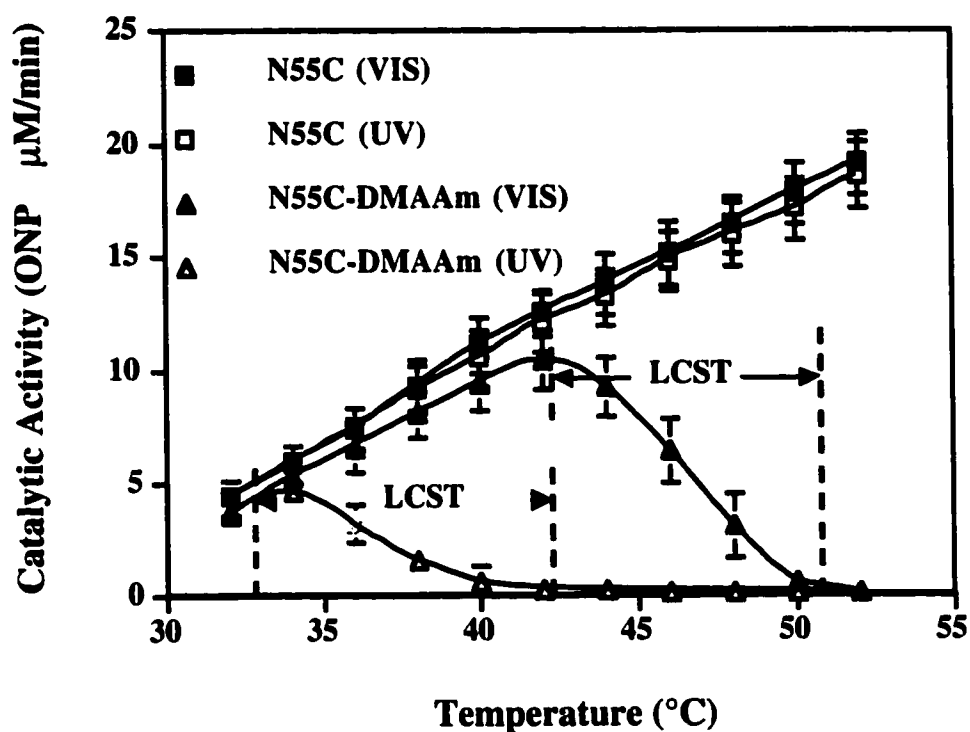


Figure 5.12. Effects of temperature and photo-irradiation on catalytic activity of N55C-DMAAm conjugate toward ONPC.

The activity was measured for 100 nM N55C or N55C-DMAAm (10 kDa) conjugate with free polymer as an initial velocity of the product (ONP) using 8 mM ONPC as a substrate in 50 mM sodium acetate buffer pH5.5. The phase transition temperature ranges of the conjugated polymers are shown as LCST. The UV and VIS light was irradiated for 10 min and 3 h, respectively, before the measurement.

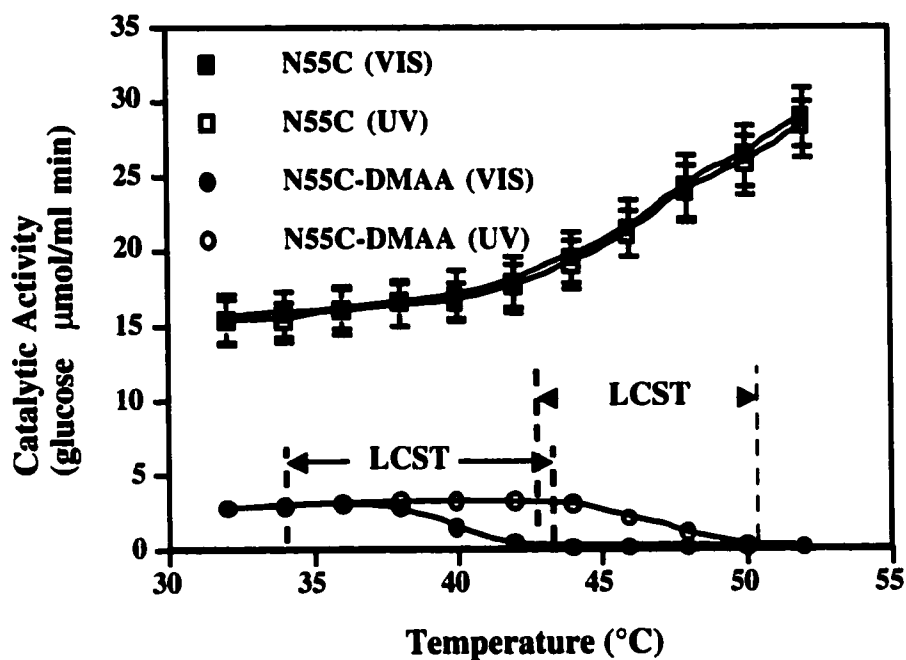


Figure 5.13. Effects of temperature and photo-irradiation on catalytic activity of N55C-DMAA conjugate toward HEC.

The activity was measured for 100 nM N55C or N55C-DMAA (11 kDa) conjugate with free polymer as an initial velocity of the product (glucose) using 20 mg/ml HEC as a substrate in 50 mM sodium acetate buffer pH5.5. The phase transition temperature ranges of the conjugated polymers are shown as LCST. The UV and VIS light was irradiated for 10 min and 3 h, respectively, before the measurement.

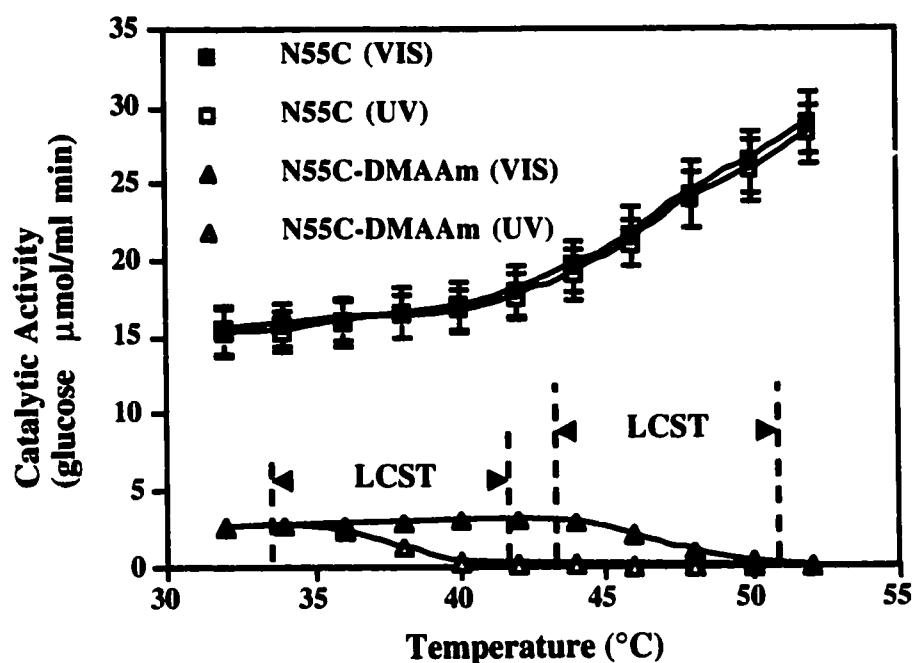


Figure 5.14. Effects of temperature and photo-irradiation on catalytic activity of N55C-DMAA conjugate toward HEC.

The activity was measured for 100 nM N55C or N55C-DMAAm (10 kDa) conjugate with free polymer as an initial velocity of the product (glucose) using 20 mg/ml HEC as a substrate in 50 mM sodium acetate buffer pH5.5. The phase transition temperature ranges of the conjugated polymers are shown as LCST. The UV and VIS light was irradiated for 10 min and 3 h, respectively, before the measurement.

The photo-responsive relative activity changes of the conjugates toward ONPC and HEC are shown in Figure 5.15. The activity was measured isothermally at 45 °C. Although both conjugates showed photo-responses lesser in magnitude with HEC, they exhibited the same photo-responsive patterns as seen with ONPC. The DMAA conjugate exhibits significant shut-off of activity upon VIS irradiation. On the contrary, the DMAAm conjugate is switched off upon UV irradiation. Therefore, under isothermal conditions at 45 °C, we can control the catalytic activities of the conjugates significantly in the opposite direction by UV and VIS irradiations.

5.3.4 PHOTO-RESPONSIVE ACTIVITY CHANGES OF EG III – AZOBENZENE (AZ) CONJUGATE

To elucidate the effect of ‘polymer’ on the photo-switching activity, we have investigated the photo-switching activity changes of the EG III-AZ conjugate. AZ was directly conjugated to S25C and N55C. Figure 5.16 shows UV-VIS spectra of the EG III-AZ conjugates. The S25C-AZ and N55C-AZ conjugates have more absorbance at 325 nm than the WT due to the conjugated AZ. The molar ratio of AZ to EG III was calculated by comparing the absorbance data at 280 nm for EG III and at 325 nm for AZ. The ratios were determined as 2.77 for S25C-AZ and 1.50 for N55C-AZ conjugates, suggesting that AZ was successfully conjugated to the mutants. Figure 5.17 shows the photo-responsive relative activity changes of these conjugates toward ONPC and HEC. They exhibited similar activities as each mutant, and the activities did not change in response to UV and VIS irradiation. Thus, we can conclude that the direct conjugation of an azobenzene at the 25 or the 55 position of EG III does not provide a photo-switchable EG III, and the polymer is necessary in the development of photo-responsive enzymes.

5.3.5 PHOTO-SWITCHING HYDROLYSIS OF COTTON CLOTH BY THE CONJUGATES

In order to examine the practical possibility of the conjugates, the photo-switching activity toward cotton cloth was investigated. Figure 5.18 shows the photo-switching activities of the N55C-DMAA (11 kDa) and N55C-DMAAm (10 kDa) conjugates toward cotton cloth. The DMAA conjugate was turned on upon UV irradiation, while the DMAAm was turned on upon VIS irradiation. Thus, they showed opposite photo-responses on the cotton hydrolysis. However, the activities of the conjugate in the on state were less than 6 % of the unconjugated N55C. This might be due to the sterical hindrance by the conjugated polymer to the access of solid cotton fiber. Therefore, although the conjugates exhibited photo-switching activity toward solid cellulose, the activity changes were much lower than the activity toward a small substrate, ONPC. This result suggests that it might be difficult to apply our concept to develop photo-switchable proteins for large substrates or ligands.

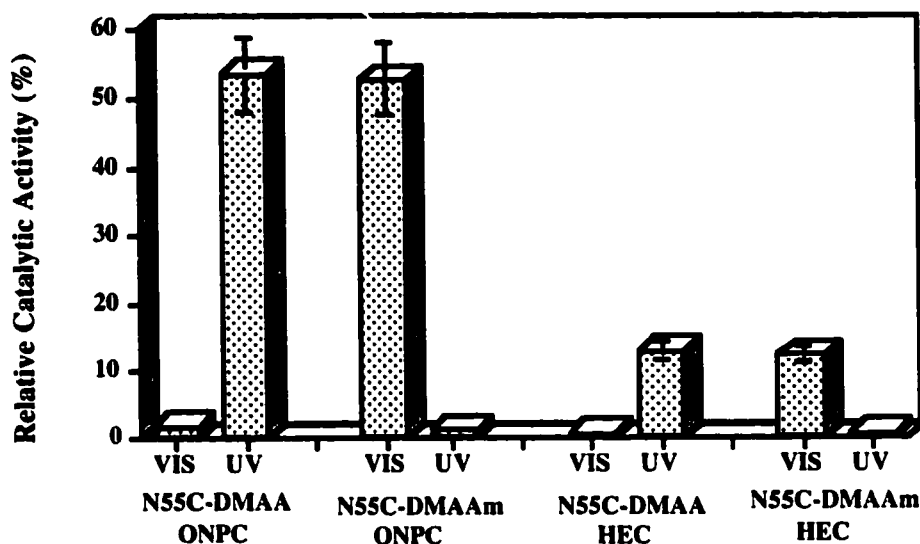


Figure 5.15. Photo-responsive relative activity changes of N55C-DMAA and N55C-DMAAm conjugates.

The activity was measured for 100 nM conjugates with free polymer using 8 mM ONPC or 20 mg/ml HEC as a substrate in 50 mM sodium acetate buffer pH5.5 at 45 °C, and normalized to the activity of N55C upon UV or VIS irradiation as 100%. The UV and VIS light was irradiated for 10 min and 3 h, respectively, before the measurement.

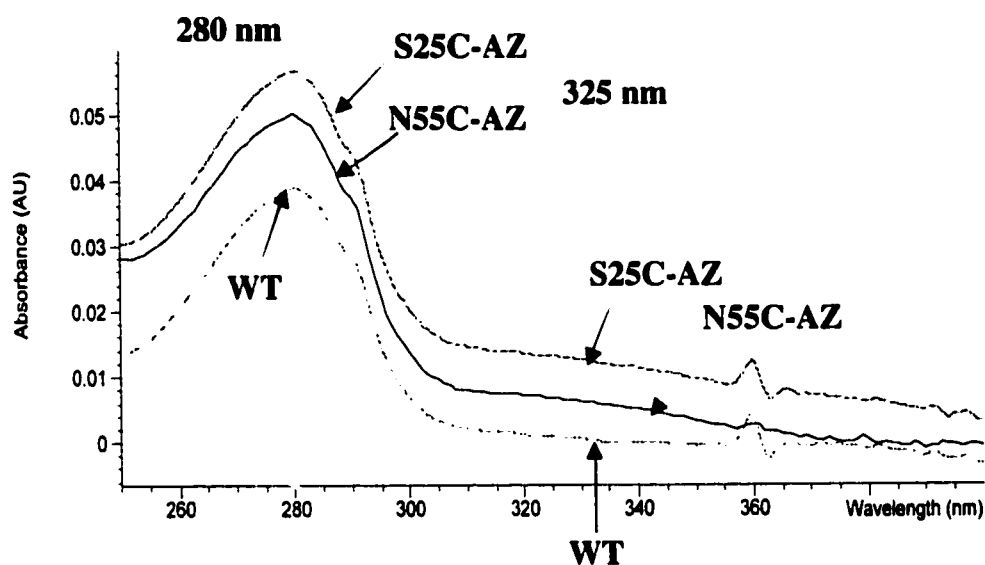


Figure 5.16. UV/VIS spectra of EG III-AZ conjugates.

The absorbance at 280 nm was due to EG III, and that at 325 nm was due to azobenzene. The wild type (WT) EG III didn't show any absorbance at 325 nm, while the conjugates showed some shoulder at 325 nm.

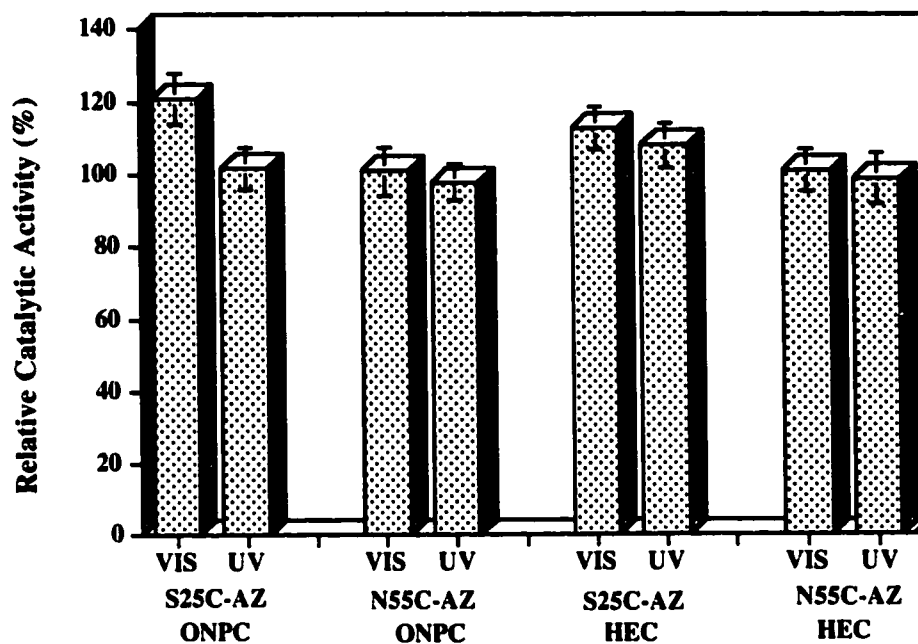


Figure 5.17. Photo-responsive relative activity changes of N55C-AZ and S25C-AZ conjugates.

The activity was measured for 100 nM conjugates using 8 mM ONPC or 20 mg/ml HEC as a substrate in 50 mM sodium acetate buffer pH5.5 at 45 °C, and normalized to the activity of the each mutant as 100 %. The UV and VIS light was irradiated for 10 min and 3 h, respectively, before the measurement.

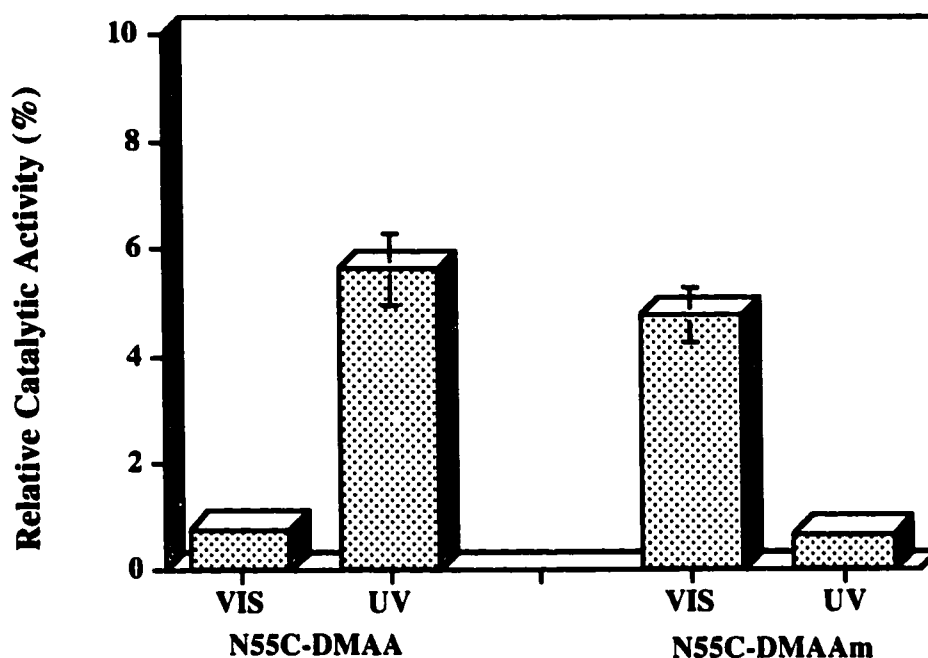


Figure 5.18. Photo-responsive relative activity changes of the N55C conjugates toward cotton cloth.

The activity was measured for 100 nM conjugates using 2 mg of cotton cloth (gauze) as a substrate in 50 mM sodium acetate buffer pH5.5 at 45 °C, and normalized to the activity of the N55C as 100 % upon UV or VIS irradiation. The UV and VIS light was irradiated for 10 min and 3 h, respectively, before the measurement.

5.3.6 TEMPERATURE-RESPONSIVE ACTIVITY CHANGES OF THE IMMOBILIZED CONJUGATES

To investigate the switching activity of the conjugates in the absence of free polymer, the conjugates were biotinylated and immobilized onto streptavidin magnetic beads. The beads were washed intensively to remove free polymer.

The primary amino group on the N-terminus of EG III, glutamate, has a pK_a around 9.1. The amino groups on lysine residues have a pK_a around 10.5. At pH 7.4, only the N-terminal primary amino groups are partially deprotonated and capable of reacting with the N-hydroxysuccinimide ester group (NHS) of the Sulfo-NHS-LC-LC-Biotin. This selective reaction allowed us to approach a degree of biotinylation of one. Table 5.2 shows the degree of biotinylation of the conjugates and WT EG III detected by HABA assay.

Table 5.2. Degrees of biotinylation of the conjugates.

Conjugate	Mn of the polymer (kDa)	Number of biotin (# / EG III conjugate)
N55C-DMAA	11	1.12
N55C-DMAAm	10	1.35
N55C-DMAAm	6	1.42
N55C-DMAAm	3	1.55
S25C-DMAA	11	1.21
S25C-DMAAm	10	1.32
S25C-DMAAm	6	1.38
S25C-DMAAm	3	1.54
WT	-	1.51

The HABA assay has been commonly used to determine biotin content. Biotin binds to avidin with a binding affinity six orders of magnitude higher than that of HABA. Thus, the absorbance at 500 nm, which stems from the HABA-avidin complex, is decreased

upon addition of free biotin. The difference in the binding affinity results in stoichiometric replacement of avidin bound HABA by free biotin.

Table 5.3 shows the amounts of the conjugates and WT EG III immobilized on the SA-magnetic beads. The biotinylated conjugates were immobilized on the magnetic beads effectively.

Table 5.3. Immobilized amount of the conjugates and WT EG III.

Conjugate	Mn of the polymer (kDa)	Immobilized amount ($\mu\text{g} / \text{mg beads}$)
N55C-DMAA	11	19.0
N55C-DMAAm	10	18.8
N55C-DMAAm	6	19.3
N55C-DMAAm	3	19.5
S25C-DMAA	11	19.2
S25C-DMAAm	10	19.0
S25C-DMAAm	6	19.5
S25C-DMAAm	3	19.8
WT	-	19.8

Figure 5.19 and 5.20 show comparisons of the catalytic activities of the immobilized and purified S55C and S25C conjugates toward ONPC and HEC at 32 °C and 52 °C, respectively. The activity was normalized to the activity of the immobilized WT EG III. Although the conjugates showed less activity at 52 °C compared to 32 °C, the shut-off abilities of the immobilized conjugates were lower than the conjugates in the presence of free polymer (c.f. Figure 5.7 and 5.8). Similar to the results for the conjugates with free polymer, the conjugate with higher MW polymer at the 55 position exhibited the higher switch-off activity. In particular, S25C-M6 and S25C-M3 conjugates exhibited higher relative activities at 52 °C than that at 32 °C. This result suggests that the conjugate with a small polymer at a remote position to the active site has less sterical hindrance to a

large substrate in the shrunken state of the polymer than in the expanded state. Thus, the balance between the distance of the conjugation from the active site and the size of the conjugated polymer determines the switching direction.

5.3.7 THE EFFECT OF ADDITION OF FREE POLYMER ON SWITCHING ACTIVITY

To investigate the effect of free polymer on the switching activity of the conjugates, the DMAA (11 kDa) or DMAAm (10 kDa) were added to the immobilized and purified conjugates of the respective polymers. Figure 5.21 shows the effect of addition of free polymer on the activity of the immobilized conjugates at 52 °C. Since the molar ratios of free polymer/conjugate of the unpurified states were calculated as 463 (N55C-DMAA), 258 (N55C-DMAAm), 309 (S25C-DMAA), and 213 (S25C-DMAAm) based on conjugation yields, free polymer up to 400 molar times the conjugates was added. The addition of the free polymer enhanced the switch-off ability for both S25C and N55C conjugates, and reached almost zero activity for N55C conjugates when more than 200 molar times of the free polymer was added. These results suggest that the free polymer might cause physical aggregation with the conjugated polymer, acting together as a higher MW polymer, leading to more effective blocking of the substrate from the active site. This same effect was observed for the SA conjugates in Chapter 3.

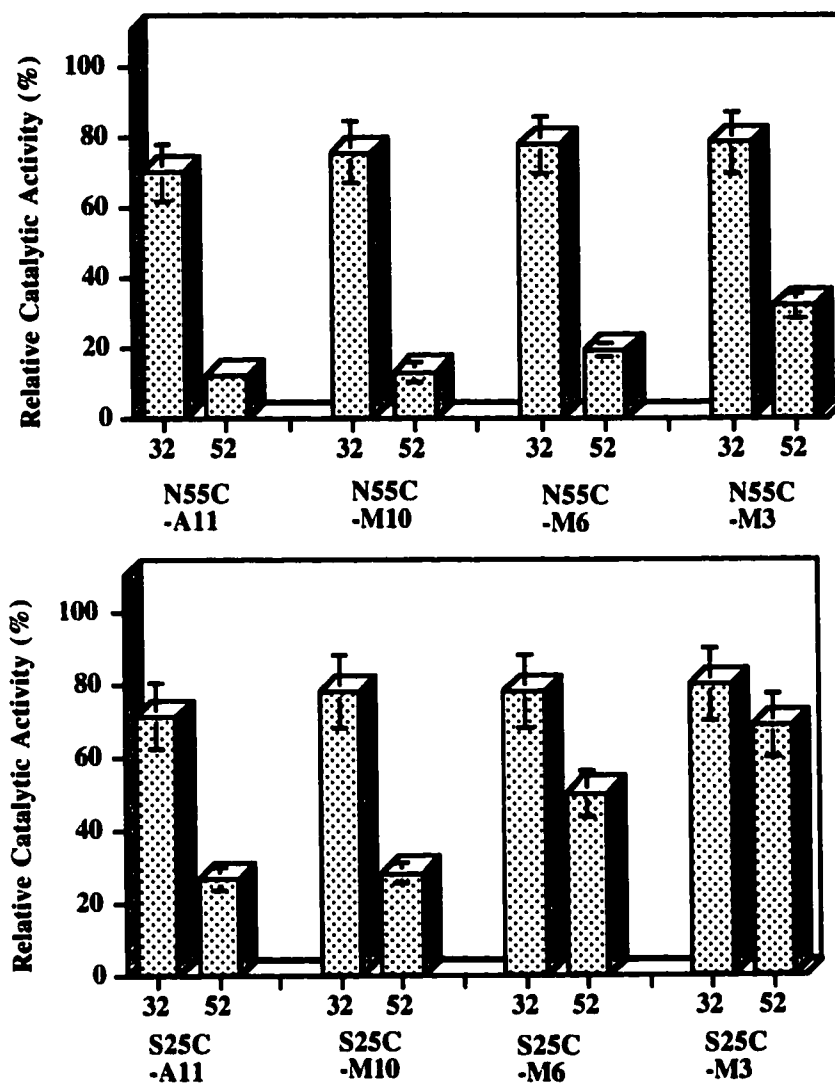


Figure 5.19. Thermo-responsive activity changes of the conjugates immobilized on magnetic beads.

The activities were measured for 100 nM purified conjugates using ONPC (8mM) as a substrate, and normalized to the activity of the immobilized WT EG III as 100 % at each temperature. A11: DMAA (11 kDa), M10: DMAA.m (10 kDa), M6: DMAAm (6 kDa), M3: DMAAm (3 kDa).

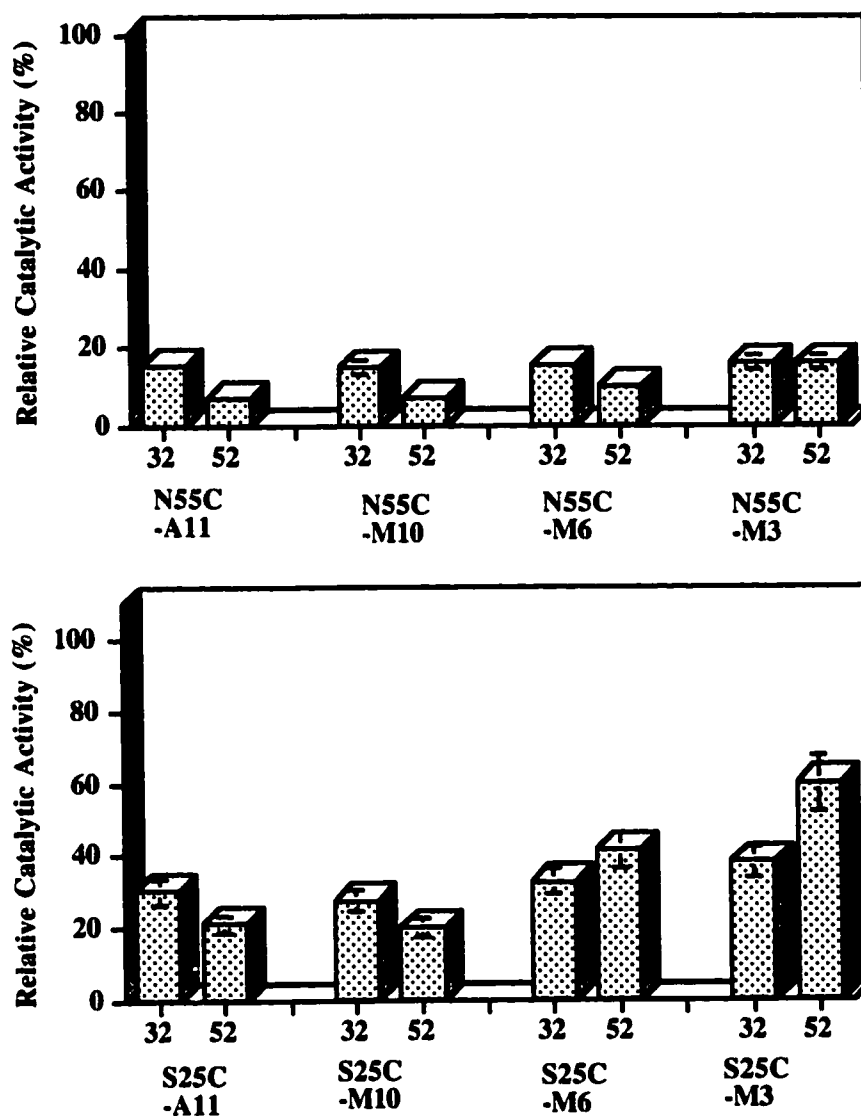


Figure 5.20. Thermo-responsive activity changes of the conjugates immobilized on magnetic beads.

The activities were measured for 100 nM purified conjugates using HEC (20 mg/ml) as a substrate, and normalized to the activity of the immobilized WT EG III as 100 % at each temperature. A11: DMAA (11 kDa), M10: DMAAm (10 kDa), M6: DMAAm (6 kDa), M3: DMAAm (3 kDa).

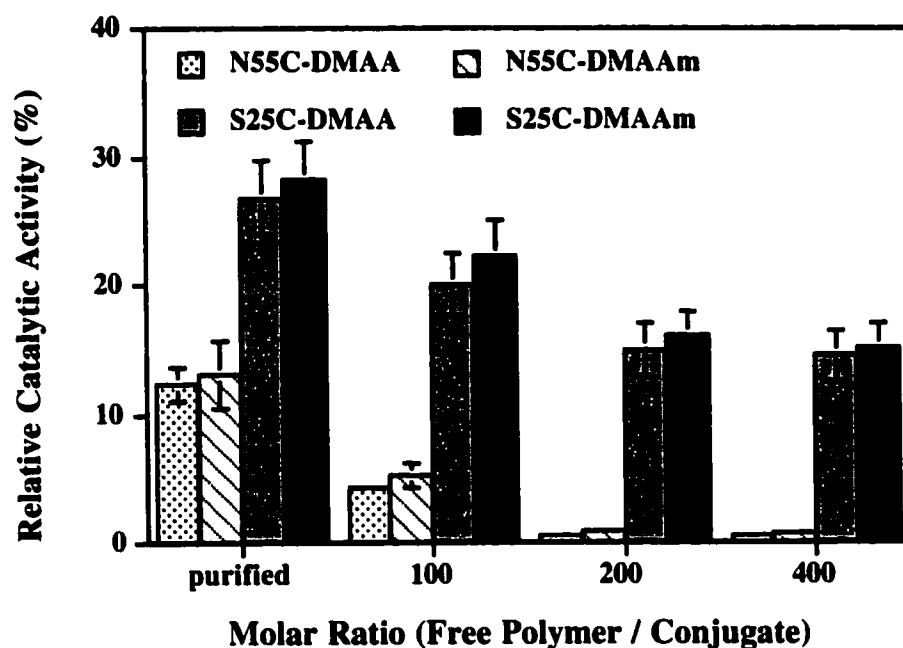


Figure 5.21. Effect of addition of free polymer on the shut-off activity of the conjugates immobilized on magnetic beads.

The same DMAA (11 kDa) or DMAAm (10 kDa) was added into the conjugate immobilized on magnetic beads. The activities were measured for 100 nM conjugates using ONPC (8 mM) as a substrate at 52 °C in 50 mM sodium acetate buffer pH5.5, and normalized to the activity of immobilized WT EG III at each temperature.

5.3.8 PHOTO-RESPONSIVE ACTIVITY CHANGES OF THE IMMOBILIZED CONJUGATES

Figure 5.22 shows the photo-responsive activity changes of the immobilized and purified conjugates for ONPC and HEC measured isothermally at 45 °C. The DMAA conjugate exhibited lower activity upon VIS irradiation, while the DMAAm conjugate showed reduced activity upon UV irradiation. These results are similar to the conjugates in the

presence of free polymer (c.f. Figure 5.15). However, the magnitudes of the switching responses were less than those of the unpurified conjugates. Therefore, we can conclude that the free polymer enhanced the photo-responses of the conjugates as well as the thermal responses.

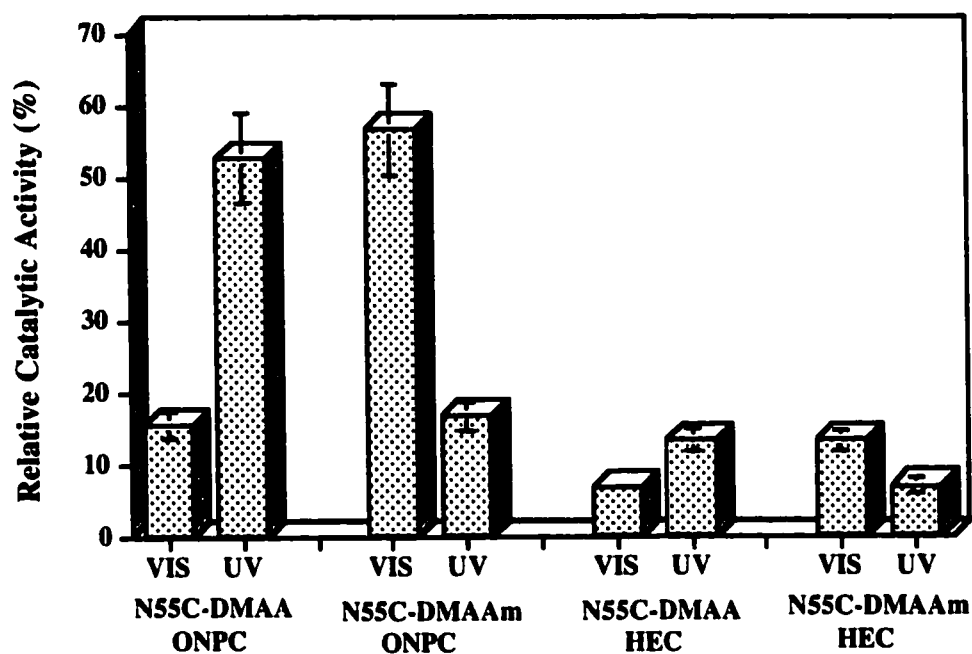


Figure 5.22. Photo-responsive activity changes of the conjugates immobilized on magnetic beads.

The activities were measured for 100 nM purified conjugates using ONPC (8 mM) or HEC (20 mg/ml) as a substrate at 45 °C in 50 mM sodium acetate buffer pH5.5, and normalized to the activity of immobilized WT EG III as 100 % upon UV or VIS irradiation.

5.3.9 CYCLIC SWITCHING OF THE ACTIVITY

As a molecular switch, the time course of on-off switching behavior and the switching durability are important properties. These properties were evaluated for the N55C-DMAA (11 kDa) and N55C-DMAAm (10 kDa) conjugates in the presence of free polymer.

Figure 5.23 and 5.24 show the sequential thermo- and photo-switching responses of N55C-DMAA and N55C-DMAAm conjugates toward ONPC. Both conjugates were in the “on” state at lower temperature (32 °C) and in the “off” state at higher temperature (52 °C). In addition, they showed almost complete shut-off of the activity at 52 °C. The response time was within 1 min. As for the photo-responses, the DMAA conjugate was in the “on” state upon UV irradiation, while the DMAAm conjugate was in the “on” state upon VIS irradiation. The response time to VIS irradiation was longer than that to UV light, which may be due to the slower photo-isomerization rate of azobenzene (from *cis* to *trans*) under VIS light (c.f. Figure 2.4 and 2.5). One of the reason might be the different power level between UV and VIS light.

Figure 5.25 and 5.26 show the effects of thermo- and photo- cycling on the activity of the conjugates for up to three cycles. The conjugates exhibited reversible on-off switching in response to temperature change or UV/VIS photo-irradiation. Figure 5.27 and 5.28 show the effect of the number of temperature cycles between 32 °C and 52 °C or UV/VIS photo-cycles on the catalytic activity of the N55C-DMAA and N55C-DMAAm conjugates, respectively. N55C was used as a control. For the thermal cycling, the activities of both N55C and the conjugates decreased with increasing cycle number; however, the conjugates retained almost same activity as N55C. As for the photo-cycling, while the conjugates were vulnerable similar to the thermal cycling, N55C retained its activity for more cycles. This suggests that the phase transition of the conjugated polymer might reduce the residual activity. The polymer repeatedly changes its configuration between loose coil and dense globule in the cyclic phase transition. The cyclic collapse

and expansion of the polymer chains might lead to micro-environmental stresses, resulting in unfolding of some EG III molecules. On the other hand, the N55C didn't suffer from such stresses because it has no covalent attachments to the polymers. Therefore, the N55C was more stable during the photo-recycling under isothermal condition. However, quick temperature changes between 32 °C and 52 °C might elicit the gradual denaturation even for the unconjugated N55C, resulting in similar vulnerability of the N55C towards thermal cycling.

Although the activity decreased with increasing thermo- and photo-cycle number, the conjugates still retained more than 70 % activity after 10 cycles.

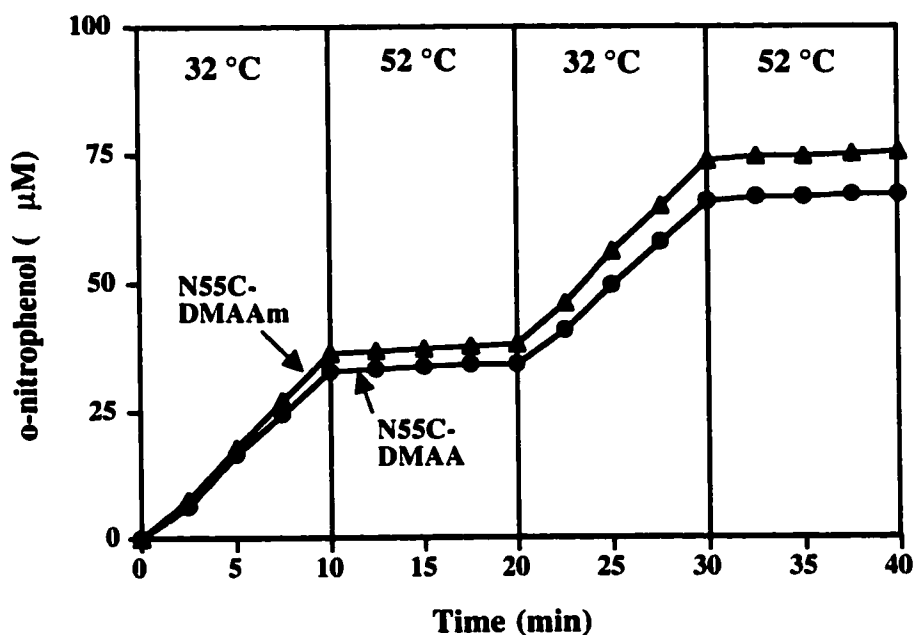


Figure 5.23. Sequential thermo-switching of activity of N55C-DMAA and N55C-DMAAm conjugates.

The product (o-nitrophenol) concentration was measured for 100 nM conjugates with free polymer using ONPC (8 mM) as a substrate in 50 mM sodium acetate buffer pH5.5.

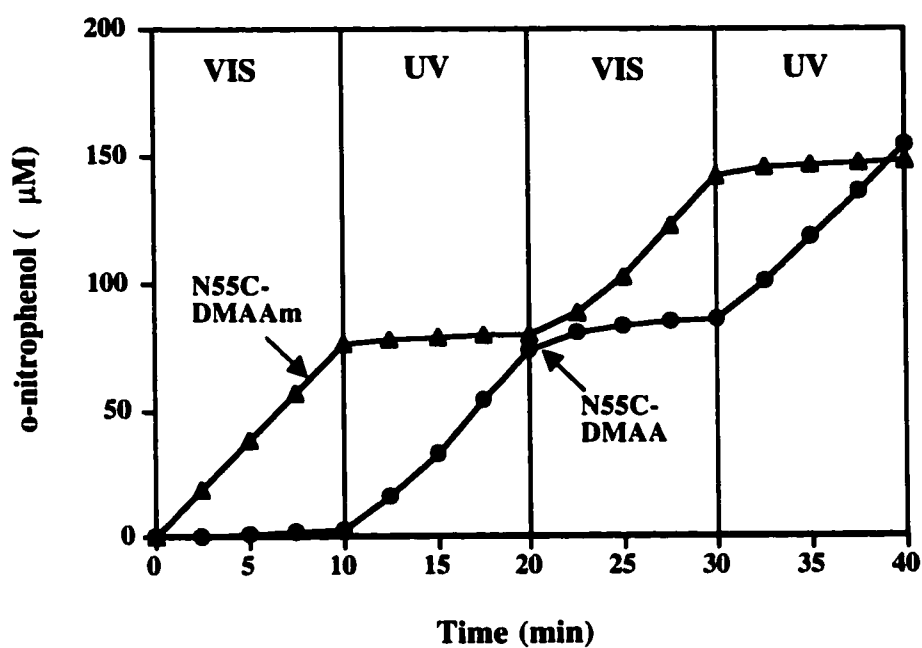


Figure 5.24. Sequential photo-switching of activity of N55C-DMAA and N55C-DMAAm conjugates.

The product (o-nitrophenol) concentration was measured for 100 nM conjugates with free polymer using ONPC (8 mM) as a substrate at 45 °C in 50 mM sodium acetate buffer pH5.5.

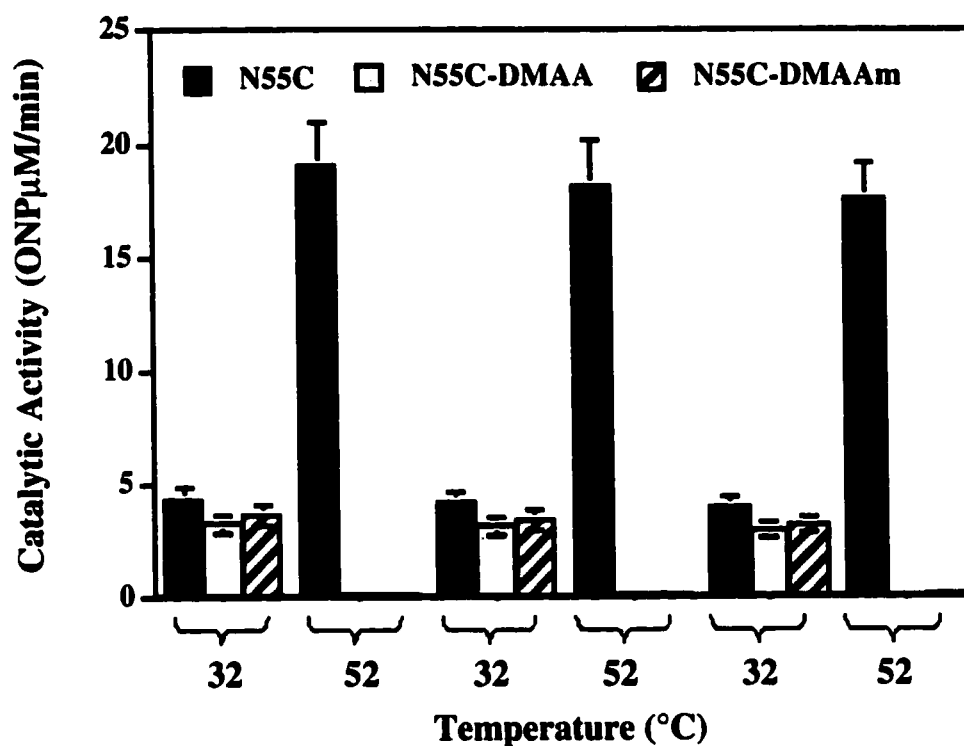


Figure 5.25. Effect of thermal cycling on the activity of N55C, N55C-DMAA and N55C-DMAAm conjugates.

The activities were measured for 100 nM N55C or the conjugates with free polymer using ONPC (8 mM) as a substrate after incubation for 20 min at each temperature in 50 mM sodium acetate buffer pH5.5.

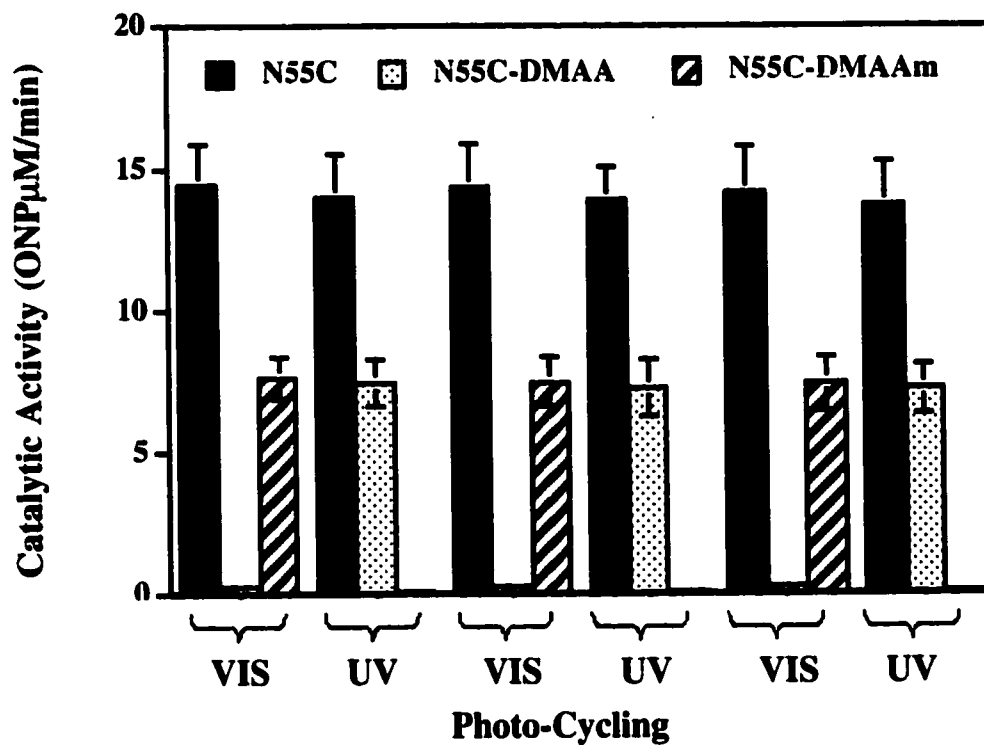


Figure 5.26. Effect of photo-cycling on the activity of N55C, N55C-DMAA and N55C-DMAAm conjugates.

The activities were measured for 100 nM N55C or the conjugates with free polymer using ONPC (8 mM) as a substrate at 45 °C isothermal condition after UV or VIS irradiation for 20 min in 50 mM sodium acetate buffer pH5.5.

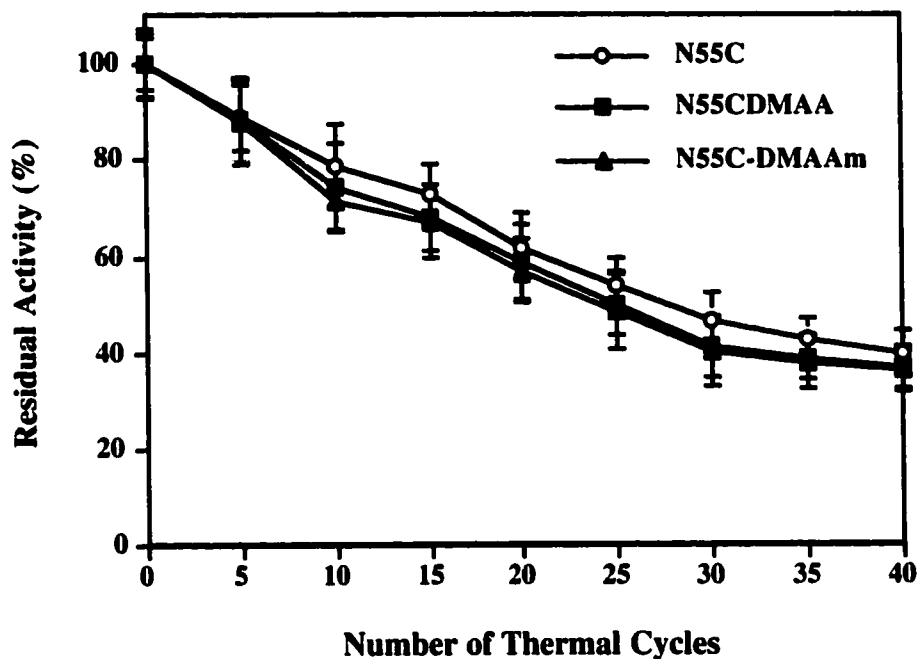


Figure 5.27. Retained activities of N55C, N55C-DMAA and N55C-DMAAm conjugates as a function of the number of thermal cycling.

The temperature was cycled between 32 °C and 52 °C for 2 min each. The activities were measured for 100 nM N55C or the conjugates with free polymer using ONPC (8 mM) as a substrate at 32 °C after incubation for 20 min in 50 mM sodium acetate buffer pH5.5.

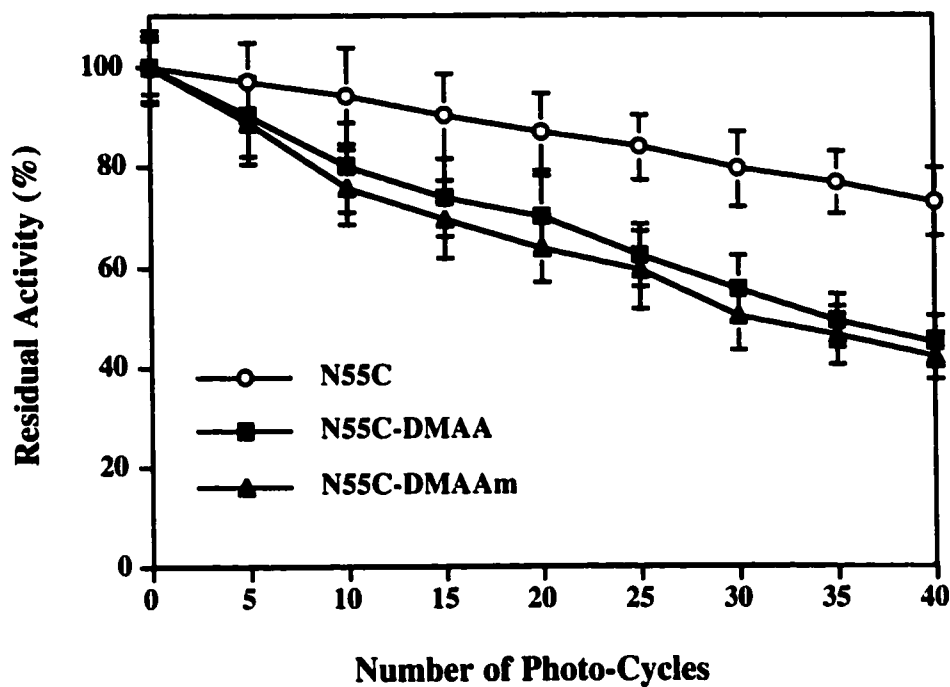


Figure 5.28. Retained activities of N55C, N55C-DMAA and N55C-DMAAm conjugates as a function of the number of photo-cycling.

The UV and VIS light was irradiated for 10 min each at 45 °C and cycled. The activities were measured for 100 nM N55C or the conjugates with free polymer using ONPC (8 mM) as a substrate at 32 °C after 20 min incubation in 50 mM sodium acetate buffer pH5.5.

5.3.10 MECHANISM ANALYSIS OF THE THERMO- AND PHOTO-RESPONSE

From kinetic analysis of the catalytic activity data, the mechanism of the thermo- and photo-responses of the conjugates were elucidated. If the k_{cat} of the conjugate is strongly dependent on the temperature changes or the photo-irradiations compared to the unconjugated mutant, the switching response can be attributed to a change in the catalytic

site directly. While, if the K_m is changed significantly by the stimulus, we can conclude that the affinity change between EG III and the substrate is the driving force of the switching.

Figure 5.29 and 5.30 show the effect of temperature change and UV/VIS photo-irradiation on the kinetic parameters of N55C, N55C-DMAA (11 kDa) and N55C-DMAAm (10 kDa) conjugates for the hydrolysis of ONPC and HEC, respectively. By increasing the temperature from 32 °C to 52 °C, the K_m values of the conjugates were drastically increased (more than 50 times). The k_{cat} values of the conjugates did not differ from those of N55C compared to the changes in K_m . This suggests that the activity-off at high temperature is mainly due to a drastic decrease in the affinity between the conjugate and the substrates. This may stem from the physical blocking of the substrate from reaching the active site of EG III by the shrunken polymers. The smaller k_{cat} values of the conjugates at 52 °C compared to N55C indicates that the active site is a little perturbed by the shrinkage of the polymers; however, the effect is small compared to the large changes in K_m .

Concerning the photo-responsive kinetic changes at 45 °C, the DMAA conjugate showed much higher K_m values upon VIS irradiation, whereas the DMAAm conjugate showed an increase in K_m upon UV irradiation. The k_{cat} values upon UV and VIS irradiation were almost the same. Thus, the photo-switching of the catalytic activity is also due to affinity changes between the conjugates and the substrates.

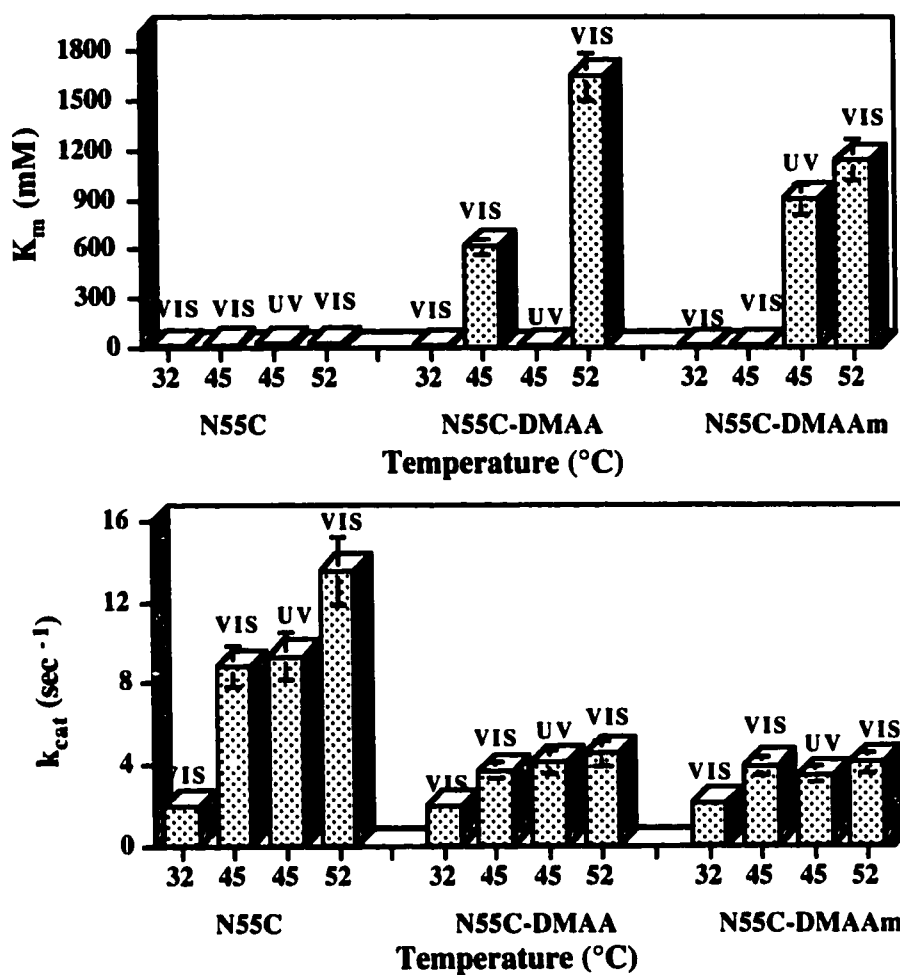


Figure 5.29. Kinetic parameters of the conjugates toward ONPC in response to temperature and photo-irradiation.

The activities were measured for 100 nM N55C or the conjugates with free polymer using ONPC as a substrate after 20 min incubation in 50 mM sodium acetate buffer pH5.5.

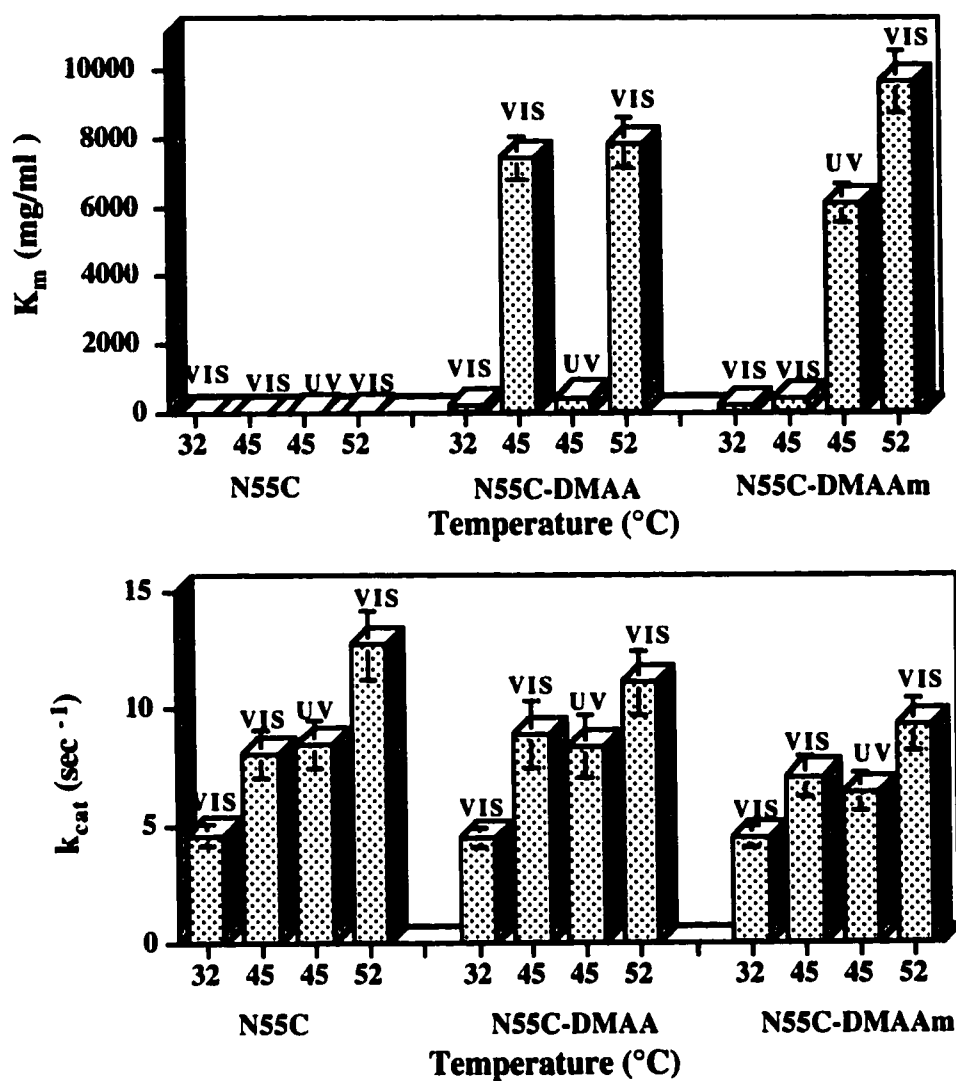


Figure 5.30. Kinetic parameters of the conjugates toward HEC in response to temperature and photo-irradiation.

The activities were measured for 100 nM N55C or the conjugates with free polymer using HEC as a substrate after 20 min incubation in 50 mM sodium acetate buffer pH5.5.

For the hydrolysis of HEC, the conjugates exhibited larger K_m values (180-187 mg/ml) than the unconjugated N55C (14.4 mg/ml) even in the expanded state of the polymer at 32 °C. This result suggests that the reason for the small activity of the conjugates at 32 °C toward HEC (Figure 5.8) is due to a decrease in affinity between the conjugates and HEC. The conjugated polymers in the expanded state might physically prevent the access of the large substrate, HEC, to the active site of the conjugates.

5.4 CONCLUSIONS

The EG III mutants, S25C and N55C, were conjugated to the polymers, DMAA and DMAAm, successfully. The best yields of the conjugates were obtained for conjugation with VS-terminated polymers at pH 8.0.

The conjugates exhibited temperature-responsive activity changes. The activity was switched on at lower temperature (32°C), and switched off at higher temperature (52 °C). The higher the MW of the conjugated polymer, the more effectively the activity was shut off. The N55C conjugates showed higher shut-off activity than the S25C conjugates and the WT conjugates. The size of the substrate also influenced the activity. The conjugates showed much less activity for a larger substrate (HEC) even at low temperature where the polymer was expanded, while they showed almost the same activity as WT for the small substrate, ONPC. Thus, we can conclude that the MW of the conjugated polymer, the position of conjugation and the size of the substrate are key factors to design such molecular switches.

The photo-responsive activity changes of the conjugates were evaluated under isothermal conditions at 45 °C. The DMAA conjugate and DMAAm conjugate exhibited opposite and complete photo-responses; N55C-DMAA conjugate was turned on, while N55C-DMAAm conjugate was turned off upon UV irradiation. These responses agree with the opposite photo-responsive phase transitions of the conjugated polymers.

Azobenzene was directly conjugated to S25C or N55C. They exhibited almost the same activity as unconjugated mutants, and the activities did not change in response to UV or VIS irradiation. Therefore, we can conclude that the photo-induced shrinkage of the polymer turns off the catalytic activity, and the polymer effect is significant for the switching of the activity.

Although the N55C conjugates exhibited photo-switching activities toward cotton cloth, the activities in the on state were less than 6 % of the activity of the unconjugated N55C. This might be due to the sterical hindrance of the conjugated polymer to the binding of cotton fiber. Therefore, it might be difficult to apply this methodology for switching the activity toward large substrates.

The immobilized and purified conjugates without free polymer exhibited lower shut-off effect on the activity in response to both temperature changes and UV/VIS irradiation. The addition of the free polymer into the purified conjugates enhanced and recovered the switching ability to the same level as the unpurified conjugates. This suggests that the free polymer may cause physical aggregation with the conjugated polymer, acting together as a higher MW polymer, leading to more effective blocking of the substrate from the active site.

The temperature- and photo-cyclic activity changes of the conjugates were examined. The conjugates maintained more than 70 % activity even after 10 cycles. The response rate to complete thermal switching-off was less than 1 min. The photo-switching triggered by UV light was also completed within 1 min, while VIS light-triggered switching took 5 min to complete. This may be due to the slow cis-trans photo-isomerization of azobenzene.

The mechanisms of such stimuli-responsive activity changes were elucidated by kinetic studies. When the activity was turned off either by temperature change or light irradiation, the K_m values of the conjugates were drastically increased. Thus, the shut-off

of the activity might be mainly ascribed to the decrease in the affinity between the conjugates and the substrate, stemming from the inhibition of the access of the substrate to the catalytic site of EG III by the shrunken polymers.

Therefore, we have successfully developed photo-switchable enzymes in which the catalytic activity can be switched on and off reversibly, oppositely and completely by UV and VIS irradiations.

CHAPTER 6 CONCLUSIONS AND RECOMMENDATIONS

6.1 CONCLUSIONS

Light-regulated switches that reversibly control protein functions have been attracting many researchers' interests. An ideal photo-switchable protein system should turn on and off the function of the protein sharply, reversibly and completely by specific light irradiation. In addition, it is desirable to be able to select the wavelength of the light to control the function depending on the application.

Our rationale to develop such photo-switchable proteins is the site-specific conjugation of a light-responsive polymer near the critical site of the protein in order to regulate the function. This provides control of the protein function associated with the photo-induced phase transition of the polymer. We have selected SA and EGIII as model target proteins to control ligand binding affinity or catalytic activity in response to light irradiation, respectively.

6.1.1 CONCLUSIONS OF PHOTO-RESPONSIVE POLYMER RESEARCH

We synthesized two kinds of temperature- and photo- dual stimuli-responsive polymers, DMAA and DMAAm. They exhibited LCSTs, which shifted upon UV or VIS irradiations. Thus, under isothermal conditions at a temperature between the LCSTs upon UV and VIS irradiations, these polymers underwent photo-responsive phase transitions. In addition, they showed opposite photo-responses from each other under UV and VIS irradiations; that is, DMAA became soluble and DMAAm became insoluble under the same UV light irradiation. This can be useful as oppositely photo-switchable devices. The

photo-responsive temperature range of the polymer was dependent on the content of azobenzene, MW of the polymer, concentration of the polymer and the buffer condition. Therefore, we could design and tailor appropriate polymers for various condition and applications.

6.1.2 CONCLUSIONS OF SA-PHOTO-RESPONSIVE POLYMER CONJUGATE RESEARCH

To prepare site-specific conjugates of SA to photo-responsive polymers, we have constructed two streptavidin mutants; one contains a unique cysteine residue at a critical site for biotin-binding (E116C) and another has a cysteine at a remote position to the biotin-binding site (S139C).

These mutant SAs were conjugated site-specifically to DMAA and DMAAm. The E116C conjugates exhibited reversible switching of biotin binding between 52 °C and 4 °C. They bound biotin at 4°C, where the polymer was hydrated, and released biotin completely at 52 °C, where the polymer was collapsed. Kinetic studies of biotin release demonstrated that the off-rate of biotin was unperturbed, and that the thermally triggered release of biotin with the E116C conjugates was due to blocking of biotin reassociation. The E116C-DMAA conjugate showed higher response than the E116C-DMAAm conjugate, which might be attributed to the higher MW of DMAA than DMAAm. The biotin binding switching activity was strongly dependent on conjugation position, as the E116C conjugates displayed a large thermal response while the S139C conjugates displayed only small effects. Moreover, the addition of free polymer to purified conjugates was also shown to increase the blocking and release properties of the switch. This effect was site-dependent, suggesting that the conjugated polymers were directing a physical aggregation near the binding site that effectively enhanced the switching activity. Therefore, three key factors to improve the thermal switching property of the conjugate have been elucidated. They are the position of the conjugation, the MW of the

conjugated polymer, and the addition of free polymer. When the conjugation position is close to the binding site, when the MW of the polymer is high, and when free polymer is added to the conjugate solution, the thermal response will be maximized.

The photo-responses of these conjugates for biotin binding and release were investigated upon UV/VIS light cyclic irradiation under isothermal conditions at 40 °C. The conjugates demonstrated reversible blocking and release of biotin in response to UV/VIS cyclic irradiation. In addition, they exhibited the opposite photo-responses. The DMAA conjugate bound biotin upon UV irradiation, while the DMAAm conjugate bound it upon VIS irradiation. The off-rates of biotin from the conjugates were only three times larger than the off rate of wild type SA, suggesting that the photo-induced release of biotin might be due to the blocking of reassociation of the released biotin.

Therefore, we have succeeded in controlling the SA-biotin association reversibly and oppositely by UV and VIS irradiations.

6.1.3 CONCLUSIONS OF EG III - PHOTO-RESPONSIVE POLYMER CONJUGATE RESEARCH

We have constructed four site-directed mutant EG III genes, S25C, N55C, N107C and N151C. The activity measurements, SDS-PAGE and peptide mapping for the expressed mutants have shown that S25C and N55C were expressed successfully, but N107C and N151C were not. The N55C locates a genetically introduced Cys at a position closer to the catalytic active site than the S25C. The kinetic parameters of the catalytic activity of WT, S25C and N55C EG IIIs were evaluated with ONPC and HEC as substrates. The N55C mutant showed higher K_m values than WT, but similar k_{cat} values as WT, indicating that the 55 residue is involved in binding of the substrate but does not participate in the catalytic event. The S25C mutant exhibited higher K_m values only for

HEC, but not for ONPC, suggesting the 25 residue influences the binding of the large substrate, but does not affect the binding of the small substrate.

The mutants were conjugated to DMAA and DMAAm of various MWs. The effects of pH (pH7.0 vs. pH8.0) and chemistry (VS vs. AA) of the conjugation were investigated. The best yields of the conjugates were obtained for conjugation with VS-terminated polymers at pH8.0. The conjugates exhibited temperature-responsive activity changes. The activity was switched on at lower temperature (32°C), and switched off at higher temperature (52 °C). The MW of the conjugated polymer affected the switching activity. The higher the MW of the conjugated polymer, the more effectively the activity was shut off. The position of the conjugation was also shown to be important. The N55C conjugates showed higher shut-off activity than the S25C conjugates and the WT conjugates. The size of the substrate influenced the activity as well. The conjugates showed much less activity for the larger substrate, HEC, even at low temperature where the polymer was expanded. However, they showed almost the same activity as WT for the small substrate, ONPC. Thus, we can conclude that the MW of the conjugated polymer, the position of the conjugation, and the size of the substrate are key factors in the design of such molecular switches.

The photo-responsive activity changes of the conjugates were evaluated under isothermal conditions at 45 °C. The DMAA conjugate and DMAAm conjugate exhibited opposite and complete photo-responses; the N55C-DMAA conjugate was turned on, while N55C-DMAAm conjugate was turned off upon the same UV irradiation. These responses agree with the opposite photo-responsive phase transitions of the conjugated polymers. In both cases, the conjugates assumed the “off” state when the polymers were shrunken. Therefore, the photo-induced shrinkage of the polymer leads to a turning off of the catalytic activity. Since the conjugate of only one azobenzene to the mutants didn't induce photo-responsive activity changes, we can conclude that the polymer effect is significant for switching the activity.

The possibility of a practical application of the conjugates was investigated using cotton cloth as a substrate. The conjugates exhibited photo-switching hydrolysis activities toward cotton, however, they exhibited less than 6 % of the activity of the unconjugated mutant even in the “on” state. This may be due to sterical hindrance of the conjugated polymer.

The conjugates were immobilized onto magnetic beads and separated from free polymer. The immobilized conjugates exhibited a lower shut-off effect on the activity in response to both temperature change and UV/VIS irradiation. The addition of free polymer to the immobilized conjugates enhanced and recovered the switching ability to the same level as the unpurified conjugates. This suggests that the free polymer may cause physical aggregation with the conjugated polymer, acting together as a higher MW polymer, leading to more effective blocking of the substrate from the active site.

In order to investigate the switching response and the durability of the conjugates, the temperature- and photo-cyclic activity changes of the conjugates were examined. The conjugates maintained more than 70 % activity even after 10 cycles. The response rate to complete thermal switching-off was within 1 min. The photo-switching triggered by UV light was also completed within 1 min; however, the VIS light-triggered switching took 5 min to complete. This may be due to the slow cis-trans photo-isomerization of azobenzene.

The mechanisms of such stimuli-responsive activity changes were elucidated by kinetic studies of the activity. When the activity was turned off either by temperature change or light irradiation, the K_m values of the conjugates were drastically increased, while the k_{cat} values showed slight decreases. Thus, the shut-off of the activity might be mainly due to a decrease in the affinity between the conjugates and the substrate, stemming from the inhibition of the access of the substrate to the catalytic site of EG III by the shrunken polymers.

Therefore, we have succeeded in developing photo-switchable enzymes in which the catalytic activity can be switched on and off reversibly, oppositely and completely by UV and VIS irradiations. The site-specific conjugation of such photo-responsive polymers to genetically-engineered proteins could provide a general approach to the design and development of photo-switchable proteins, where the specific molecular recognition and binding processes or the catalytic activity is controlled by external specific light signals.

6.2 RECOMMENDATIONS FOR THE FUTURE RESEARCH

6.2.1 IMPROVEMENT OF THE CONJUGATE

6.2.1.1 Switching Response

Since separation of the conjugate from free polymer led to lower switching responses in the present system, it is clear that free polymer is required to achieve zero activity in the off state. This may not be ideal for some applications. From the results of our research, it was suggested that a conjugate with a higher MW polymer at a position closer to the active site enhanced the shut-off ability. Thus, a conjugate of higher MW polymer, such as 20 – 50 kDa, to N55C or another mutant that locates a Cys closer to the active site, might exhibit complete zero activity in the off state even in the purified state.

Purification of the conjugates might also improve the switching response rate of the conjugates, since the slow step of dissolution and diffusion of the phase separated free polymer might retard the response speed. The tight aggregation of the free polymer with the conjugated polymer might reduce the expanding and dissolving speed of the conjugated polymer chain, resulting in the slow response to return to the “on” state. Therefore, the isolation of the conjugate from the free polymer might also enhance the switching rate of the conjugate.

The immobilization reduced the activity of the conjugates to 20 - 30 % of the unimmobilized states. Thus, the purified solution state of the conjugates would be ideal. In order to separate the conjugate from the free polymer, we tried to use cationic exchange chromatography and hydroxyapatite chromatography. However, capture of the conjugates was inadequate, and the yields were less than 20%. Usually cellulase has high affinity to cellulose, which can be used for affinity separation of cellulase. However, EG III does not have a separated cellulose binding domain, thereby the affinity to cellulose is rather weak. One of the best methods might be to utilize a His-tag – Ni affinity separation. A His-tag domain could be introduced at the C-terminus of the mutants, and the His-tag could bind to a Ni-NTA solid substrate (Qiagen, CA). The trapped His-tag mutant can be eluted by competition with imidazole. Since the C-terminus is remote to the active site of EG III, the His-tag may not influence the catalytic activity.

Another method to improve the switching efficacy might be related to the conjugated polymers. To regulate the protein activity by stimuli-responsive phase transition of the polymer more sharply, the conjugated polymer has to be uniform. The MW should be mono-dispersed and the composition of the copolymer should be uniform, because the transition temperature is dependent on the MW and the composition of the polymer. The polymer synthesized by free radical copolymerization has both MW and composition distribution. For this purpose, living polymerization methods have to be employed for the copolymerization of photo-responsive polymers.

6.2.1.2 Conjugation Reaction Efficacy on the Yield

The conversions of the conjugates were only 10 – 20 %. This might be due to sterical hindrance between the macromolecules, the polymer and the protein, for the specific reaction of the end group of the polymer to the thiol group in the protein. Thus, one possible method to increase the conversion might be to use the polymer with lower MW. Since both the position of conjugation and the MW of the polymer influence the

switching activity, a smaller MW polymer conjugated to a position closer to the active site might have the same effect on the switching as a larger remotely-positioned polymer.

6.2.2 PRACTICAL PROCESS USING OUR PHOTO-SWITCHABLE EG III

EG III has been industrially utilized for the surface treatment of fabrics to add stone-wash feeling on it by partial hydrolization of the cotton surface. A problem on this treatment is fiber strength loss due to the difficulty of the activity control. Fine and sharp control of the catalytic activity might be possible by using our conjugates. Figure 6.1 illustrates a possible process using our conjugates. The cloth is introduced in the EG III treatment bath. The bath includes the N55C-DMAA (11 kDa) conjugate with 200 molar times excess amount of the free polymer to the conjugate, and is controlled at 45 °C isothermal condition. The cloth is exposed to UV light at the UV zone, then exposed to VIS light at the VIS zone. Since the N55C-DMAA conjugate is switched on by UV irradiation and switched off by VIS irradiation, the treatment efficacy is controlled by the line speed or the distance between the UV and VIS exposure zones. This reactor might enable us fine tuning of the extent of the surface hydrolysis treatment.

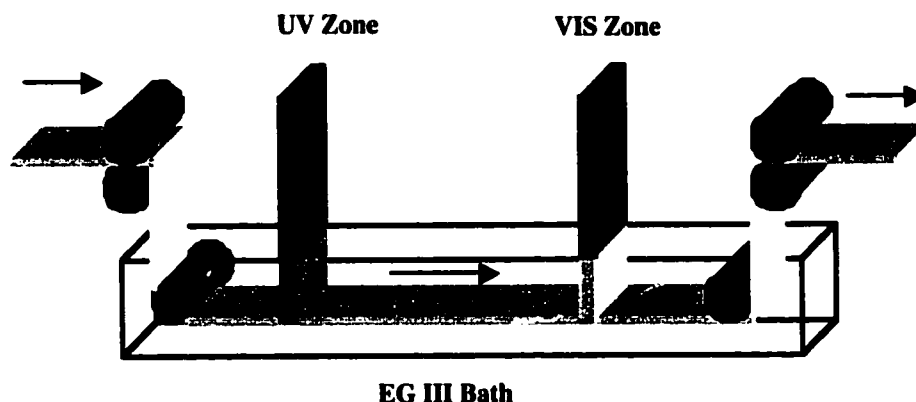


Figure 6.1. EG III reactor.

The temperature of the reactor bath is controlled at 45 °C isothermal condition. The reactor includes the N55C-DMAA (11 Ka) conjugate with free polymer (200 molar times excess to the conjugate) in 50 mM sodium acetate buffer pH5.5. The reaction time is controlled by the line speed or the distance between UV and VIS zone.

6.2.3 APPLICATION OF OUR METHODOLOGY

We could design and develop other important photo-responsive proteins using the same methodology. The advantage of our system is that we could develop reversibly, oppositely and completely photo-switchable proteins. For example, when DMAA and DMAAm are conjugated to two kinds of enzymes, which can catalyze a sequential series of reactions in a cascade, alternative UV and VIS irradiation could regulate the enzymatic cascade stepwise.

Another interesting example is to regulate the direction of the opposite enzymatic reaction. When two kinds of enzymes, which catalyze opposite reactions, are conjugated to each of these opposite photo-responsive polymers, the direction of the reactions could be regulated by the alternative switching of UV and VIS irradiations.

6.2.4 OPPOSITELY PHOTO-RESPONSIVE POLYMERS AND HYDROGELS

Since the DMAA-AA or DMAAm-AA has a polymerizable end terminus, acrylate, these polymers can be used as photo-responsive macromers. They can be co-polymerized with any other monomers and also can be grafted to radically activated surfaces by plasma treatment or gamma irradiation. In addition, VS or AA terminated DMAA or DMAAm can be grafted to thiol-containing polymers or surfaces to introduce photo-sensitivity into them.

Another application is a photo-responsive hydrogel, which can swell and collapse by external UV and VIS irradiation reversibly and oppositely. When DMAA is copolymerized with DMA and a crosslinker, the resultant hydrogel could swell upon UV light and collapse upon VIS light. If instead DMAAm is copolymerized, the gel would exhibit the opposite photo-response. When a drug is incorporated in the gel, we could control the release of the drug by UV/VIS photo-irradiation.

BIBLIOGRAPHY

1. W. Haupt, *Philos. Trans. R. Soc. London B* **303**, 467 (1983)
2. H. Smith, *Photochrome and Photomorphogenesis*, McGraw-Hill, London, p22 (1975).
3. G. Feher, J. P. Allen, M. Okamura, D. C. Rees, *Nature* **339**, 111 (1989).
4. L. Stryer *Am. Rev. Neurosci.* **9**, 87 (1986).
5. *Photochromism* (Ed.: G. H. Brown) Wiley, New York (1971).
6. *Organic Photochromism* (Ed.: A. V. Elston) Plenum, New York, (1990).
7. *Photochromism: Molecules and Systems* (Ed.: H. Durr, H. Bouas – Laurent), Elsevier, Amsterdam (1990).
8. *Applied Photochromic Polymer Systems* (Ed.: C. B. McArdle), Chapman & Hall, New York (1992).
9. A. D. Turner, S. V. Pizzo, G. W. Rozakis and N. A. Porter, *J. Am. Chem. Soc.* **109**, 1274 (1987).
10. M. S. Ferritto and D. A. Tirrell, *Macromol.* **21**, 3119 (1988).
11. M. S. Ferritto and D. A. Tirrell, *Biomaterials*, **11**, 645 (1990).
12. I. Willner and S. Rubin, *J. Am. Chem. Soc.* **114**, 3150 (1992).
13. R. Pamela, J. P. Kelly and B. D. Smith, *J. Am. Chem. Soc.* **115**, 3416 (1993)
14. I. Willner, M. L. Dagan, S. Rubin, J. Wonner, F. Effenberger and P. Bauerle, *Photochem. Photobiol.* **59**, 491 (1994).
15. M. Harada, M. Sisido, J. Hirose and M. Nakanishi, *Bull. Chem. Soc. Jpn.* **67**, 1380 (1994)
16. T. Hoshaka, K. Kawashima and M. Sisido, *J. Am. Chem. Soc.* **116**, 413 (1994).
17. T. Hoshaka, K. Sato, M. Sisido, K. Takai and S. Yokoyama, *FEBS. Lett.* **344**, 171 (1994).
18. R. Felicioli, L. Nannicini, E. Balestreri and G. Montagnoli, *Eur. J. Biochem.* **51**, 467 (1975).

19. G. Montagnoli, S. Monti, L. Nannicini and R. Felicioli, *Photochem. Photobiol.* **23**, 29 (1976).
20. G. Montagnoli, S. Monti, L. Nannicini, M. P. Giovannitti and M. G. Ristori, *Photochem. Photobiol.* **27**, 43 (1978).
21. I. Willner, S. Rubin and A. Riklin, *J. Am. Chem. Soc.* **113**, 3321 (1991).
22. P. R. Westmark, J. P. Kelly and B. D. Smith, *J. Am. Chem. Soc.* **115**, 3416 (1993).
23. D. Liu, J. Karanickolas, C. Yu, Z. Zhang and G. A. Woolley, *Bioorg. Med. Chem. Lett.* **7**, 2677 (1997).
24. I. Willner and S. Rubin, *Angew. Chem. Int. Ed. Engl.* **35**, 367 (1996).
25. K. Namba and S. Suzuki, *Chem. Lett.* **9**, 947 (1975).
26. I. Karube, Y. Nakamoto, K. Namba and S. Suzuki, *Biochim. Biophys. Acta.* **429**, 975 (1976).
27. M. Aizawa, K. Namba and S. Suzuki, *Arch. Biochem. Biophys.* **180**, 41 (1977).
28. M. Aizawa, K. Namba and S. Suzuki, *Arch. Biochem. Biophys.* **182**, 305 (1977).
29. I. Willner, S. Rubin, R. Shatzmiller and T. Zor, *J. Am. Chem. Soc.* **115**, 8690 (1993).
30. R. C. Rathi, P. Kopeckova and J. Kopecek, *Macromol. Chem. Phys.* **198**, 1165 (1997).
31. I. Willner, S. Rubin and T. Zor, *J. Am. Chem. Soc.* **113**, 4013 (1991).
32. V. N. R. Pillai, *Synthesis* **1** (1990)
33. R. W. Binkley and T. W. Flechtner, *Synthetic Organic Photochemistry* (Ed.: W. M. Horspool), Plenum, New York, p375 (1984)
34. A. D. Turner, S. V. Pizzo, G. Rozakis, N. A. Porter, *J. Am. Chem. Soc.*, **110**, 244 (1988).
35. N. A. Porter and J. D. Bruhnke, *Photochem. Photobiol.*, **51**, 37 (1990).

36. P. M. Koenig, B. C. Faust and N. A. Porter, *J. Am. Chem. Soc.* **115**, 9371 (1993).
37. J. Nargeot, J. M. Nerbonne, J. Engels and H. A. Lestner, *Proc. Natl. Acad. Sci. USA* **80**, 2395 (1983).
38. J. M. Nerbonne, S. Richard, J. Nargeot and H. A. Lestner, *Nature* **310**, 74 (1984).
39. J. H. Kaplan and R. J. Hollis, *Nature* **288**, 587 (1980).
40. A. Mamada, T. Tanaka, D. Kungwachakun and M. Irie, *Macromolecules* **23**, 1517 (1990).
41. S. R. Adams, J. P. Y. Kao and Y. Tsien, *J. Am. Chem. Soc.* **111**, 7957 (1989).
42. G. C. R. Ellis-Davies and J. H. Kaplan, *J. Org. Chem.* **53**, 1966 (1988).
43. R. Warmuth, E. Grell, J. M. Lehn, J. W. Bats and G. Quinkert, *Helv. Chim. Acta* **74**, 671 (1991).
44. O. Pieroni, J. L. Houben, A. Fossi, P. Costantino and F. Ciardelli, *J. Am. Chem. Soc.*, **102**, 5913 (1980).
45. J. L. Houben, A. Fossi, D. Baccida, N. Rosato, O. Pieroni and F. Ciardelli, *Int. J. Biol. Macromol.* **5**, 94 (1983).
46. B. R. Malcolm, O. Pieroni, A. Fossi and J. L. Houben, *Biopolymers*, **23**, 1423 (1984).
47. A. Fossi, *Macromolecules*, **29**, 4680 (1996).
48. F. Ciardelli, D. Fabbri, O. Pieroni and A. Fossi, *J. Am. Chem. Soc.* **111**, 3470 (1989).
49. O. Pieroni, A. Fossi, A. Viegi, D. Fabbri and F. Ciardelli, *J. Am. Chem. Soc.* **114**, 2734 (1992).
50. M. Sato, *Macromolecules*, **21**, 3419 (1988).
51. S. Rubin and I. Willner, *Mol. Cryst. Liq. Cryst.*, **246**, 201 (1994).
52. M. Harada, M. Sisido, J. Hirose and M. Nakanishi, *FEBS Lett.* **286**, 6 (1991).

53. T. Ueda, K. Murayama, T. Yamamoto, S. Kimura and Y. Imanishi, *J. Chem. Soc. Perkin. Trans. 1*, 225 (1994).
54. A. S. Hoffman, *Materials Research Society Bulletin*, XVI. **9**, 42 (1991).
55. A. S. Hoffman, *Artificial Organs*, **19**, 458 (1995).
56. M. Heskins, J. E. Guillet, *Macromol. Sci., Chem.*, **A2**, 1441 (1968).
57. H. G. Schild, *Probes of the lower critical solution temperature of poly(N-isopropylacrylamide)*;; Ed.: H. G. Schild, pp 259 (1991).
58. R. Lovrien, *Proc. Nat. Acad. Sci.* **57**, 236 (1967).
59. M. Irie and K. Hayashi, *J. Macromol. Sci., Chem.* **A13**, 511 (1979).
60. M. Iria, K. Hirano, S. Hashimoto, K. Hayashi, *Macromolecules* **14**, 202 (1981).
61. G. C. Hampson and J. M. Robertson, *J. Chem. Soc.* 409 (1941).
62. M. Irie and M. Hosoda, *Makromol. Chem. Rapid Commun.*, **6**, 533 (1985).
63. M. Irie, A. Menju and K. Hayashi, *Macromolecules*, **12**, 1176 (1981).
64. A. Menju, K. Hayashi and M. Irie, *Macromolecules*, **14**, 755 (1981).
65. D. Kungwatchakun and M. Irie, *Macromol. Chem. Rapid Commun.* **9**, 243 (1988).
66. M. Irie and D. Kungwatchakun, *Proc. Japan Acad.* **68**, 127 (1992).
67. R. Kröger, H. Menzel and M. L. Hallensleben, *Macromol. Chem. Phys.* **195**, 2291 (1994).
68. H. Menzel, R. Kröger and M. L. Hallensleben, *Macromol. Rep.* **A32**, 779 (1995).
69. M. Sanger, F. Borle, M. Heller and H. Sigrist, *Bioconj. Chem.* **3**, 308 (1992).
70. H. Sigrist, A. Collioud, J. F. Clemence, H. Gao, R. Luginbuhl, M. Sanger and G. Sundarababu, *Opt. Eng.* **34**, 2339 (1995).
71. H. Menzel, R. Kroger and M. L. Hallensleben, *ACS Polym. Preprints*, **39**, 330 (1998).
72. G. Z. Pelzl, *Chem.* **17**, 294 (1977).

73. U. Wiesner, M. Antonietti, C. Boeffel and H. W. Spiess, *Macromol. Chem.* **191**, 2133 (1990).
74. H. Menzel, B. Weichart, A. Schmidt, S. Paul, W. Knoll, J. Stumpe and T. Fischer, *Langmuir* **10**, 1926 (1994).
75. M. Brinkley, *Bioconj. Chem.*, **3**, 2 (1992).
76. L. Chalet, T. W. Miller, F. Tausing and F. J. Wolf, *Antimicrob. Agents Chemother.* **3**, 28 (1963).
77. L. Chalet and F. J. Wolf, *Arch. Biochem. Biophys.* **106**, 1 (1964).
78. N. M. Green, *Methods Enzymol.* **184**, 51 (1990).
79. N. M. Green, *Adv. Protein Chem.*, **29**, 85 (1975).
80. E. P. Diamandis and T. K. Christopoulos, *Clinical Chemistry*, **37**, 625 (1991).
81. W. A. Hendrichson, A. Pahler, J. L. Smith, Y. Satow and E. A. Merritt, *Proc. Natl. Acad. Sci. USA*, **86**, 2190 (1989).
82. P. C. Weber, D. H. Ohlendorf, J. J. Wendoloski and F. R. Salemme, *Science* **243**, 85 (1989).
83. P. C. Weber, J. L. Wendoloski, M. W. Pantoriano and F. R. Salemme, *J. Am. Chem. Soc.* **114**, 3197 (1992).
84. A. Pahler, W. A. Hendrickson, M. A. Gawinowicz Kolks, A C. E. ragana and C. R. Cantor, *J. Biol. Chem.* **262**, 13933 (1989).
85. A. Chilkoti, P. H. Tan and P. S. Stayton, *Proc. Natl. Acad. Sci. USA* **92**, 1754 (1995).
86. T. Sano and C. R. Cantor, *Proceedings Of The National Academy Of Sciences Of The United States Of America*, **92**, 3180 (1995).
87. P. S. Stayton, T. Shimoboji, C. Long, A. Chilkoti, G. Chen, J. M. Harris, A. S. Hoffman, *Nature*, **378**, 472 (1995).
88. Z. Ding, C. J. Long, Y. Hayashi, E. V. Bulmus, A. S. Hoffman and P. S. Stayton, *Bioconj. Chem.* **10**, 395 (1999).

89. V. Bulmus, Z. Ding, C. J. Long, P. S. Stayton and A. S. Hoffman, *Bioconj. Chem.* **11**, 78 (2000).
90. P. Beguin and J. P. Aubert, *FEMS Microbiol. Rev.* **13**, 25 (1994).
91. S. Pedersen, K. N. Lange and A. M. Nissen, *Ann. NY Acad. Sci.* **750**, 376 (1995).
92. J. D. McCarter and S. G. Withers, *Curr. Opin. In Stru. Biol.* **4**, 885 (1994).
93. M. Ward, S. Wu, J. Darberman, G. Weiss, E. Larenas, B. Bower, M. Rey, K. Clarkson and R. Bott, *Found. Biotech. Ind. Ferment. Res.* **8**, 153 (1993)
94. U. Arunachalam and J. T. Kellis, *Biochemictry*, **35**, 11379 (1996).
95. T. M. Wood and K. M. Bhat, *Methods in Enzymology*, **160**, 87 (1988).
96. K. Igarashi, M. Samejima and K. L. Eriksson, *Euro. Biochem.* **253**, 101 (1998).
97. H. Tilbeurgh, M. Claeysens and C. K. Bruyne, *FEBS Lett.*, **149**(1), 152 (1982).
98. G. L. Miller, R. Blum, W. E. Glennon and A. L. Burton, *Anal. Biochem.*, **1**, 127 (1960).
99. N. Nelson, *J. Biol. Chem.*, **153**, 376 (1944).
100. Method N-2bI/II. Technicon Instruments Corp. Tarrytown, N. Y. 10591 (1965).
101. SMA 6/60 and 12/60 system method manuals. Technicon Instruments Corp. Tarrytown, N. Y. 10591 (1970).
102. N. C. Suddith, B. S. Widish and J. L. moore, *Amer. J. Clin. Pathol.*, **53**, 181 (1970).
103. B. Fingerhut, *Clin. Chem.* **19**(9), 1022 (1973).
104. H. Flohe, R. Giertz and R. Beckmann, *Handbook for Information*, Vol 5, Elsevier, Amsterdam (1985).
105. K. Lechner, *Blutgerinnungsstorungen*, Springer, Berlin (1982).

106. J. Elisseeff, K. Anseth, D. Sims, W. McIntosh, M. Randolph, and R. Langer, *Proc. Natl. Acad. Sci. USA*, **96**, 3104 (1999).
107. Biosensors: Fundamentals and Applications (Eds: A. P. F. Turner, I. Karube and G. S. Wilson), Oxford University Press (1989).
108. F. Scheller and F. Schubert, *Tech. Instrum. Anal. Chem.*, **11** (1992).
109. K. Cammann, U. Lemke, A. Rohen, J. Sander, H. Wilken and B. Winter, *Angew. Chem.*, **103**, 519 (1991).
110. I. Willner and B. Willner, Bioorganic Photochemistry, (Ed.: H. Morrison), Wiley, **1** (1993).
111. Y. Morishima, M. Seki, S. Nomura and M. Kamachi, *ACS Symp. Ser.* **548**, 243 (1994).
112. T. Noda and Y. Morishima, *Macromol.* **32**(14), 4631 (1999).
113. J. P. Gallivan, H. A. Lester and D. A. Dougherty, *Chemistry and Biology* **4**, 739 (1997).
114. J. Peranen, *Biotechniques* **13**, 546 (1992).
115. G. King, S. Payne, F. Walker and G. I. Murray, *Journal of Pathology* **183**, 237 (1997).
116. F. M. Narendja and G. Sauermann, *Analytical Biochemistry* **220**, 415 (1994).
117. B. R. Stevenson, C. L. Richards, A. G. Howarth, V. A. Maraj and J. G. Hibbard, *Journal of Experimental Zoology* **268**, 224 (1994).
118. H. J. Hoeltke, I. Ettl, E. Strobel, H. Leying, M. Zimmermann and R. Zimmermann, *Biotechniques* **18**, 900 (1995).
119. R. W. Stephens, A. N. Pedersen, H. J. Nielsen, M. J. A. G. Hamers, H. G. Hoyer, E., Ronne, E., Dybkjaer, K. Dano, and N. Bruenner, *Clinical Chemistry* **43**, 1868 (1997).
120. R. Gutierrez, T. Garcia, I. Gonzalez, B. Sanz, P. E. Hernandez and R. Martin, *Journal of Applied Microbiology* **83**, 518 (1997).
121. R. Muller, *Biotechnology and Applied Biochemistry* **26**, 73 (1997).

122. M. Schlosser, J. Hahmann, B. Ziegler, P. Augstein and M. Ziegler, *Journal of Immunoassay* **18**, 289 (1997).
123. G. Shankar and D. A. Cohen, *Journal of Immunoassay* **18**, 371 (1997).
124. S. Kossek, C. Padeste and L. Tiefenauer, *Journal of Molecular Recognition* **9**, 485 (1996).
125. D. R. Kim and C. S. McHenry, *Journal of Biological Chemistry* **271**, 20690 (1996).
126. U. H. Refseth, B. M. Fangan and K. S. Jakobsen, *Electrophoresis* **18**, 1519 (1997).
127. A. Rolfs and I. Weber, *Biotechniques* **17**, 782 (1994).
128. B. Pettersson, K. E. Johansson and M. Uhlen, *Applied and Environmental Microbiology* **60**, 2456 (1994).
129. V. R. Muzykantov, V. D. Gavriluk, A. Reinecke, E. N. Atochina, A. Kuo, E. S. Barnathan and A. B. Fisher, *Analytical Biochemistry* **226**, 279 (1995).
130. D. Oupicky, K. Ulbrich and B. Rihova, *J. Bioact. Compat. Polym.* **14**, 213 (1999).

CURRICULUM VITA**TSUYOSHI SHIMOBOJI****EDUCATION****University of Washington, Seattle, WA, USA**

Ph.D., Department of Bioengineering 3 - 2001

Kyoto University, Kyoto, JAPAN

M.E., Department of Polymer Chemistry 3 - 1988

Kyoto University, Kyoto, JAPAN

B.E., Department of Polymer Chemistry 3 - 1986

WORK EXPERIENCE**Mitsubishi Chemical Corporation (MCC), Yokohama, JAPAN**

Yokohama Research Center: Research Scientist 1988 - 1997

University of Washington, Seattle, WA, USA

Department of Bioengineering

Visiting Scholar from MCC to Prof. A.S. Hoffman Lab. 1993 - 1995

RESEARCH EXPERIENCE (at Kyoto University, MCC, and UW)**Monomer and polymer synthesis and characterization**

- Synthesis of intelligent (stimuli-responsive) polymers

- Synthesis of self-assembling and ion-transporting polymers for solid polymer electrolytes
- Polyelectrolyte modification for polyion complex processing
- Utilized the following equipment and measurements: WAXD, SAXS, USAXS, DLS, DSC, TG, DTA, SEM, HPLC, GPC, LC, GC, NMR, IR, UV spectroscopy, XRD, Gas permeability, Electrical impedance, Mechanical properties, Viscometers
- Structure analysis of polymer and molecular assemblies in solution: microemulsions, polyion complexes, coacervates
- Polymer processing: polymer mixing, pelletizing, blending, heat press, multilayered extrusion processing (inflation film molding, T-die sheet molding), orientation processes (film and tubular biaxial elongation)
- Pilot plant scale-up of monomer synthesis and film processing: solid polymer electrolyte monomer synthesis
- Multilayered functional film processing: oxygen barriers, freshness preservation, antibiotic incorporation, cloud-free films

Biotechnology

- Polymer surface modification for biomaterials and biotech applications: hydrophilic modification, crosslinking, functional group (amino, sulfhydryl) immobilization, functional molecule (biotin, streptavidin, heparin) immobilization, RFGD (plasma gas discharge), chemical modification, corona discharge
- Gene design for recombinant and mutant protein expression: site-directed mutagenesis, gene cloning, gene design (GCG), PCR, gel filtration, miniprep, transformation, gel electrophoresis, sequencing
- Protein-polymer conjugates: conjugation between mutant proteins (protein G, streptavidin, IgG) and intelligent polymers (temperature- and photo-sensitive polymers)

Agriculture

- Computer simulation of gas composition in the plant respiratory system
- Freshness preservation testing of fruits, fungi, and flowers

PUBLICATIONS

1. T. Shimoboji, H. Matsuoka and N. Ise, "Small Angle X-ray Scattering Study on Nonionic Microemulsions", Physical Review, **A39**, 4125-4131 (1989).
2. T. Shimoboji, "Design of Controlled Atmosphere Films for Preserving Fresh Produce", Mitsubishi Kasei R&D Review, **5** (2), 84-90 (1991).
3. P. S. Stayton, T. Shimoboji, C. Long, A. Chilkoti, G. Chen, J. M. Harris and A. S. Hoffman, "A Novel Method for Control of the Protein - ligand Recognition Process: Site-specific Conjugation of a Temperature-sensitive Polymer in the Binding Pocket of a Genetically-engineered Protein", Nature, **378**, 472, (1995).
4. P. S. Stayton, K. E. Nelson, T. C. McDevitt, V. Bulmus, T. Shimoboji, A. Ding and A. S. Hoffman, "Smart and biofunctional streptavidin", Biomolecular Engineering, **16**, 93-99 (1999).
5. T. Shimoboji, P. S. Stayton and A. S. Hoffman, "Photo-responsive polymers for protein conjugation", prepa.ed.
6. T. Shimoboji, P. S. Stayton and A. S. Hoffman, "Photo-switched Gating of Biotin Association with Light-Responsive Polymer-Streptavidin", prepared.
7. A. S. Hoffman, P. S. Stayton, T. Shimoboji. *et al.*, "Really Smart Bioconjugates of Smart Polymers and Receptor Proteins", J. Biomed. Mat. Res., **52**(4), 577-586 (2000).
8. T. Shimoboji, D. Zhongli, , P. S. Stayton and A. S. Hoffman, "Mechanistic Investigation of Smart Polymer-Protein Conjugates", Bioconj. Chem. Accepted.
9. T. Shimoboji, E. Larenas, T. Flower, P. S. Stayton and A. S. Hoffman, "Thermo-Switching of Enzymatic Activities by Site-Specific Conjugation of Temperature-Responsive Polymers to Genetically-Engineered Enzymes", prepared.
10. T. Shimoboji, E. Larenas, T. Flower, P. S. Stayton and A. S. Hoffman, "Photo-Switchable Enzyme-Polymer Conjugate", prepared.
11. T. Shimoboji and A. S. Hoffman, "Covalent Immobilization of Heparin on Inert Polymer Supports", US Patent Application, disclosure 1024DL.
12. 26 Patents applied for at Mitsubishi Chemical Co.

SCIENTIFIC PRESENTATIONS

1. "Small Angle X-ray Scattering Study on Nonionic Microemulsions", Conference of Polymer Science in Japan, 1987, Kobe, Japan
2. "Relationship between the microstructure and oxygen barrier property of Poly(vinylalcohol-ethylene)-copolymer film", POVAL Conference, 1990, Kyoto, Japan
3. "A New Process Combining Gas Discharge Treatment and Adsorption of a Cationic Polymer to Enhance Immunoassay Tests", The 21st Annual Meeting of Society for Biomaterials, 1995, San Francisco, CA, U.S.A.
4. "Site-specific Conjugation of a Temperature-sensitive Polymer to a Genetically Engineered Protein", The 5th World Biomaterials Congress, 1996, Toronto, Canada
5. "A New Method for Amination of Biomaterial Surfaces", The 5th World Biomaterials Congress, 1996, Toronto, Canada
6. "Photo-switched Gating of Biotin Association with Light-Responsive Polymer-Streptavidin", The 6th World Biomaterials Congress, 2000, Hawaii, U.S.A.
7. "Thermo-switching of Enzymatic activity by Site-Specific Conjugation of Temperature-Responsive Polymers to Genetically-Engineered Enzymes", 27th Annual Meeting of Soc. For Biomaterials, 2001, Saint Paul, U.S.A.